

For Reference

NOT TO BE TAKEN FROM THIS ROOM

For Reference

NOT TO BE TAKEN FROM THIS ROOM

Ex LIBRIS
UNIVERSITATIS
ALBERTAENSIS





Digitized by the Internet Archive
in 2020 with funding from
University of Alberta Libraries

<https://archive.org/details/Alpaslan1969>

THE UNIVERSITY OF ALBERTA

SPECTRAL BEHAVIOR OF SHORT PERIOD BODY WAVES AND
THE SYNTHESIS OF CRUSTAL STRUCTURE IN WESTERN CANADA

BY



TÜMER ALPASLAN

A THESIS

SUBMITTED TO THE FACULTY OF GRADUATE STUDIES
IN PARTIAL FULFILLMENT OF THE REQUIREMENTS
FOR THE DEGREE OF MASTER OF SCIENCE

DEPARTMENT OF PHYSICS

EDMONTON, ALBERTA

NOVEMBER, 1968

UNIVERSITY OF ALBERTA
FACULTY OF GRADUATE STUDIES

The undersigned certify that they have read and recommend to the Faculty of Graduate Studies for acceptance, a thesis entitled SPECTRAL BEHAVIOR OF SHORT PERIOD BODY WAVES AND THE SYNTHESIS OF CRUSTAL STRUCTURE IN WESTERN CANADA, submitted by Tüner Alpaslan, in partial fulfillment of the requirements for the degree of Master of Science.

ABSTRACT

In Project Early Rise, the University of Alberta recorded arrivals at distances of 1100 to 2000 kilometers from the source. At some locations a cluster of one vertical and two horizontal components of ground motion were recorded.

A very fast and efficient program for Butterworth band-pass filter has been written and was used to enhance the data without introducing any phase distortion. This algorithm based on the Butterworth filter has given very good results in various geophysical problems involving time sequence analysis.

Theoretical spectral ratios have been compared with the spectral ratios of field records from Project Early Rise. The theoretical spectral ratios for a southern Alberta crustal model with five layers has been calculated using the Thomson-Haskell matrix formulation. The basic Alberta model has been modified by changing the thickness of various layers to obtain a better fit between theoretical and experimental spectral ratios at various locations where data was available. From this limited amount of comparisons it is found that the spectral ratio favors a crustal thickness of about 43 kilometers in Saskatchewan and increasing to 48 kilometers on the Alberta-Saskatchewan boundary to a possible maximum of 53

kilometers near Viking, Alberta. No uniqueness can be claimed for these models and it is probable that further calculations would yield models which give a better fit over the frequency range that was recorded.

Comparison of field results were also made using theoretical seismograms which were calculated by a fast Fourier program which inverted the transfer function obtained with a Thomson-Haskell matrix formulation. It was noticed that at certain locations the theoretical seismograms agree with the field records while at other locations the comparison was not good. Possibly, the crustal model will need major modification at these locations or the assumption of plane layering in the model calculations is not justified.

ACKNOWLEDGEMENTS

I wish to thank sincerely Dr. E.R. Kanasewich who made possible this research problem.

I would also like to thank Mr. C.M. McCloughan for his assistance and Mrs. M. Lybacki for her job in typing.

Project Early Rise was supported by a grant obtained for the United States Air Force (Grant No. AF-AFOSR-1140-66) through the offices of the Arctic Institute of North America.

During the course of this study, the author was supported by a Graduate Teaching Assistanship from the Department of Physics, University of Alberta and a bursary from the National Research Council of Canada.

TABLE OF CONTENTS

	Page
CHAPTER I	
SEISMIC INVESTIGATION OF THE CRUST	1
Introduction	1
Previous Work	2
Experimental data	5
CHAPTER II	
ZERO PHASE DIGITAL FILTERS	8
Introduction	8
Recursion filters	12
Synthesis of recursion filters in the z-plane	14
The Bilinear z-transform	16
Butterworth filters	19
Poles and zeros of a low-pass Butterworth filter	21
Frequency transformation for high-pass filter	28
Frequency transformation for a band-pass filter	31
Zero phase filters	47
Conclusion	52
CHAPTER III	
THE CRUSTAL TRANSFER FUNCTION AND SPECTRAL RATIOS	58
Theory	58
Properties of the transfer function	61
Application of the crustal transfer function	63

CHAPTER III (cont'd.)		Page
	Analysis of data	72
	Conclusion	76
CHAPTER IV	SYNTHETIC SEISMOGRAMS	80
	Theory	80
	Generation of synthetic seismograms	80
	Field records and theoretical seismograms	91
REFERENCES		
Appendix 1	THOMSON-HASKELL MATRIX FORMULATION	A. 1
	Introduction	A. 1
	Wave equations and plane wave solution	A. 4
	Equations of stress	A.11
	Matrix formulation and transfer function	A.12
Appendix 2	LISTING OF COMPUTER PROGRAMS	A.26

LIST OF ILLUSTRATIONS

<u>Figure</u>		<u>Page</u>
1. 1	Project Early Rise	6
2. 1	Ideal low-pass filter	8
2. 2	Evaluation of the recursive equation 2.16	13
2. 3	Z-plane representation of poles and zeros	15
2. 4	Non-linear warping of frequency scale in the bilinear z-transformation	18
2. 5	Square of the transfer function for a normalized low-pass filter using a Butterworth function	20
2. 6	Poles of a fourth order low-pass Butterworth filter	23
2. 7	Zero phase impulse response of a Butterworth low-pass filter for $f_c=10.0$ c.p.s., $\Delta t=1/118$ sec. and $n=4$	26
2. 8	Zero phase amplitude response of Butterworth low-pass filter for $f_c=10.0$ c.p.s., $\Delta t=1/118$ sec. and $n=4$	27
2. 9	Square of the transfer function for an n^{th} order Butterworth high-pass filter	29
2.10	Zero phase impulse response of a Butterworth high-pass filter for $f_c=10.0$ c.p.s., $\Delta t=1/118$ sec. and $n=4$	32
2.11	Zero phase amplitude response of a Butterworth high-pass filter for $f_c=10.0$ c.p.s., $\Delta t=1/118$ sec. and $n=4$	33
2.12	Transformation from a low-pass to a band-pass filter	35
2.13	Poles and zeros of a Butterworth band-pass filter with cut-off frequencies at 1 and 10 cycle per second	41

<u>Figure</u>		<u>Page</u>
2.14	Location of poles and zeros of equation 2.88	43
2.15	Zero phase impulse response of Butterworth band-pass filter with a cut-off at 1 c.p.s. and 10.0 c.p.s., for $n=4$ and $\Delta t=1/118$ sec.	44
2.16	Zero phase amplitude response of Butterworth band-pass filter with a cut-off frequencies at 1 c.p.s. and 10.0 c.p.s. for $n=4$ and $\Delta t=1/118$ sec.	45
2.17	Phase response of Butterworth band-pass filter with a cut-off frequencies at 1 c.p.s. and 10 c.p.s. for $n=4$ and $\Delta t=1/118$ sec.	46
2.18	Impulse response of zero phase shift Butterworth filter for cut-off frequencies at 1 c.p.s. and 5 c.p.s. The sampling interval is $1/118$ sec.	53
2.19	Amplitude response of zero phase shift Butterworth filter for cut-off frequencies at 1 c.p.s. and 5 c.p.s. The sampling interval is $1/118$ sec.	54
2.20	Example of 4 unfiltered seismic records from Project Early Rise	55
2.21	Four seismic records from Project Early Rise filtered by a zero phase shift band pass recursive digital Butterworth filter with cut-off frequencies at 1 c.p.s. and 5 c.p.s.	56
2.22	Four seismic records from Project Early Rise filtered by a zero phase shift band pass recursive digital Butterworth filter with cut-off frequencies at 0.5 c.p.s. and 3.0 c.p.s.	57
3. 1	Notation used for a crustal system of n layers	60

<u>Figure</u>		<u>Page</u>
3. 2	Modulus of transfer functions and their ratios for plane waves incident on a southern Alberta crustal section at an angle of incidence of 80° . The depth has been increased in the third layer by 3 kilometers. The crosses denote the thicker model	64
3. 3	Modulus of the transfer function, their ratios and the phase of the ratios for plane waves incident on a southern Alberta model at an angle of incidence of 80° . The velocity has been increased in the third layer from 6.50 to 7.50 km/sec. (see table 1). The crosses denote the higher velocity model	65
3. 4	Modulus of transfer function and their ratios for plane waves incident on a southern Alberta crustal model at an angle of incidence of 60° . The depth has been increased in the third layer by 3 kilometers. The crosses denote the thicker model	66
3. 5	Phase curves for transfer functions of a southern Alberta crustal model. This corresponds to the modulus of transfer function shown in figure 3.2.	67
3. 6	Truncation of transfer function for Alberta model using frequency interval of $\Delta f = 0.05$ and time interval of $\Delta t = 1/50$	73
3.7	Vertical and horizontal spectrum of a field record at location WC 25 and comparison of the spectral ratios with a theoretical model which is represented by a dashed line	77
3. 8	Vertical and horizontal spectrum of a field record at location WC 34 and a comparison of spectral ratios with the theoretical model which is represented by a dashed line	78

<u>Figure</u>		<u>Page</u>
3. 9	Vertical and horizontal spectrum of a field record at location WC 39 and a comparison of the spectral ratios with the theoretical model which is represented by a dashed line	79
4. 1	Source function	81
4. 2	Calculation of theoretical seismogram using fast Fourier algorithm	83
4. 3	Theoretical seismogram calculated for Hanon's (1964) model	85
4. 4	Conversion in a single layer model	88
4. 5	Theoretical ground motions for a southern Alberta model using a frequency interval $\Delta f = 0.02$ c.p.s.	89
4. 6	Theoretical ground motions for a southern Alberta model using a frequency interval $\Delta f = 0.005$ c.p.s.	90
4. 7	Theoretical seismograms for a southern Alberta model and its filtered version using a Butterworth band-pass filter whose cut-off frequencies are 1 c.p.s. and 5 c.p.s.	93
4. 8	Comparison of vertical and horizontal components of a field record with the theoretical seismograms for a southern Alberta model	94
4. 9	Additional comparison of vertical and horizontal components of a field record with the theoretical seismograms for a southern Alberta model	95

CHAPTER 1

SEISMIC INVESTIGATION OF THE CRUST

1.1 Introduction

An investigation of the deep structure of the Earth will help us to interpret its historical evolution, the nature of some destructive events, and it will even give us a better understanding about other planets. In the study of the Earth's interior refraction and reflection seismology have been two of the most powerful tools. From the variation of velocity with depth the Earth has been divided into a number of zones which are separated by first or second order discontinuities. The uppermost part of these zones is called the crust and it has an average thickness of 35 km under the continents and 5 km under the oceans. The Mohorovičić (M) discontinuity separates the crust from another zone called the mantle having different elastic parameters.

The crust has been found to consist of many discrete layers whose properties change from place to place. This layered medium produces a reverberation which makes it difficult to interpret deeper arrivals from the mantle. This aspect of the problem will be investigated at length in this thesis. Apart from this effect a study of a layered system as a linear filter is useful because of the economic

importance of the crust.

1.2 Previous Work.

Observations of the effects of the crust on seismic reverberations were begun by Imamura (1929) who studied terrestrial vibrations induced by the arrival of seismic waves from earthquakes. He observed that the period of the waves varied with different soils and geological strata. Nasu (1931) continued studying vibrations of the Earth and concluded that earthquake motion at short periods (less than 1 sec.) is much influenced by the nature of the soil and he explained the oscillations as due to a superficial layer being excited by a sudden arrival of an impulse originating from an earthquake. Suzuki (1932) observed changes in the period of waves with the angle of incidence. His observational study showed that beyond certain epicentral distances the angle of incidence does not change with distance. Gutenberg (1957) studied earthquake damage at different locations as a function of the elastic properties of the soil. Nuttli (1964) observed that for long-period P waves generated by earthquakes of magnitude 6, the amplitude of ground motion was not effected by crustal layering.

The theoretical response of such a layered system has been calculated by different authors under certain

simplifying assumptions. For example, Sezawa (1930) calculated the free oscillations of a single layer excited by a dilatational pulse of a purely plane type propagated vertically upwards in an elastic solid medium. Later Sezawa and Kanai (1932 a,b, 1937) studied transmission of seismic waves of oscillatory type and of finite extent through a strata for obliquely incident waves. Theoretical seismograms were compared by changing the thickness of the layers and the frequency of the waves. Kanai (1952, 1953, a,b) in a series of studies, calculated the oscillations of doubly stratified visco-elastic layers excited by seismic waves at vertical incidence and the relation between the amplitude at the surface, the impedance ratio of the two media, the coefficients of viscosity and the thickness of the surface layer. He showed that as the velocity of a weak layer decreases, the amplitude of the seismic motion at the free surface increases.

Thomson (1950), Haskell (1953) and Dorman (1962) generalized the theory to yield the response of a layered system to plane waves at any angle of incidence. They expressed the solution in terms of products of four by four matrices whose members are a function of the parameters of each layer; the angle of incidence and the wavelength of the incident harmonic wave. Thomson (1950) made the original formulation of propagation of plane waves through

a system of plane parallel layers. Haskell (1953) corrected an error in Thomson's work and discussed the application of the method to the dispersion of Love and Rayleigh waves. In 1962 Dorman formulated the solution for the boundary conditions at a boundary between a liquid and a solid. Later Haskell (1962) gave the transfer function for the vertical and horizontal components of ground motion.

Fast digital computers have made it practical to use the Thomson-Haskell matrix formulation for calculating the response of a media with any number of layers. Phinney (1964) compared the ratio of long-period spectra of vertical and horizontal seismograms for large earthquakes with the ratio of the vertical to horizontal transfer function, using the Thomson-Haskell matrix formulation. Hanon (1964) first attempted the calculation of a synthetic seismogram by taking the inverse Fourier transform of the transfer function for different models. Fernandez (1965) calculated spectral ratios for long-period data giving model curves to determine crustal structure. Recently Leblanc (1966) and McCamy (1967) applied the transfer function and spectral ratios to short period data in an attempt to obtain crustal structure.

In this study, the transfer function for an ALBERTA crustal model has been calculated using the Thomson-Haskell matrix formulation. The theoretical ratio of verti-

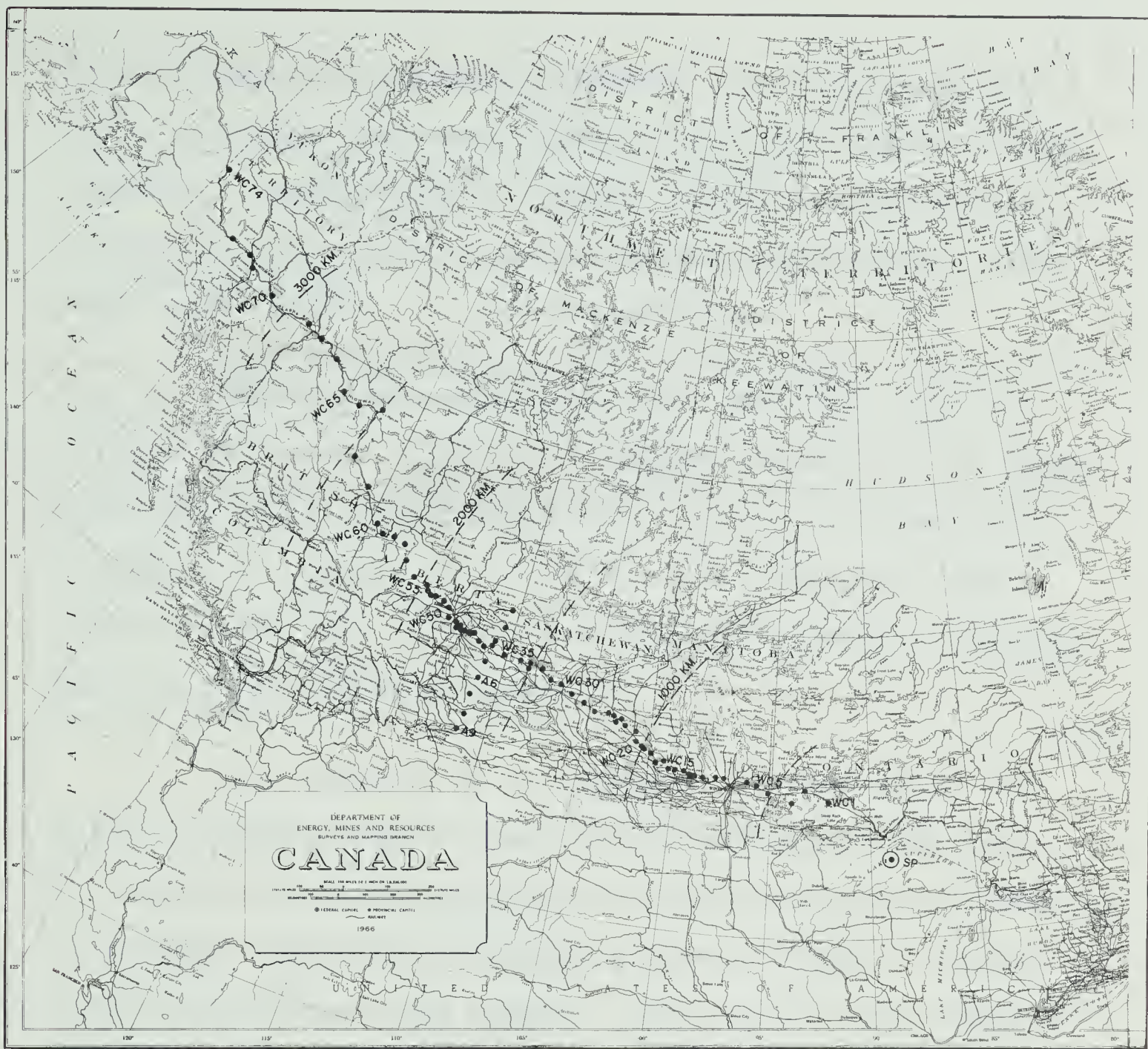
cal to horizontal transfer function was compared with the ratio of the spectra of vertical and horizontal seismograms. A time synthesis of ground motion was obtained for a $\text{Sin } X/X$ shaped pulse. Comparisons were carried in the time domain.

1.3 Experimental Data.

Project Early Rise was planned to study the upper mantle under North America by seismic waves generated by chemical explosives detonated in Lake Superior. The University of Alberta recorded the arrivals at a distance of 1100 to 2000 kilometers from the source. Arrivals are recorded also by a 400 kilometers arc line from Cold Lake to Bow Island, Alberta. Nine stations on this arc line have a distance of 1675 kilometers from the source. The United States Geological Survey extended this profile from 350 to 1100 and 2000 to 3500 kilometers from the shot to the Alaska-Yukon border. The seventy-four locations are labelled from WC 1 to WC 74 (Figure 1.1).

In this project the University of Alberta had two mobile recording units equipped with tape recorders and two stationary observatory sites also recording on magnetic tape. Each mobile unit had 9 Texas instrument S-36 2 c.p.s. seismometers, 12 channel V.L.F. amplifiers, an

Figure 1.1. Project Early Rise



RS-8U 24-trace oscillograph with 200 c.p.s. galvanometers and a precision instrument model PS 207 F.M. magnetic tape recorder. Occasionally a cluster of one vertical and two horizontal components of ground motion was recorded using Hall Sears (HS-10) 2 c.p.s. seismometers.

Most of the recordings were made with high-cut filters on 8 c.p.s. The low frequency cut-off is not adjustable but falls off rapidly below 2 c.p.s. Attenuation of arrivals was usually set to 18 db on the amplifier panel. A chronometer, WWV receiver and standard broadcast receiver were used for timing purposes.

The accuracy of the results obtained about the Earth's interior depend upon the reliability of the data. The use of precisely located and timed explosion is preferred to studies employing earthquake generated waves. Current recording systems using magnetic tape allows us to enhance the data with various data processing techniques on the digital computer. Useful data was obtained during Project Early Rise and in Chapter 2 attempts have been made at enhancing this data with distortionless digital band-pass filters. The results were then used in Chapter 3, to evaluate the usefulness of present day theoretical studies as applied to the calculation of theoretical seismograms.

CHAPTER 2

ZERO PHASE DIGITAL FILTERS

2.1 Introduction.

Zero phase filters are most important because they are the best filters in a least-mean square sense for extracting signals whose spectra overlap slightly with that of noise. It is possible to obtain data with no phase distortion by digital filters since past and future values of the data are available in the memory of the computer. This is one of the major advantages of digital over analog filters.

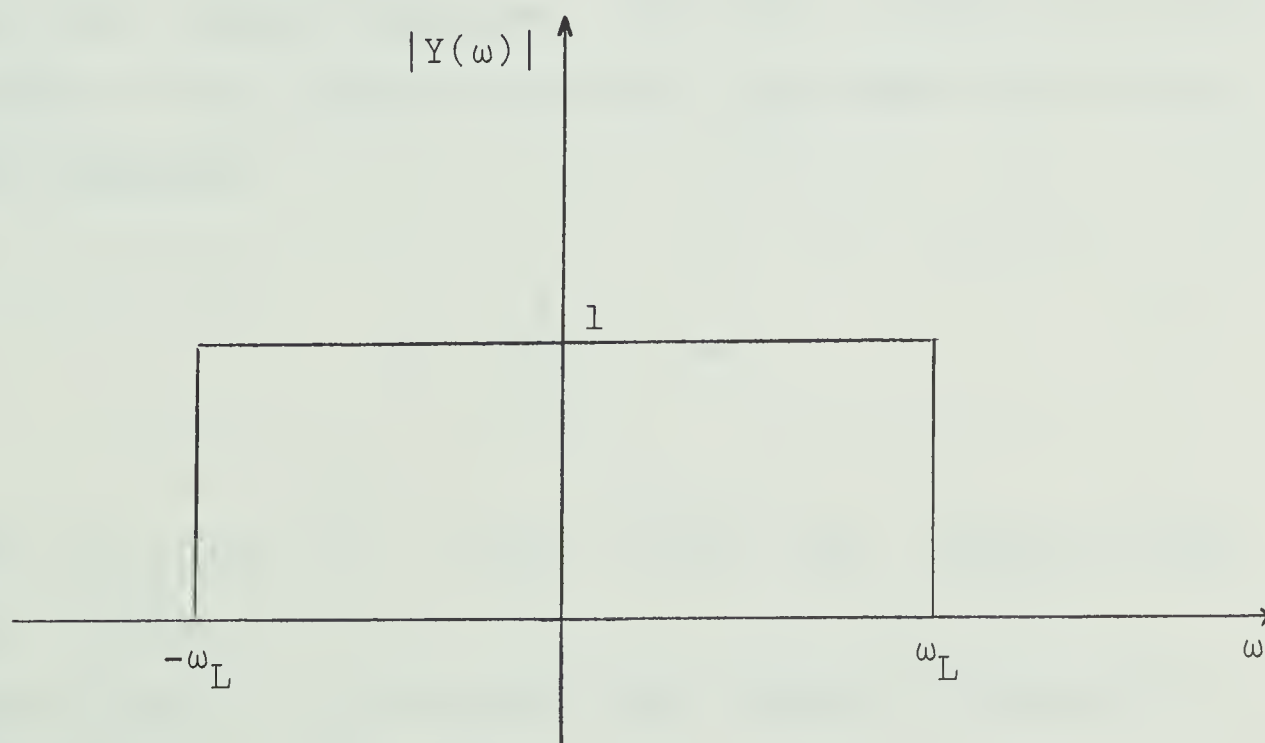


Figure 2.1. Ideal low-pass filter

An ideal filter is the one with unit response in the desired region and zero elsewhere (Figure 2.1) in the frequency domain. An approximation to such a filter can be realized by a number of methods which are discussed by Baum (1948), Guillemin (1957), Ormsby (1961), Weinberg (1962), Kaiser (1963), Holtz and Leondes (1966), Stalling (1966), Shanks (1967) and Wood (1968).

In the digital domain the unit impulse function is

$$\delta_t = \begin{cases} 1 & t = 0 \\ 0 & t \neq 0 \end{cases} \quad 2.1$$

The output of a filter whose input is a unit impulse is called the impulse response. The filter operation is then defined as the convolution of the input data with the impulse response:

$$y_n = \sum_{i=0}^n f_i x_{n-i} \quad 2.2$$

where $(x_0, x_1, x_2, \dots, x_m)$ are the $m+1$ values of the input series;

$(f_0, f_1, f_2, \dots, f_n)$ are the $n+1$ values of impulse response;

$(y_0, y_1, y_2 \dots y_{n+m})$ are the $n+m+1$ values of the output series.

For a filter to be stable the sum of the squares of the impulse response must be bounded i.e.,

$$\sum_{t=-\infty}^{\infty} |f_t|^2 < \infty \quad 2.3$$

A filter is called realizable if f_t is one-sided so that no response can occur prior to its stimulus. In equation 2.3 the lower limit can be set to $t=0$ for a realizable filter.

For digital computation and analysis of filter stability a z -transform is used (Jury, 1964), since convolution in the digital time domain is equivalent to multiplication in the domain of the z -transform. The z -transform of a continuous function $f(t)$ which has a sampling interval of Δt is

$$F(z) = \sum_{n=-\infty}^{\infty} f(n\Delta t) z^n \quad 2.4$$

where $n=0,1,2 \dots$ and z is a complex variable. The z -transform of a realizable stable system can be written as

$$Y(z) = \sum_{t=0}^{\infty} y(t) z^t \quad 2.5$$

where $y(t)$ is the impulse response of the filter. The z -transform can also be obtained by replacing $e^{-\Delta t s}$ or $e^{-i\omega \Delta t}$ with z in the Laplace and Fourier transform (Jury, 1964). Therefore z -transforms can also be expressed as

$$z = e^{-\Delta t s} \quad 2.6$$

$$z = e^{-i\omega \Delta t} \quad 2.7$$

Here z represents the delay of a signal one sample interval and z^2 represents a delay of two sample intervals (Robinson, 1964), etc. Using the equation 2.7 in the equation 2.5 for $\Delta t=1$, that is, on the unit circle in the z -plane, it can be written

$$Y(\omega) = \sum_{t=0}^{\infty} y(t) e^{-i\omega t} \quad -\pi \leq \omega \leq \pi \quad 2.8$$

The function $Y(\omega)$ is called the transfer function of the filter. In polar form it can be written as

$$Y(\omega) = |Y(\omega)| e^{i\theta(\omega)} \quad 2.9$$

where $|Y(\omega)|$ is called the Gain and $\theta(\omega)$ the phase shift. The delay of the system is defined as

$$\tau_g = - \frac{d\theta(\omega)}{d\omega} \quad 2.10$$

2.2 Recursion filters.

The filter operation in the z -domain can be written as

$$Y(z) = F(z) \cdot X(z) \quad 2.11$$

where

$$X(z) = x_0 + x_1 z + x_2 z^2 + \dots + x_m z^m$$

$$F(z) = f_0 + f_1 z + f_2 z^2 + \dots + f_n z^n$$

$$Y(z) = y_0 + y_1 z + y_2 z^2 + \dots + y_{m+n} z^{m+n}$$

2.12

Often the transfer function of a filter can be expressed as

$$F(z) = \frac{A(z)}{B(z)} = \frac{a_0 + a_1 z + a_2 z^2 + \dots + a_n z^n}{b_0 + b_1 z + b_2 z^2 + \dots + b_m z^m} \quad 2.13$$

Such a transfer function can be programmed more efficiently by a recursion relation involving a feedback loop. As an example consider an impulse response with the form

$$F(z) = \frac{a_0 + a_1 z}{1 + b_1 z + b_2 z^2} \quad 2.14$$

From equation 2.11 the output will be

$$Y(z) = F(z) \cdot X(z) = \frac{a_0 + a_1 z}{1 + b_1 z + b_2 z^2} \cdot X(z) \quad 2.15$$

Multiplying both sides of equation 2.15 by the denominator and arranging terms we obtain

$$Y(z) = [a_0 + a_1 z] \cdot X(z) - z Y(z)[b_1 + b_2 z] \quad 2.16$$

Equation 2.16 can be evaluated by following the steps indicated in the flow diagram of figure 2.2.

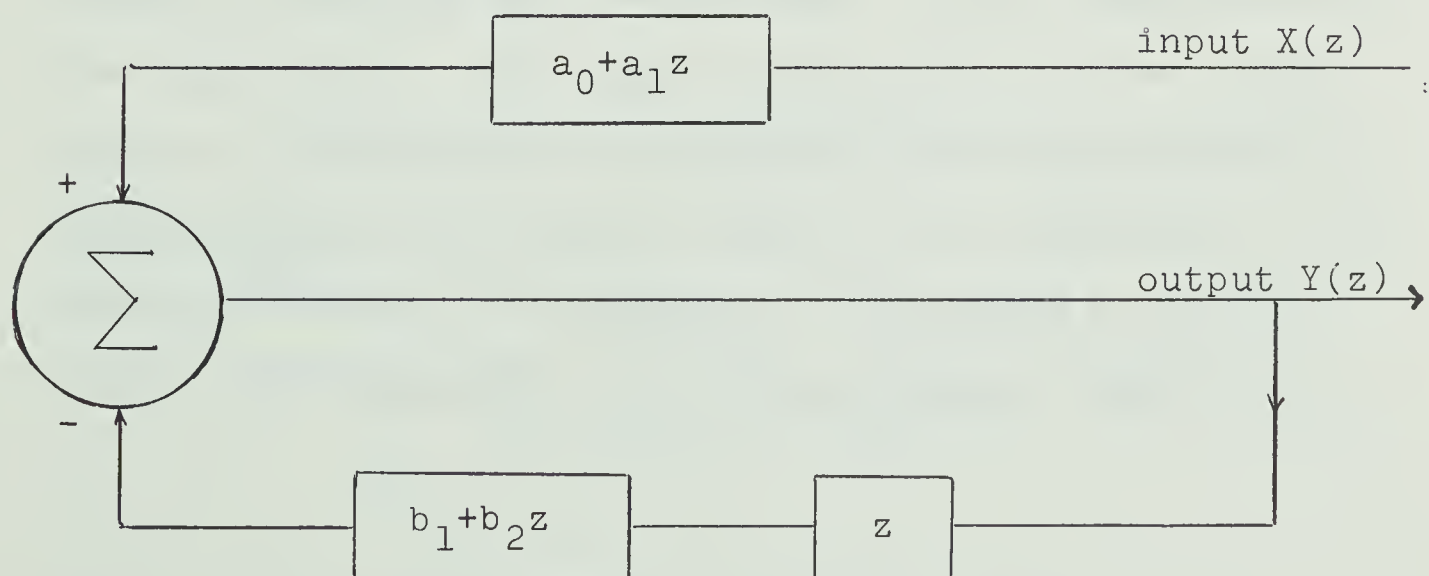


Figure 2.2. Evaluation of the recursive equation 2.16.

A general recursion equation representing equation 2.13 can be written as

$$y_n = \sum_{i=0}^n a_i x_{n-i} - \sum_{j=1}^m b_j y_{n-j} \quad 2.17$$

where the coefficient b_0 is assumed to be 1.0 for convenience in equation 2.13. The term, b_0 can always be made equal to 1.0 by division. An algorithm based on the recursive relation in equation 2.17 can save a great deal of computer time and is more precise than a standard convolution (equation 2.2). Equation 2.2 requires many more multiplications and summations and requires a large number of filter coefficients, f_i .

2.2.1 Synthesis of recursion filters in the z-plane.

It is useful to analyze rational filters in terms of roots of the z-transform of the numerator and the denominator. The roots of the numerator are called zeros of a filter while the roots of the denominator are called poles of a filter. A plot of the location of the poles and zeros in the complex z-plane may be used to predict the stability of a filter operator (Figure 2.3).

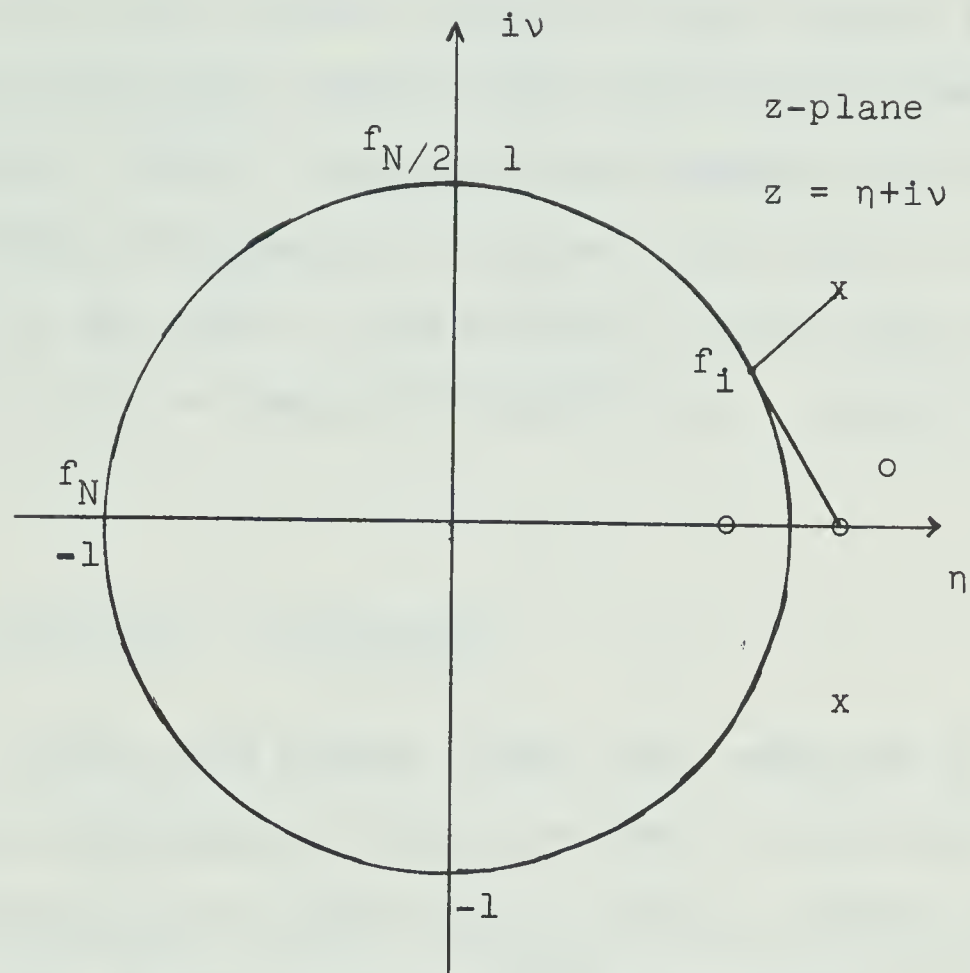


Figure 2.3. z -plane representation of poles (x) and zeros (o) .

The amplitude and phase response of a digital filter can be found by evaluating on the unit circle $|z| = 1$. From equation 2.7 the point $z = 1.0 + i 0.0$ corresponds to zero frequency and $z = -1.0 + i 0.0$ corresponds to $f_n = \omega_n/2\pi = \frac{1}{2\Delta t}$, the Nyquist, folding or alias frequency. Frequencies are linearly distributed around the unit circle between zero and the Nyquist frequency (Figure 2.3).

The z -plane can be used to design simple filters by locating poles and zeros which are known (Truxal, 1955). The poles must be located outside the unit circle since a pole inside the unit circle causes instability (Treitel and Robinson, 1964). The amplitude response of a filter at any desired frequency is related to the ratio of the distance of the zeros to the distance of the poles from the frequency point on the unit circle in the z -plane (Figure 2.3).

2.3 The Bilinear z -transform.

Golden and Kaiser (1964) have employed an algebraic transformation which converts a continuous transfer function into one which can be used on sampled data. It eliminates aliasing errors which are present in the standard z -transform (equation 2.6). The bilinear z -transformation is defined as

$$s_d = \frac{2}{\Delta t} \tanh \left(\frac{s \Delta t}{2} \right) \quad 2.18$$

using equation 2.6 we have

$$s_d = \frac{2}{\Delta t} \frac{\frac{1}{2}(e^{\frac{1}{2}s(\Delta t)} - e^{\frac{1}{2}s(\Delta t)})}{\frac{1}{2}(e^{\frac{1}{2}s(\Delta t)} + e^{\frac{1}{2}s(\Delta t)})} \quad 2.19$$

or

$$s_d = \frac{2}{\Delta t} \frac{1-z}{1+z} \quad 2.20$$

Non-linear warping caused by this transformation can be seen by setting $s_d = i\omega$ in equation 2.18 as illustrated in figure 2.4.

$$\omega_d = \frac{2}{\Delta t} \tan \frac{(\omega \Delta t)}{2} \quad 2.21$$

Since $\tanh x = -i \tan ix$

$$\frac{-\pi}{\Delta t} < \omega < \frac{\pi}{\Delta t}$$

where

ω_d = Deformed angular frequency used to calculate s_d and the bilinear z-transform.

ω = Angular frequency in the original transfer function.

A correction must be made by equation 2.21 before the poles and zeros of a filter are determined.

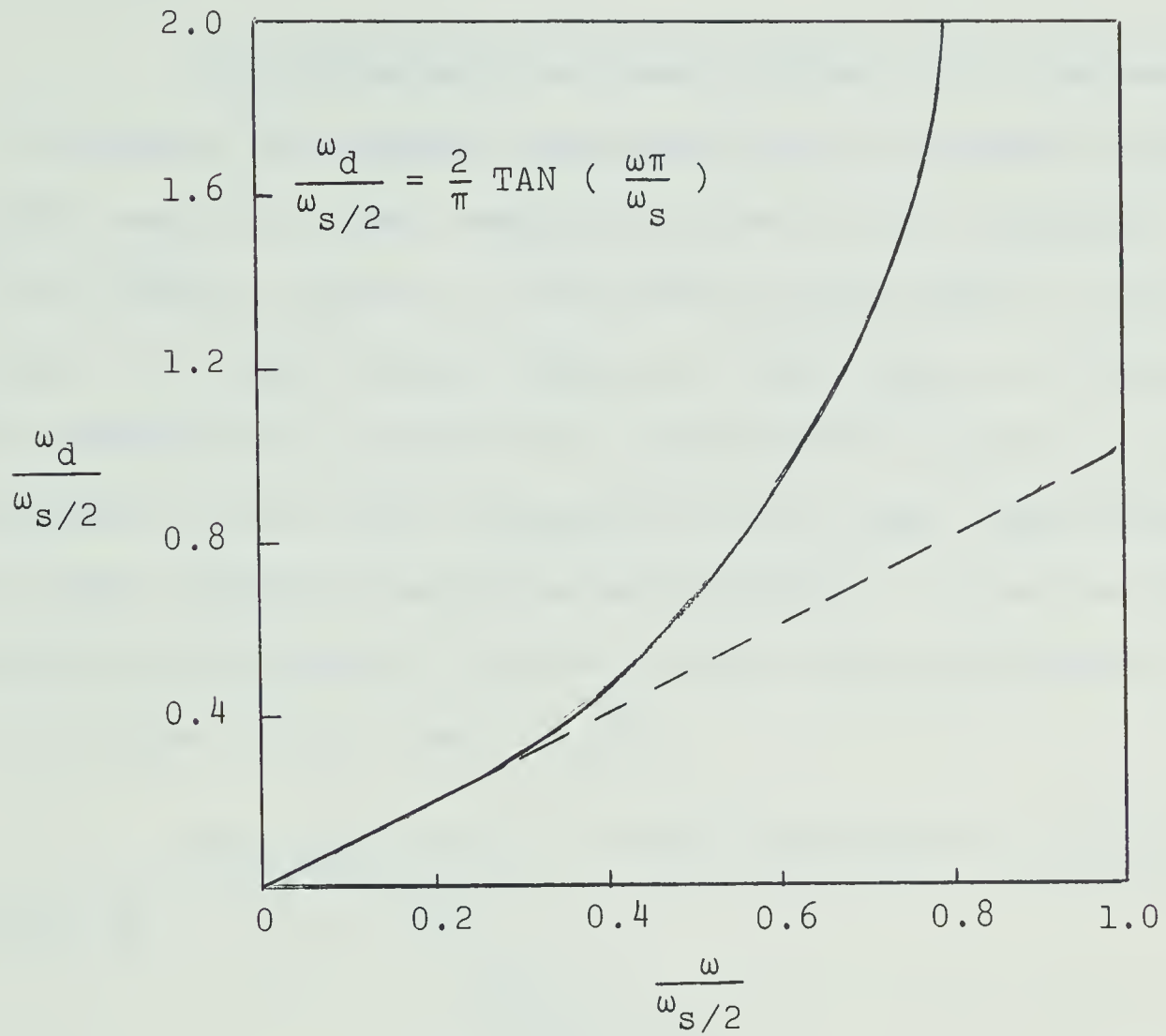


Figure 2.4. Non-linear warping of frequency scale in the bilinear z-transformation.

This transformation maps the entire ω_d into the horizontal strip bounded by Nyquist frequencies:

$$\omega_1 = -i\omega_s/2 \quad \text{and} \quad \omega_2 = +i\omega_s/2 \quad 2.22$$

The bilinear transformation is similar to the standard z-transform at low frequencies as shown in figure 2.4.

2.4. Butterworth filters.

To approximate an ideal filter, it is necessary to truncate the impulse response before it becomes negligibly small, so that computation time is not excessive. This causes a ripple or oscillation called Gibb's effect which is a very serious defect in these types of filters. To overcome this difficulty a Butterworth function is used because it has a flat response over the pass region whereas other possible functions have ripples. It can be shown that the Butterworth function is the best approximation to an ideal filter (Baum, 1948).

The Butterworth function (Butterworth, 1930) is given by

$$|Y(\bar{\Omega})|^2 = \frac{1}{1 + \bar{\Omega}^{2n}} \quad 2.23$$

The symbol $\bar{\Omega}$ is used to represent the normalized low-pass frequency. For a cut-off frequency ω_L , the normalized frequency will be

$$\bar{\Omega} = \frac{\omega}{\omega_L} \quad 2.24$$

The equation 2.23 is maximally flat over the pass region and a larger value of n gives a greater rate of

attenuation (Figure 2.5).

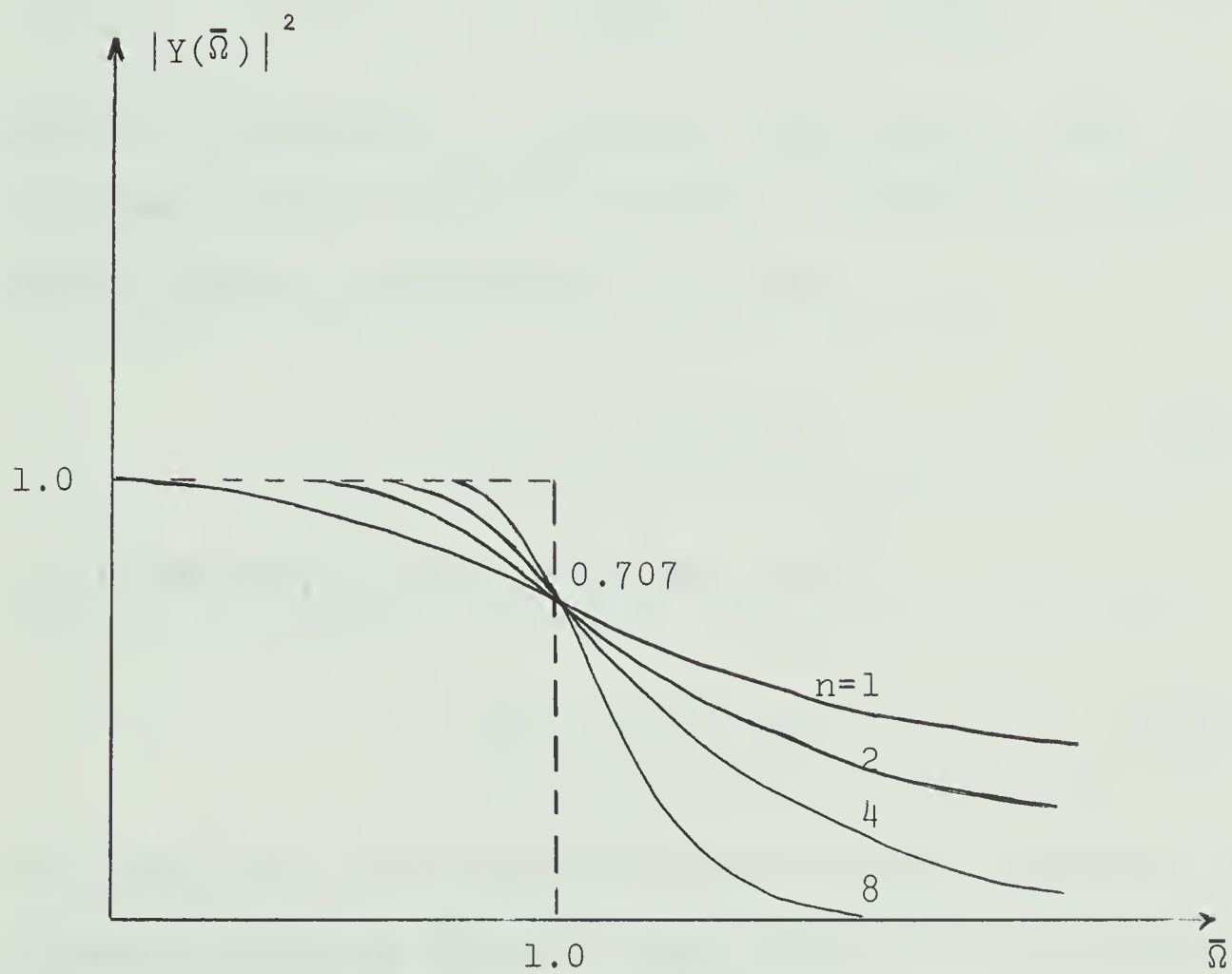


Figure 2.5. Square of the transfer function for a normalized low-pass filter using a Butterworth function.

2.4.1. Poles and zeros of a low-pass Butterworth filter.

The poles and zeros are obtained from equation 2.23 by making the frequency complex as $p = \rho + i\bar{\omega}$ with $\rho = 0$:

$$|Y_L(p)|^2 = \frac{1}{1 + (\frac{p}{i})^{2n}} = \frac{1}{1 + (-1)^n p^{2n}} \quad 2.25$$

Since the numerator is constant there are no zeros in a low-pass filter except at infinity. The poles occur at places where the denominator is zero:

$$1 + (-1)^n p^{2n} = 0 \quad 2.26$$

or if we multiply both sides by $(-1)^n$

$$p^{2n} + (-1)^n = 0 \quad 2.27$$

The poles will be arranged around the unit circle in the complex frequency domain. Only the poles on the left-hand side of the complex plane are taken to insure that we have stability and minimum phase (Weinberg, 1962).

Equation 2.23 can be written as

$$|Y_L(p)|^2 = \frac{1}{B_n(p) \cdot B_n^*(p)} \quad 2.28$$

where $B_n(p)$ is called the Butterworth polynomial. The roots of the transfer function which are on the left side of the p-plane are given by

$$p_{2v+1} = e^{i\pi/2n \cdot (2v+1+n)} \quad v=0,1,\dots,n-1 \quad 2.29$$

or by

$$p_{2v+1} = -\sin \frac{\pi}{2n}(2v+1) + i \cos \frac{\pi}{2n}(2v+1) \quad 2.30$$

The Butterworth polynomial can be written as

$$B_n(p) = \prod_{v=0}^{n-1} (p - e^{i\pi/2n \cdot (2v+1+n)}) \quad 2.31$$

This can be written (Weinberg, 1962) in the form of

$$B_n(p) = \sum_{k=0}^n a_k p^k \quad 2.32$$

where

$$a_k = \prod_{\mu=1}^k \frac{\cos(\mu-1)\gamma}{\sin \mu\gamma} \quad 2.33$$

and

$$\gamma = \frac{\pi}{2n}$$

$$a_0 = 1$$

For example the poles of a normalized fourth order low-pass filter as obtained from the equations above are:

$$p_{1,4} = -0.3826834 \pm i 0.9238795 \quad 2.34$$

$$p_{2,3} = -0.9238795 \pm i 0.3826834 \quad 2.35$$

As required by theory these occur on the unit circle in the p -plane (Figure 2.6). If the frequency is not normalized the poles will be outside the unit circle. For $n=4$ equation 2.28 can be written as

$$Y_L(p) = \frac{1}{(p-p_1)(p-p_2)(p-p_3)(p-p_4)} \quad 2.36$$

where $p_{1,2,3,4}$ are the four poles of the Butterworth function for $n=4$.

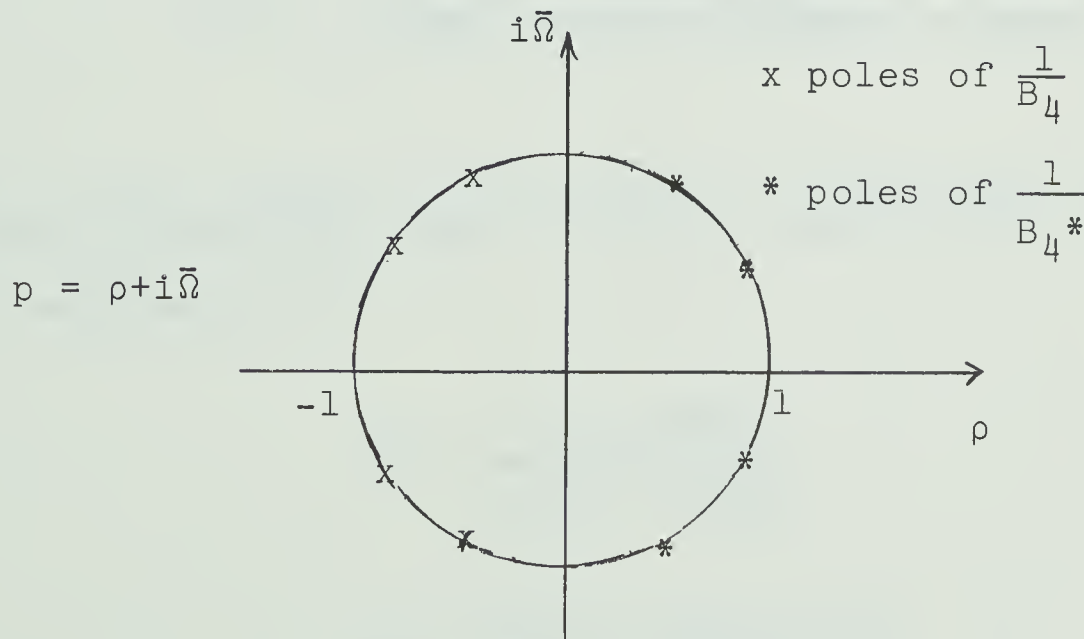


Figure 2.6. Poles of a fourth order low-pass Butterworth filter.

For a desired cut-off frequency, ω_c , the transfer function can be obtained by replacing p by

$$p_n = p \cdot \omega_c \quad 2.37$$

To obtain a recursive relation, it is convenient to express the denominator of equation 2.36 in terms of second order equations:

$$Y_L(p) = \frac{1}{(p^2 + bp + c)(p^2 + dp + e)} \quad 2.38$$

Using the bilinear z -transform, the transfer function can be written as

$$W_L(z) = \frac{(1 + z)^2}{(1 + F1 \cdot z + F2 \cdot z^2)(1 + F3 \cdot z + F4 \cdot z^2)} \quad 2.39$$

where $F1, F2, F3, F4$ are the filter coefficients, which can be calculated by

$$F1 = \frac{2 \cdot c - 8/\Delta t^2}{4/\Delta t^2 + 2b/\Delta t} \quad 2.40$$

$$F2 = \frac{4/\Delta t^2 - 2b/\Delta t + c}{4/\Delta t^2 + 2b/\Delta t + c} \quad 2.41$$

$$F3 = \frac{4 \cdot e - 8/\Delta t^2}{4/\Delta t^2 + 2d/\Delta t} \quad 2.42$$

$$F4 = \frac{4/\Delta t^2 - 2d/\Delta t + e}{4/\Delta t^2 + 2d/\Delta t + e} \quad 2.43$$

Equation 2.39 can be performed by a recursive relation in the computer. A fortran IV program has been written for IBM 360/67 to calculate filter coefficients in equations 2.40, 2.41, 2.42, 2.43 and to process any digitized data with this filter (Appendix 2). As an example, for cut-off frequency $f_c = 10$ c.p.s. the p-plane poles of a low-pass filter are

$$p_{1,2} = -59.4620 \pm i 24.6305$$

$$p_{3,4} = -24.6305 \pm i 59.4620 \quad 2.44$$

The impulse and amplitude response of this filter is shown in figure 2.7 and 2.8.

Figure 2.7. Zero phase impulse response of a Butterworth low-pass filter for $f_c=10.0$ c.p.s., $\Delta t=1/118$ sec. and $n=4$

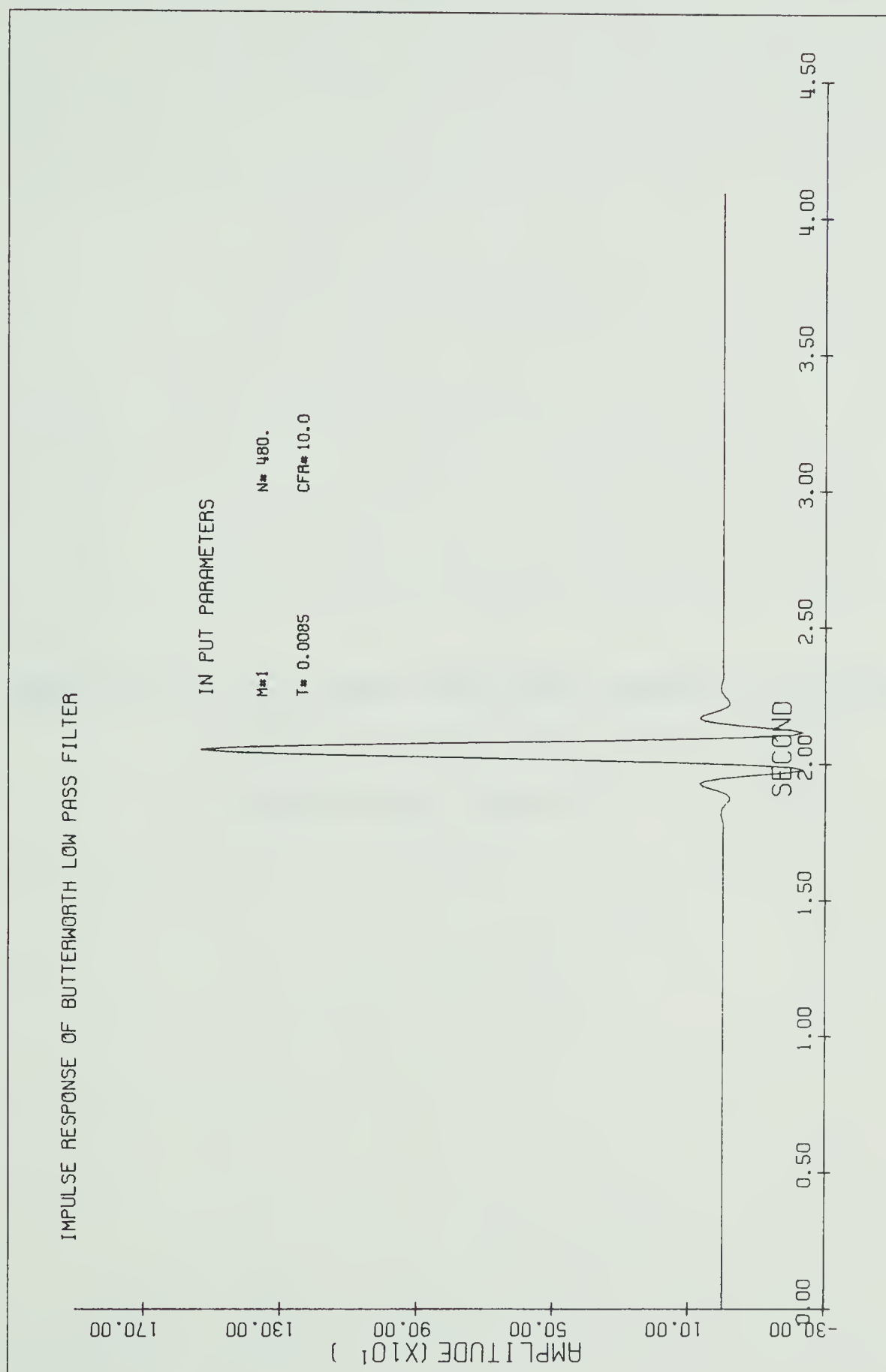
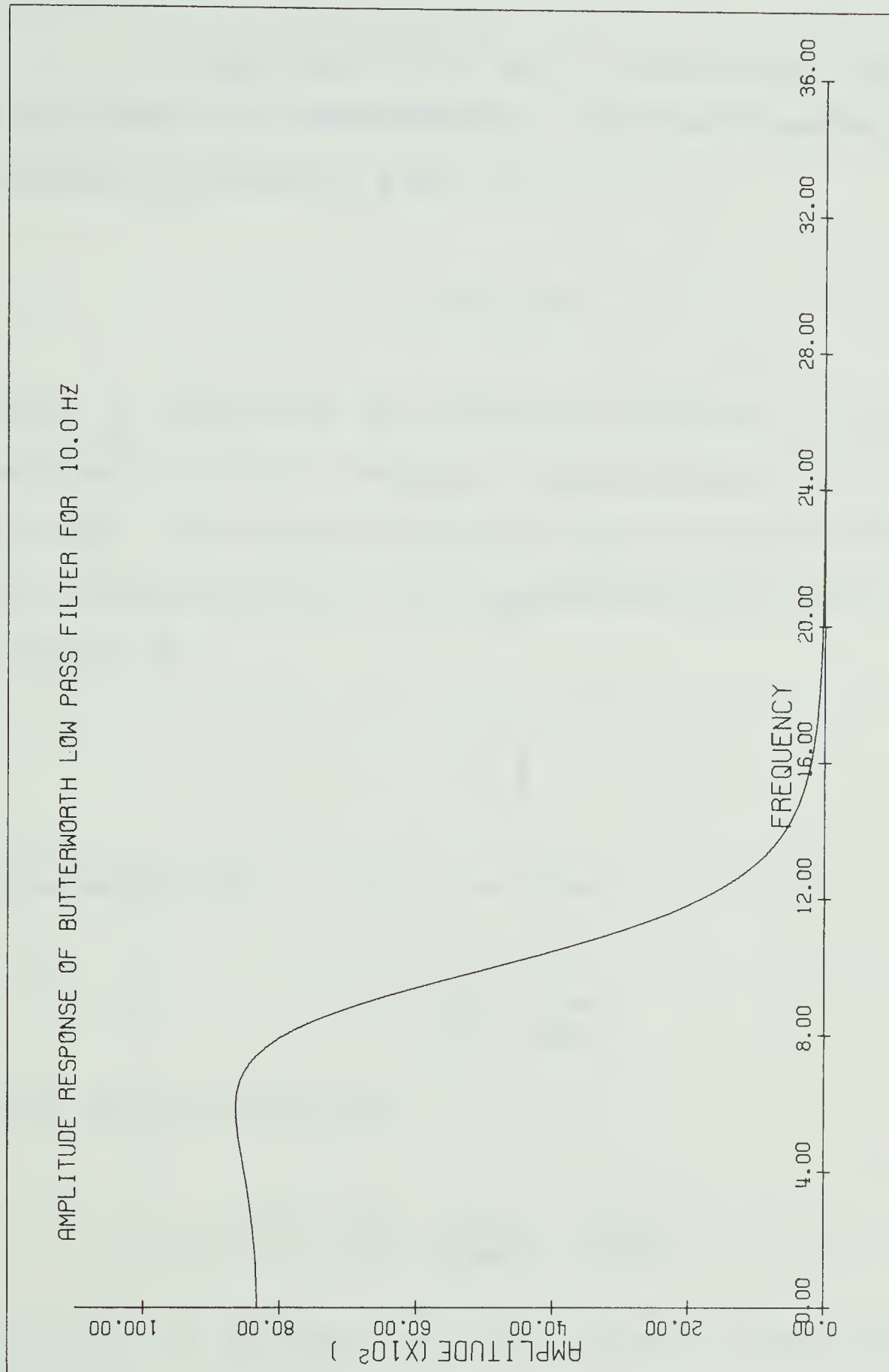


Figure 2.8. Zero phase amplitude response of Butterworth
low-pass filter for $f_c=10.0$ c.p.s.,
 $\Delta t=1/118$ sec. and $n=4$



2.4.2 Frequency transformation for high-pass filter.

A high-pass filter may be constructed from a low-pass filter by a transformation. Let the frequency in a high-pass function be given by

$$s = \partial + i\bar{\omega} \quad 2.45$$

where $\bar{\omega}$ represents the normalized frequency. It is necessary to find a frequency transformation of the type $p = \omega(s)$ which will convert one type of filter into another. For a high-pass filter the transformation is found empirically to be

$$p = \frac{1}{s} \quad 2.46$$

by substituting p and s we have

$$\rho + i\bar{\Omega} = \frac{1}{\partial + i\bar{\omega}} \quad 2.47$$

or it can be written as

$$\rho + i\bar{\Omega} = \frac{\partial}{\partial^2 + \bar{\omega}^2} + \frac{i\bar{\omega}}{\partial^2 + \bar{\omega}^2} \quad 2.48$$

If we let ∂ approach zero the frequency transformation becomes

$$\bar{\Omega} = -\frac{1}{\bar{\omega}} \quad 2.49$$

To find the n^{th} order high-pass Butterworth filter equation 2.49 is substituted in equation 2.23:

$$|Y_H(\bar{\omega})|^2 = \frac{1}{1 + \left(\frac{-1}{\bar{\omega}}\right)^{2n}} = \frac{1}{1 + \frac{1}{\bar{\omega}^{2n}}} \quad 2.50$$

or

$$|Y_H(\bar{\omega})|^2 = \frac{\bar{\omega}^{2n}}{1 + \bar{\omega}^{2n}} \quad 2.51$$

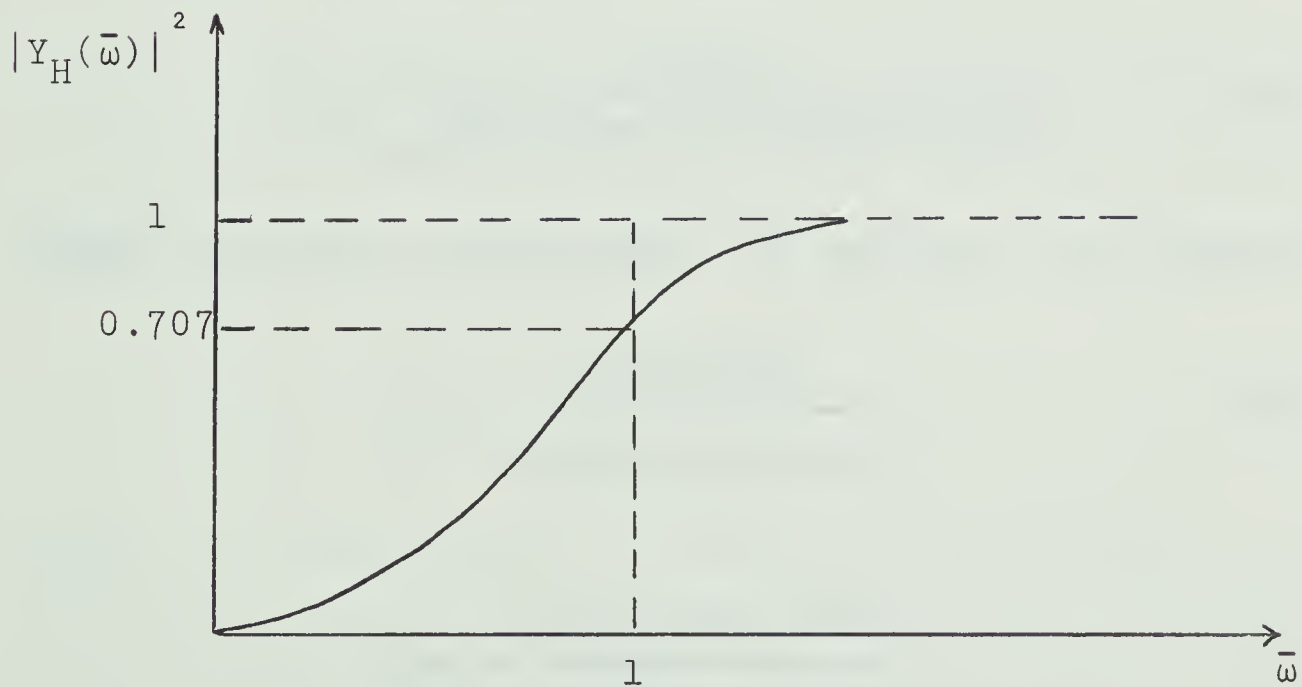


Figure 2.9. Square of the transfer function for an n^{th} order Butterworth high-pass filter.

To find the transfer function for a high-pass filter with cut-off frequency ω_c , the poles of a low-pass filter are converted to a high-pass poles using equation 2.46:

$$p = \frac{\omega_c}{s} \quad 2.52$$

Equation 2.36 is used to find the transfer function:

$$F(s) = \frac{s^2}{(s^2+bs+c)(s^2+ds+e)} \quad 2.53$$

Using the bilinear z-transform, one can obtain the impulse response in the z-plane:

$$W_H = \frac{(1-z)^4}{(1+F1.z+F2.z^2)(1+F3.z+F4.z^2)} \quad 2.54$$

where the filter coefficients $F1, F2, F3, F4$ are given by

$$F1 = \frac{\Delta t^2 \cdot c / 2 - 2}{\Delta t / 2 \cdot b + \Delta t^2 / 4 \cdot c + 1} \quad 2.55$$

$$F2 = \frac{1 - b \cdot \Delta t / 2 + c \cdot \Delta t^2 / 4}{b \cdot \Delta t / 2 + c \cdot \Delta t^2 / 4 + 1} \quad 2.56$$

$$F3 = \frac{e \cdot \Delta t^2 / 2 - 2}{d \cdot \Delta t / 2 + e \cdot \Delta t^2 / 4 + 1} \quad 2.57$$

$$F4 = \frac{1 - d \cdot \Delta t / 2 + e \cdot \Delta t^2 / 4}{d \cdot \Delta t / 2 + e \cdot \Delta t^2 / 4 + 1} \quad 2.58$$

where Δt is the digitizing interval.

A fortran IV program has been written for IBM 360/67 to process any digitized data with the high-pass filter (Appendix 2). As an example, the impulse and amplitude response of a high-pass filter has been shown in figure 2.10 and 2.11.

2.4.3 Frequency transformation for a band-pass filter.

The normalized band-pass transformation can be expressed in terms of a low-pass and high-pass transformation:

$$p = s + \frac{1}{s} \quad 2.59$$

where p is the complex frequency in the low-pass function and s is the complex frequency in the band-pass function. Substituting complex s and p values:

$$p = \sigma + i\bar{\omega} + \frac{\sigma}{\sigma^2 + \bar{\omega}^2} - \frac{i\bar{\omega}}{\sigma^2 + \bar{\omega}^2} \quad 2.60$$

Figure 2.10. Zero phase impulse response of a Butterworth high-pass filter for $f_c=10.0$ c.p.s., $\Delta t=1/118$ sec. and $n=4$

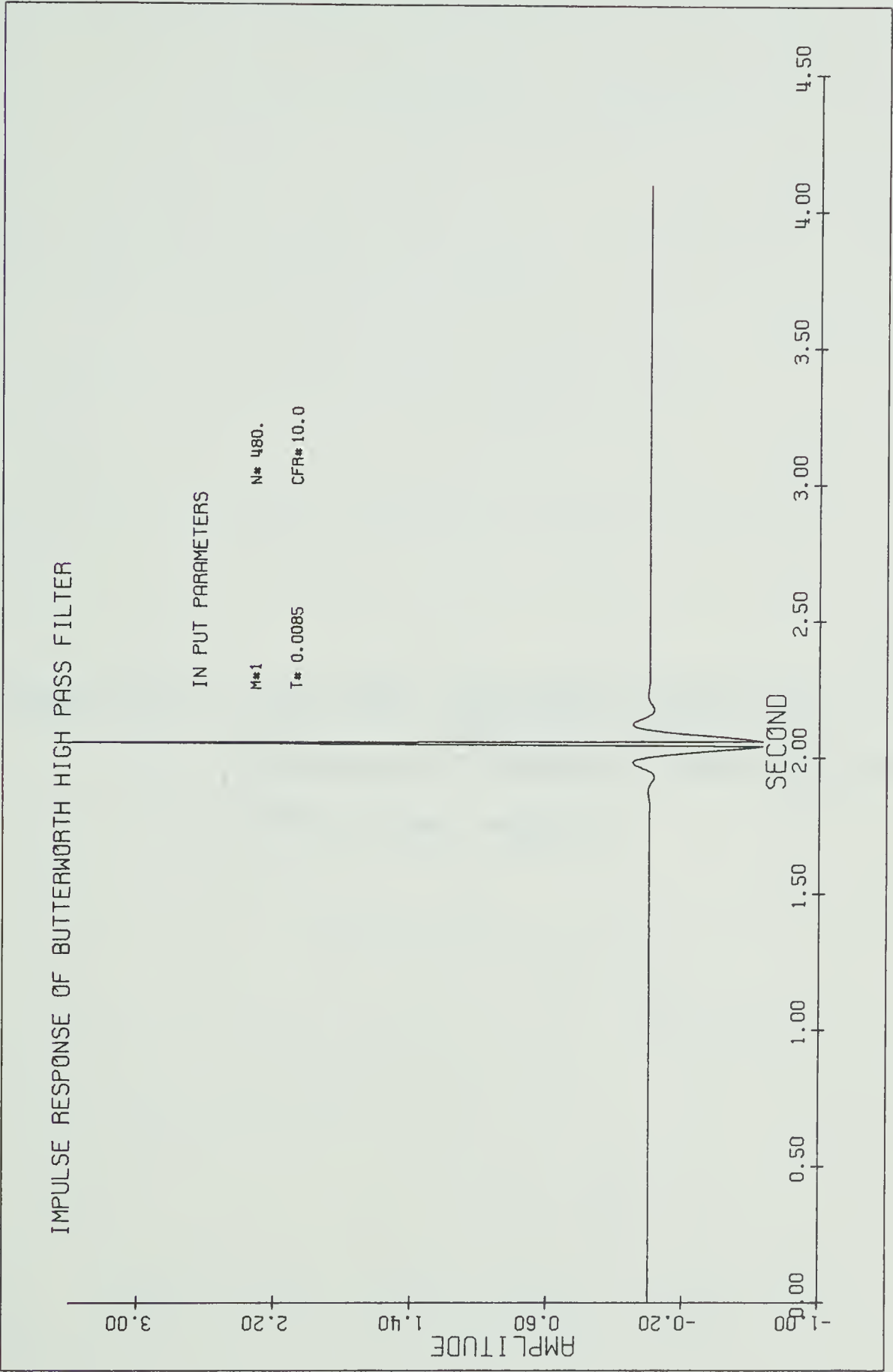
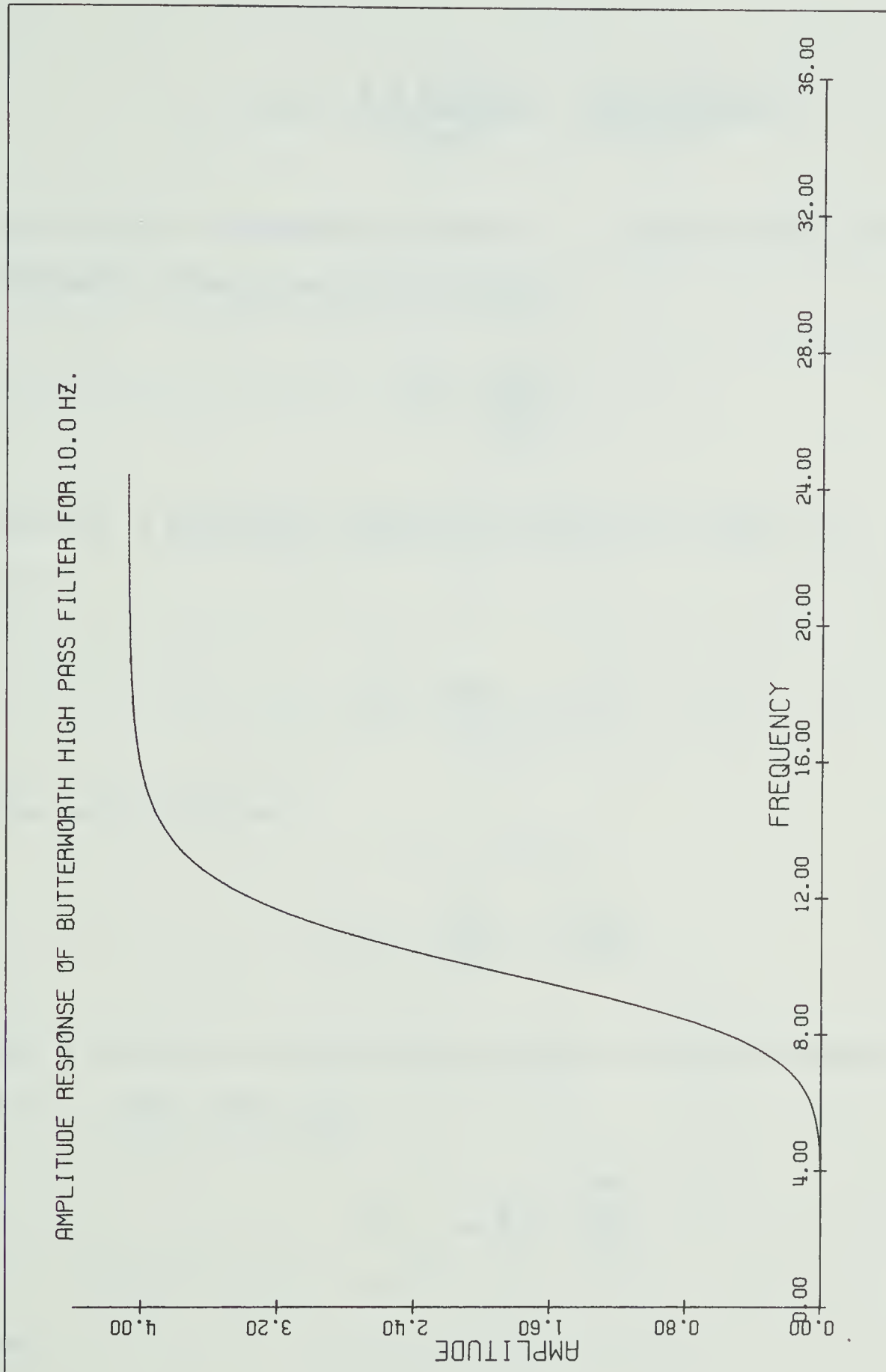


Figure 2.11. Zero phase amplitude response of a
Butterworth high-pass filter for $f_c=10.0$ c.p.s.,
 $\Delta t=1.118$ sec. and $n=4$



or

$$\rho + i\bar{\Omega} = \frac{\partial (\partial^2 + \bar{\omega}^2 + 1)}{\partial^2 + \bar{\omega}^2} + \frac{i\bar{\omega}(\partial^2 + \bar{\omega}^2 - 1)}{\partial^2 + \bar{\omega}^2} \quad 2.61$$

Letting the attenuation factor ∂ approach zero the frequency transformation becomes

$$\bar{\Omega} = \frac{\bar{\omega}^2 - 1}{\bar{\omega}} \quad 2.62$$

This is a quadratic equation having two roots, ω_1 and ω_2 :

$$\bar{\omega}^2 - \bar{\Omega}\bar{\omega} - 1 = 0 \quad 2.63$$

The two roots are

$$\bar{\omega}_{1,2} = \frac{\bar{\Omega}}{2} \pm \sqrt{\frac{\bar{\Omega}^2}{4} + 1} \quad 2.64$$

For a unit cut-off frequency in the low-pass domain i.e., $\bar{\Omega} = 1$, the roots are

$$\bar{\omega}_{1,2} = \frac{1}{2} \pm \sqrt{\frac{5}{4}} \quad 2.65$$

or

$$\bar{\omega}_1 = -0.618$$

$$2.66$$

$$\bar{\omega}_2 = 1.618$$

Setting $\bar{\Omega} = -1$ we obtain the conjugate pair of frequencies. These four roots specify the band width of the normalized band pass filter (Figure 2.12).

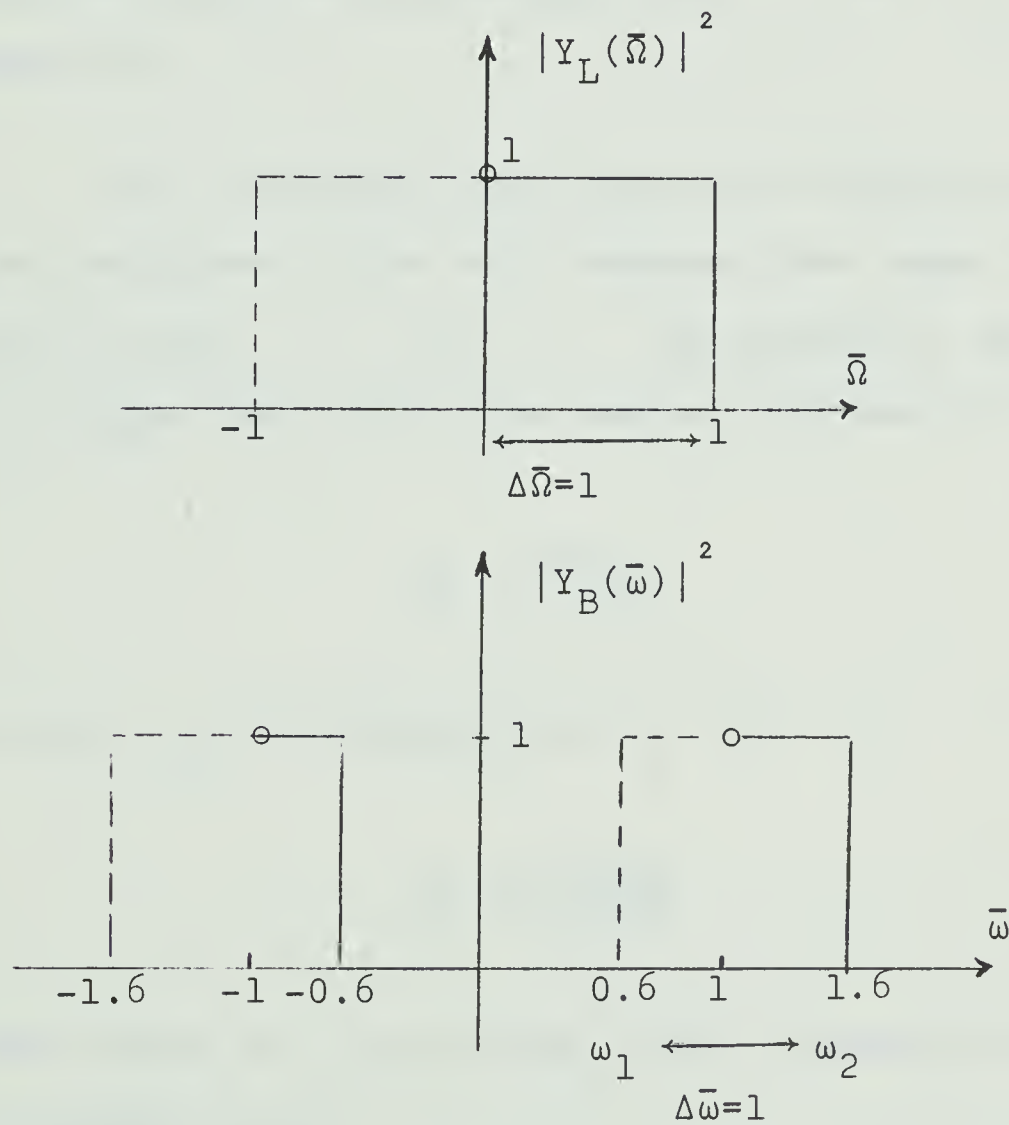


Figure 2.12. Transformation from a low-pass to a band-pass filter.

Any two arbitrary frequencies in the band-pass domain may be obtained by the appropriate transformation from a low-pass filter. For the normalized band-pass we have the relation

$$\bar{\omega}_1 \bar{\omega}_2 = 1 \quad 2.67$$

This can be verified by substituting ω_1 and ω_2 from equation 2.64.

The normalized relation can be generalized to the desired band-pass filter with unnormalized upper and lower frequency limits ω_1 and ω_2 . The geometric mean, ω_0 , which is sometimes called the center frequency is

$$\omega_0 = \sqrt{\omega_1 \omega_2} \quad 2.68$$

or for any cut-off frequencies ω_h and ω_ℓ

$$\omega_0 = \sqrt{\omega_h \omega_\ell} \quad 2.69$$

The band width $\Delta\omega$ is related to the low-pass cut-off as seen in figure 2.12.

$$\Delta\omega = \Omega_1 = \omega_2 - \omega_1 \quad 2.70$$

or

$$\Delta\omega = \Omega_h = \omega_h - \omega_\ell \quad 2.71$$

The band width will be rescaled by dividing by the geometric mean:

$$\Omega_h = \frac{\omega_h - \omega_\ell}{\omega_0} \quad 2.72$$

From equation 2.69 and 2.72 it is possible to eliminate ω_ℓ :

$$\Omega_h = \frac{\omega_h}{\omega_0} - \frac{\omega_0}{\omega_h} \quad 2.73$$

From equation 2.59, the unnormalized frequency transformation will be

$$p = \frac{s}{\omega_0} + \frac{\omega_0}{s} \quad 2.74$$

or for $\partial = 0$

$$\Omega_h = \frac{s^2 + \omega_0^2}{s\omega_0} \quad 2.75$$

In the frequency domain the band-stop filter may be obtained by taking reciprocal of the transformation for the band-pass filter:

$$p = \frac{s\omega_0}{s^2 + \omega_0^2} \quad 2.76$$

From equation 2.73 and equation 2.75

$$p = \Omega = \frac{\omega_h - \omega_l}{\omega_0} = \frac{s^2 + \omega_0^2}{s\omega_0} \quad 2.77$$

or

$$s^2 + \omega_c s + \omega_0^2 = 0 \quad 2.78$$

where

$$\omega_c = \omega_h - \omega_l$$

The roots of equation 2.78 will be poles of the band-pass filter obtained from the poles of the low-pass filter:

$$\frac{s}{s} * \left\{ = \frac{\omega_c}{2} + \sqrt{\left(\frac{\omega_c}{2}\right)^2 - \omega_1 \omega_2} \right. \quad 2.79$$

From each of the n poles of a low-pass filter there will be generated $2n$ poles, in complex conjugate pairs, in the s -plane.

The transfer function for a normalized band-pass filter can be obtained using equation 2.59 in equation 2.36:

$$Y_{NB}(s) = \frac{1}{\underbrace{(s^2 + 1 - p_1 s)}_s \underbrace{(s^2 + 1 - p_2 s)}_s \underbrace{(s^2 + 1 - p_3 s)}_s \underbrace{(s^2 + 1 - p_4 s)}_s}$$

or

$$Y_{NB}(s) = \frac{s^4}{s^8 + g_7 s^7 + g_6 s^6 + g_5 s^5 + g_4 s^4 + g_3 s^3 + g_2 s^2 + g_1 s + g_0} \quad 2.81$$

From equation 2.79 the transfer function for a unnormalized band-pass filter can be found as

$$Y_B(s) = \frac{s}{(s^2 + b_1 s + c_1)} \cdot \frac{s}{(s^2 + b_2 s + c_2)} \cdot \frac{s}{(s^2 + b_3 s + c_3)} \cdot \frac{s}{(s^2 + b_4 s + c_4)} \quad 2.82$$

The coefficients b_j and c_j are obtained from the pole positions which occur in complex conjugate pairs to make each of the terms in the bracket of equation 2.82:

$$(s - s_j)(s - s_j^*) = (s^2 + b_j s + c_j) \quad 2.83$$

The s -plane representation of equation 2.82 must be converted to the digital or z -plane representation by a bilinear z -transform:

$$\frac{s_d}{s_d^2 + b_j s_d + c_j} = \frac{\frac{2\Delta t}{(\Delta t)^2} \cdot \frac{1-z}{(1+z)^2} \cdot (1+z)}{\frac{4}{(\Delta t)^2} \cdot \frac{(1-z)^2}{(1+z)^2} + \frac{2b_j \cdot \Delta t}{(\Delta t)^2} \cdot \frac{(1-z)}{(1+z)^2} \cdot (1+z) + c_j \frac{(1+z)^2 (\Delta t)^2}{(1+z)^2 (\Delta t)^2}}$$

$$= \frac{\frac{1}{a_j} (1-z^2)}{1 + \frac{z}{a_j} (c_j \Delta t - \frac{4}{\Delta t}) + \frac{z^2}{a_j} (\frac{2}{\Delta t} - b_j + c_j \frac{\Delta t}{z})} \quad 2.84$$

where

$$a_j = \frac{2}{\Delta t} + b_j + \frac{c_j \Delta t}{2} \quad 2.85$$

Equation 2.84 can be written as

$$\frac{s_d}{s^2_d + b_j s + c_j} = \frac{\frac{1}{a_j} (1-z^2)}{B_j} \quad 2.86$$

where

$$B_j = 1 - F1_j \cdot z + F2_j \cdot z^2 \quad 2.87$$

$F1_j$ and $F2_j$ are the coefficients of z and z^2 in the equation 2.84. Omitting the static gain factor

$\frac{1}{a_1 \cdot a_2 \cdot a_3 \cdot a_4}$, the z -transform of a Butterworth band-pass filter with 8 poles is given by

$$W(z) = \frac{(1-z^2)^4}{B_1(z) B_2(z) \cdot B_3(z) \cdot B_4(z)} \quad 2.88$$

In the following example a band-pass filter with 8 poles, cut-off frequencies 1 and 10 c.p.s. and a digitizing interval of 1/118 sec. will be calculated. First the cut-off frequencies are corrected using equation 2.21 and from equation 2.79 the roots are calculated. (Figure 2.13):

σ	$j\omega$	$f(\text{c.p.s.})$
-47.0526	$\pm j25.8533$	4.03
-20.1726	$\pm j29.7337$	9.51
- 6.6029	$\pm j 3.6280$	0.58
- 2.0527	$\pm j 6.0782$	0.97

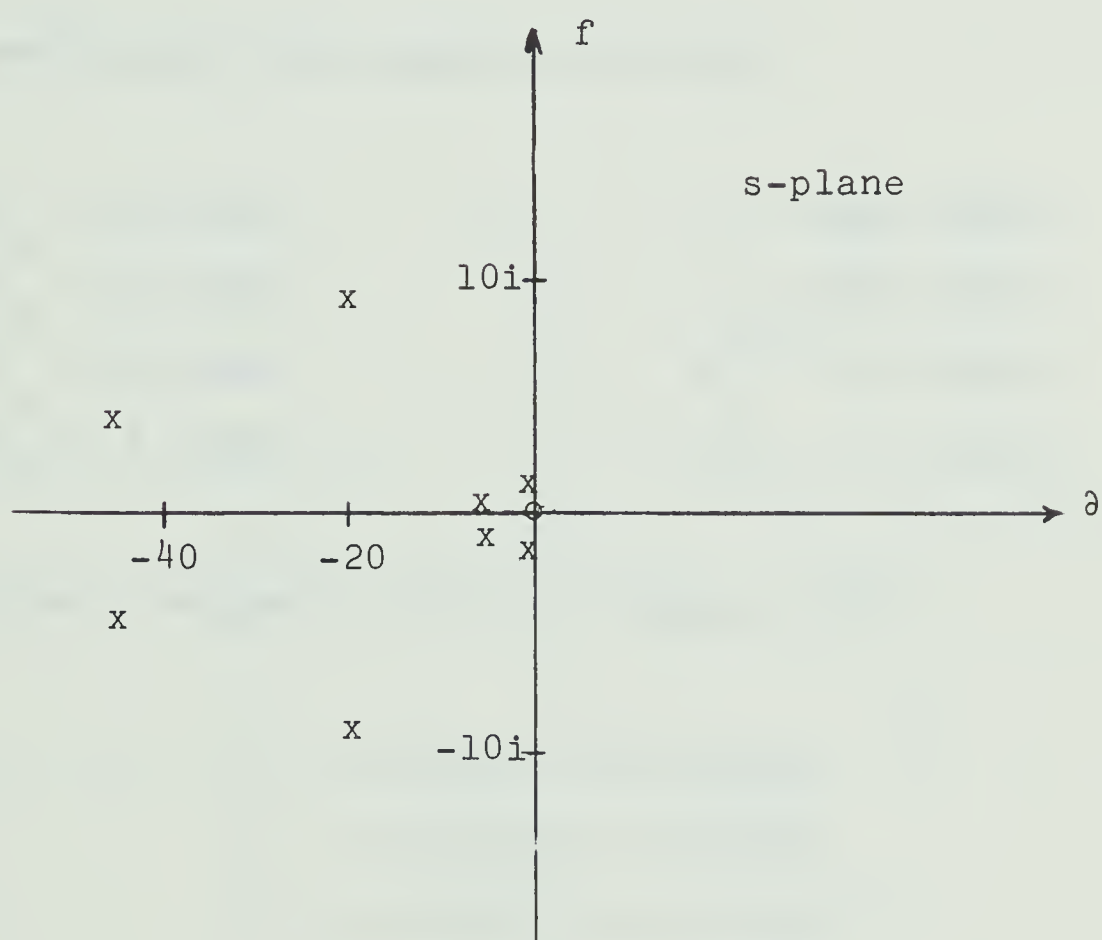


Figure 2.13. Poles and zeros of a Butterworth band-pass filter with cut-off frequencies at 1 and 10 cycle per second.

The coefficients of the polynomials in equation 2.81 are

$$\begin{aligned}
 g_0 &= 2.67661 \times 10^{10} & g_4 &= 2.16737 \times 10^7 \\
 g_1 &= 1.00427 \times 10^{10} & g_5 &= 6.96027 \times 10^5 \\
 g_2 &= 2.14872 \times 10^9 & g_6 &= 1.31337 \times 10^4 \\
 g_3 &= 2.81529 \times 10^8 & g_7 &= 1.51762 \times 10^2
 \end{aligned}$$

The coefficients for equation 2.82 are

$$\begin{aligned}
 b_1 &= 94.10519 & c_1 &= 2882.33984 \\
 b_2 &= 40.34528 & c_2 &= 3975.04687 \\
 b_3 &= 13.20584 & c_3 &= 56.76093 \\
 b_4 &= 4.10533 & c_4 &= 41.15739
 \end{aligned}$$

The poles of equation 2.88 are (Figure 2.14)

$$\begin{aligned}
 z_1 &= 1.452137 \pm i0.335533 \\
 z_2 &= 1.031333 \pm i0.562206 \\
 z_3 &= 1.057052 \pm i0.032561 \\
 z_4 &= 1.016185 \pm i0.052410
 \end{aligned}$$

The terms in the denominator of equation 2.88 are

$$\begin{aligned}
 B_1 &= 1 - 1.307476 z + 0.450190 z^2 \\
 B_2 &= 1 - 1.494986 z + 0.724783 z^2
 \end{aligned}$$

$$B_3 = 1 - 1.890261 z + 0.894119 z^2$$

$$B_4 = 1 - 1.962924 z + 0.965829 z^2$$

The impulse, amplitude and phase response of this filter are shown in figure 2.15, 2.16 and 2.17.

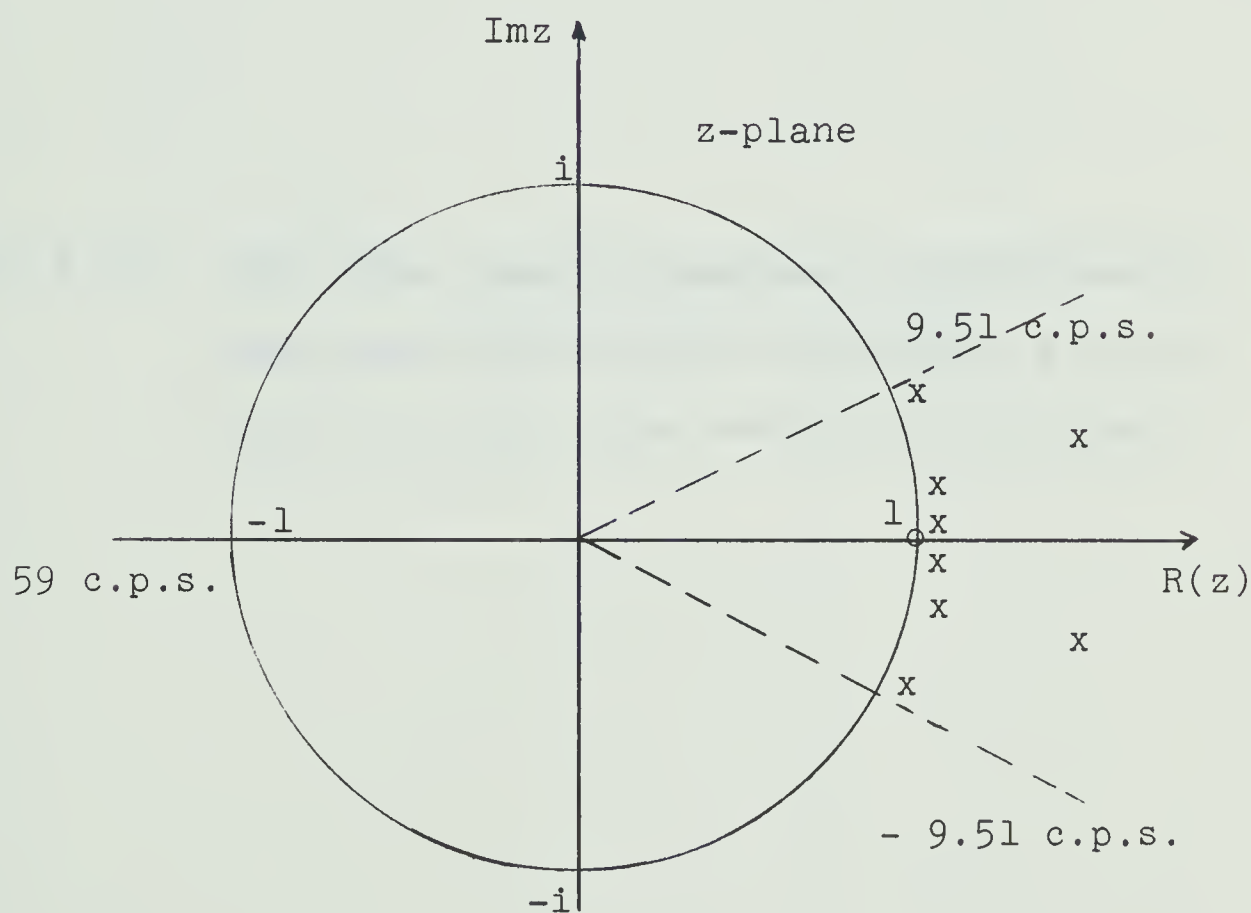


Figure 2.14. Location of poles and zeros of equation 2.88.

Figure 2.15. Zero phase impulse response of Butterworth band-pass filter with a cut-off at 1 c.p.s. and 10.0 c.p.s., for $n=4$ and $\Delta t=1/118$ sec.

IMPULSE RESPONSE OF BUTTERWORTH BAND PASS FILTER

IN PUT PARAMETERS

M# 1 LCF# 1.0
T# 0.0085 HCF# 10.0
N# 480.0

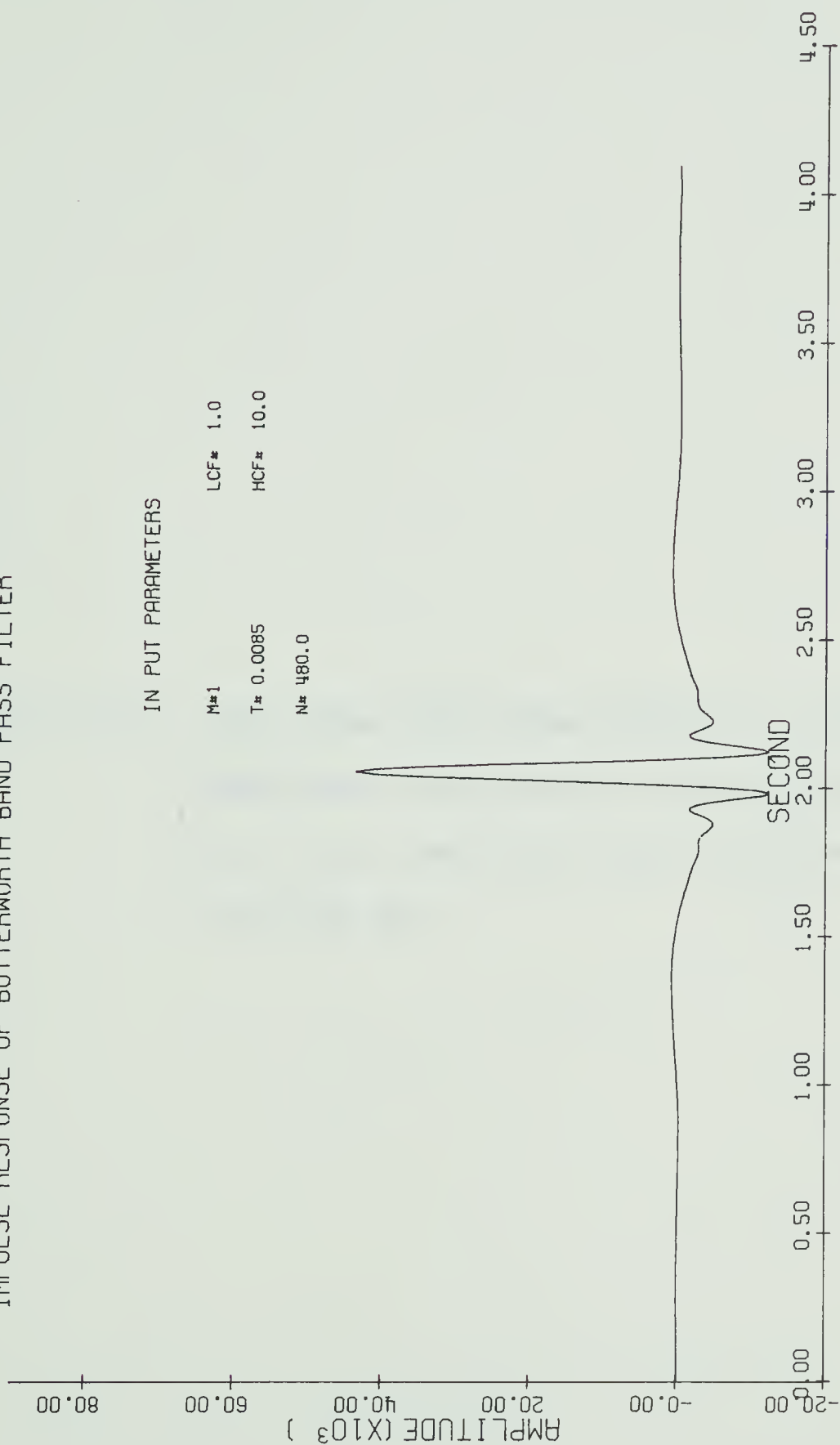


Figure 2.16. Zero phase amplitude response of Butterworth band-pass filter with a cut-off frequencies at 1 c.p.s. and 10.0 c.p.s. for $n=4$ and $\Delta t=1/118$ sec.

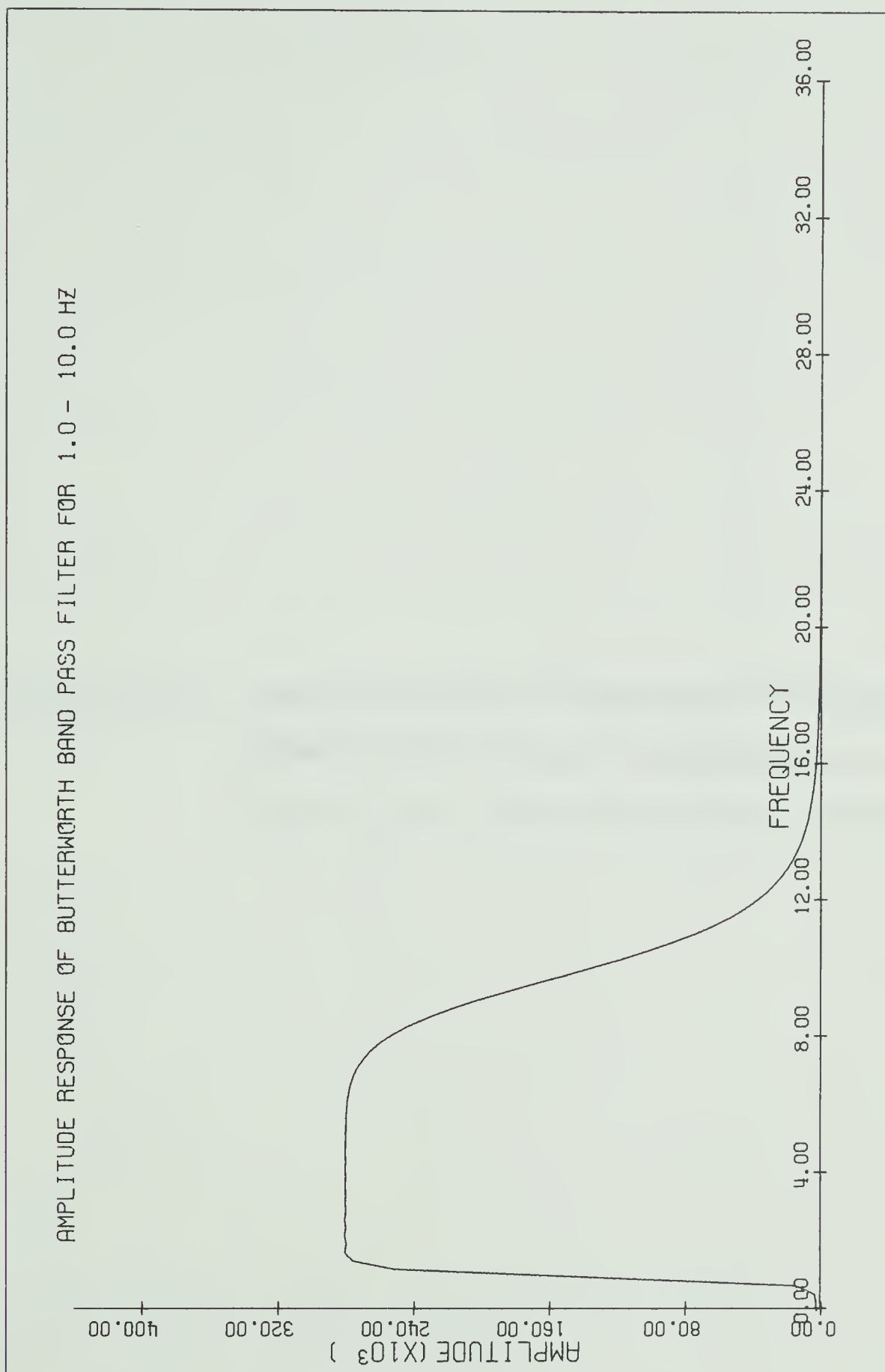
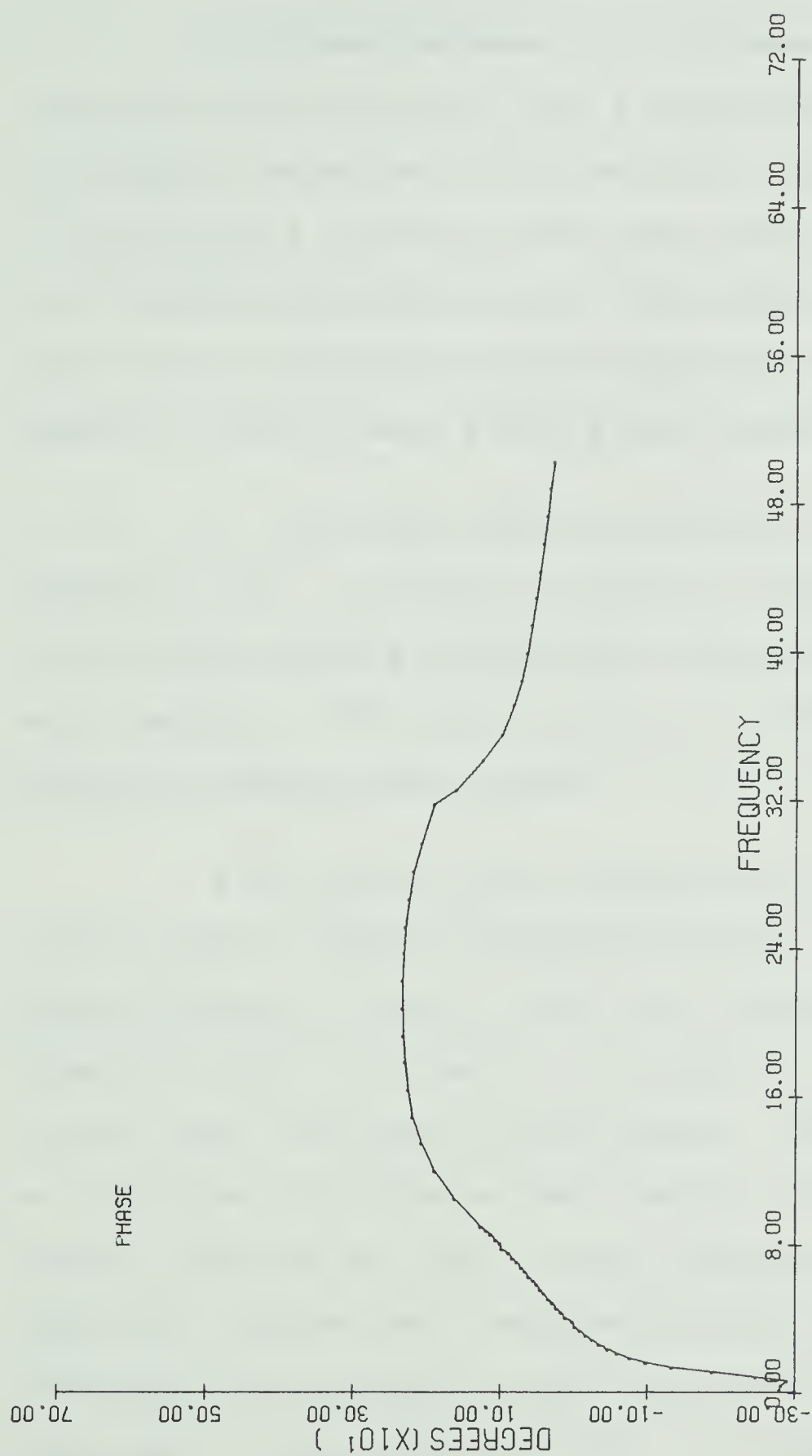


Figure 2.17. Phase response of Butterworth band-pass filter with a cut-off frequencies at 1 c.p.s. and 10 c.p.s. for $n=4$ and $\Delta t=1/118$ sec.



2.5 Zero phase filters.

The phase response of a Butterworth filter as calculated above does not have a linear phase spectrum. According to equation 2.10 it would be desirable to have a filter with a linear or zero phase shift so that different frequency components do not have differential lags. There are two methods which are applicable to a finite length of data to have a zero phase response:

1. The input data is convolved with an impulse response $F(z)$ to produce an initial output. This output is then reversed in time and convolved again with the same operator. The second output is reversed in time to obtain the final output signal.

A zero phase shift Butterworth filter was calculated and its impulse response obtained for a four second interval of time. Since the impulse response is symmetric about the time of occurrence of the impulse, we can say that the filter is zero-phase. The phase spectrum as calculated by taking a fast Fourier transform of the impulse response was zero to five significant figures. The amplitude response had a sharper cut-off because two convolutions were involved so that the amplitude spectrum is the square of the spectrum, $F(z)$, of a single Butterworth filter. That is, if we let $o(t)$ be the output from a

convolution of the input data $i(t)$, and the impulse response, $f(t)$, then the first output is:

$$o_1(t) = i(t) * f(t)$$

The reversed output is:

$$o_2(t) = o_1(-t) = i(-t) * f(-t)$$

Then data is filtered once more to give:

$$o_3(t) = \{ i(-t) * f(-t) \} * f(t)$$

The final output involves a time reversal which yields:

$$o_4(t) = \{ i(t) * f(t) \} * f(-t)$$

Taking the Fourier transform of the last output

$$O_4(f) = \{ I(f) \cdot F(f) \} \cdot F^*(f)$$

$$= I(f) \cdot \{ F(f) \cdot F^*(f) \}$$

$$= I(f) \cdot |F(f)|^2 \quad 2.89$$

where $F^*(f)$ is the complex conjugate of the transfer function. For filters in which the shape of the filter in the pass-band is important, it is necessary to design $F(z)$ to have an amplitude spectrum that is the square root of the desired spectrum.

To process field records with a zero phase filter a sufficient number of zeros must be added at the end of the data to obtain a reasonably small amplitude before the reversed data is filtered again. Generally, between 100 and 300 zeros were found to be sufficient so that the impulse response became negligible. The addition of too many zeros may give underflow problems. Therefore both the impulse response and the transfer function should be studied before a particular filter is used on any problem.

2. Shanks (1967) has advocated the use of a second method of obtaining a zero phase shift filter. First a stable positive-time and a stable negative-time filter are calculated. The negative-time filter is obtained by replacing z with $1/z$ in the theory developed previously. The zero phase output of this filter can be computed by filtering the input with the forward filter and adding to this result the input filtered backwards with the negative-time filter. Time reversal of the data is obtained by replacing z in $F(z)$ with $1/z$. Since z^{-1} represents

a time advance, using equation 2.17, a forward recursion relation can be expressed as

$$y_n = \sum_{i=0}^N a_i x_{n+i} - \sum_{j=1}^M b_j y_{n+j} \quad 2.90$$

$$n=k, k-1, k-2, \dots$$

The zero phase impulse response was calculated for a band-pass Butterworth operator, it has a symmetric impulse response about the time of the input impulse but the function is entirely different from the one calculated by method 1. The amplitude and phase spectra may be calculated using the fast-Fourier transform. It was found that it had a zero phase spectrum but the amplitude spectrum is distorted in an undesirable manner.

Steps followed in this technique can be formulated as follows:

The output from the negative recursion filter

$$o_1(t) = i(t) * f(t)$$

The output from the forward or negative time recursion filter is

$$o_2(t) = i(t) * f(-t)$$

The final output is a sum of above two equations

$$o_3(t) = o_1(t) + o_2(t) = i(t) * \{ f(t) + f(-t) \}$$

Taking a Fourier transform of last output we have

$$O_3(f) = I(f) \cdot \{ F(f) + F^*(f) \} \quad 2.71$$

If we let the real and imaginary part of $F(f)$ be $F_R(f)$ and $F_I(f)$, then

$$O_3(f) = I(f) \{ 2 F_R \}$$

whereas the required filter should have an amplitude response resembling

$$|F(f)| = \sqrt{F_R^2 + F_I^2}$$

Because the distortion due to the loss of F_I^2 is unpredictable for the Butterworth formulation this second method is not recommended.

2.6 Conclusion.

The Butterworth recursion filter is a best approximation to an ideal filter and in computation the recursive form is quite efficient and fast. The program listed in Appendix 3 is able to filter a 6 x 6300 pt. array in less than 2.27 minutes, but this time includes calculation of the filter coefficients. One can reduce this time considerably by calculating filter coefficients by a separate program. It was noticed that the calculation speed was increased by the number of records in the IBM 360/67 system. For example 3 records, each approximately 51 seconds long, took about 5 minutes to filter with the same program. The transfer function and impulse response for one filter which has proven to be very useful is shown in figures 2.18 and 2.19. Examples of unfiltered records are shown in figure 2.20 while the same data after digital filtering is shown in figure 2.21 and 2.22. It is obvious that the first and later arrivals on the records are interpreted much more easily.

Figure 2.18. Impulse response of zero phase shift
Butterworth filter for cut-off frequencies
at 1 c.p.s. and 5 c.p.s. The sampling
interval is $1/118$ sec.

IMPULSE RESPONSE OF BUTTERWORTH BAND PASS FILTER

IN PUT PARAMETERS

M#1 LCF# 1.0
T# 0.0085 HCF# 5.0
N# 480.0

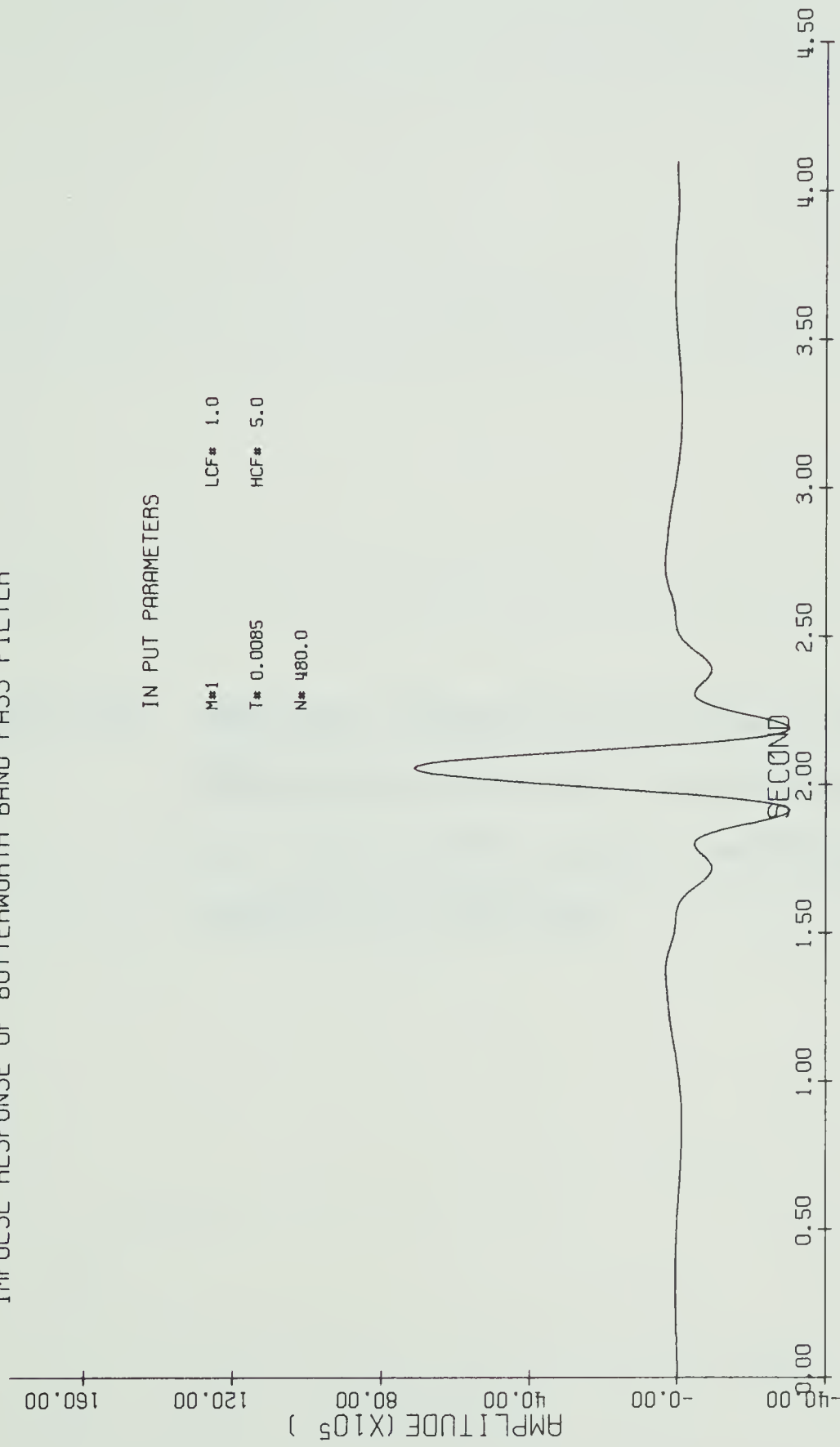


Figure 2.19. Amplitude response of zero phase shift
Butterworth filter for cut-off frequencies
at 1 c.p.s. and 5 c.p.s. The sampling
interval is $1/118$ sec.

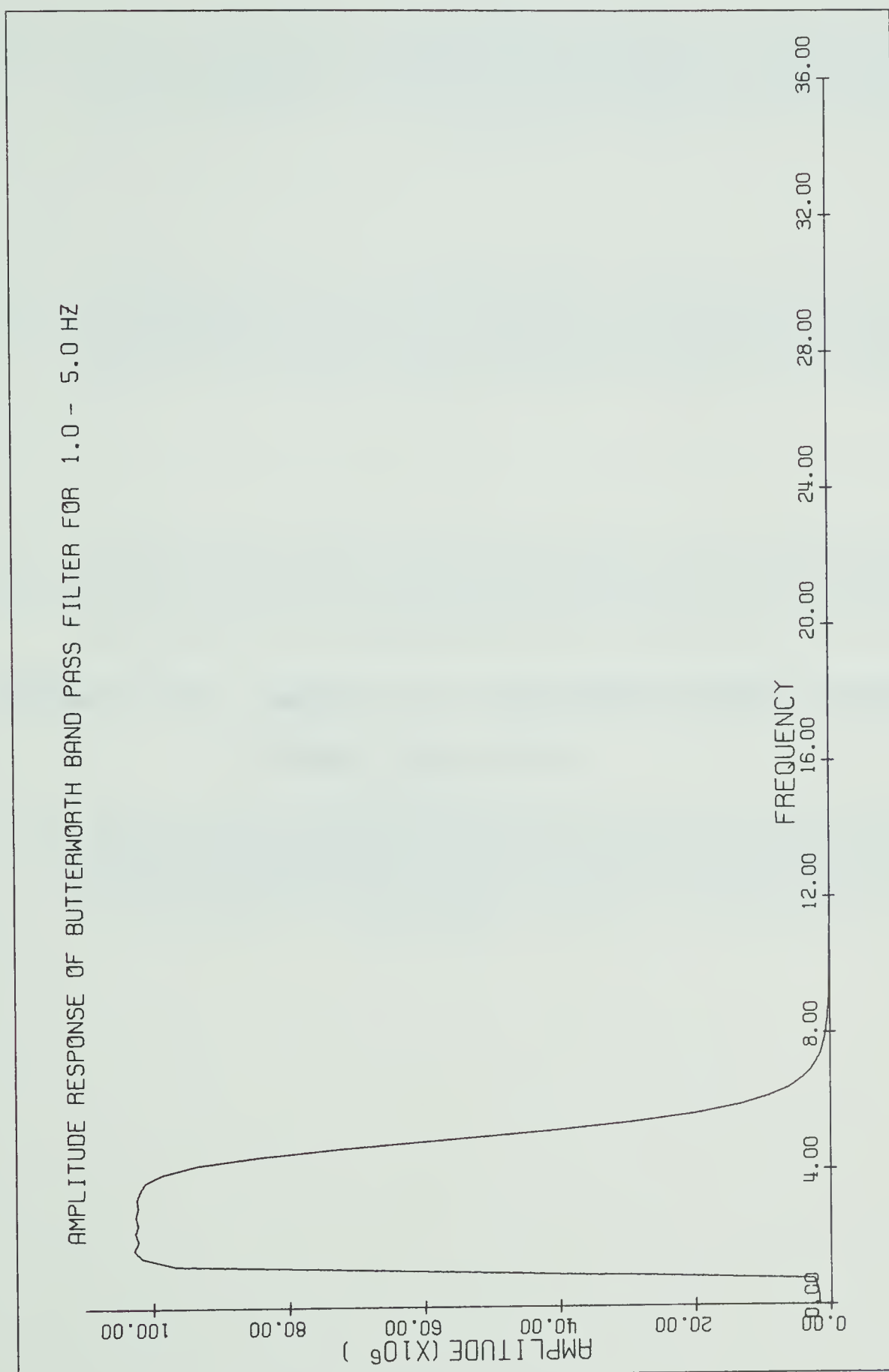


Figure 2.20. Example of 4 unfiltered seismic records from
Project Early Rise

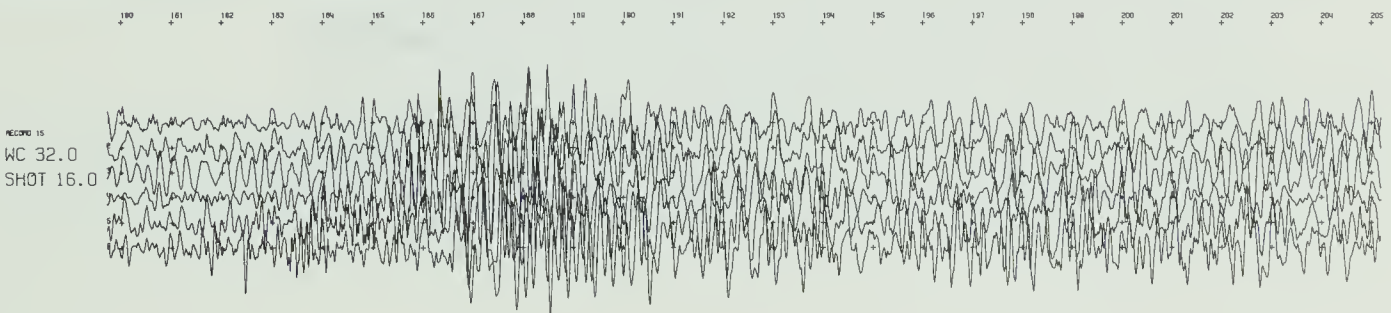
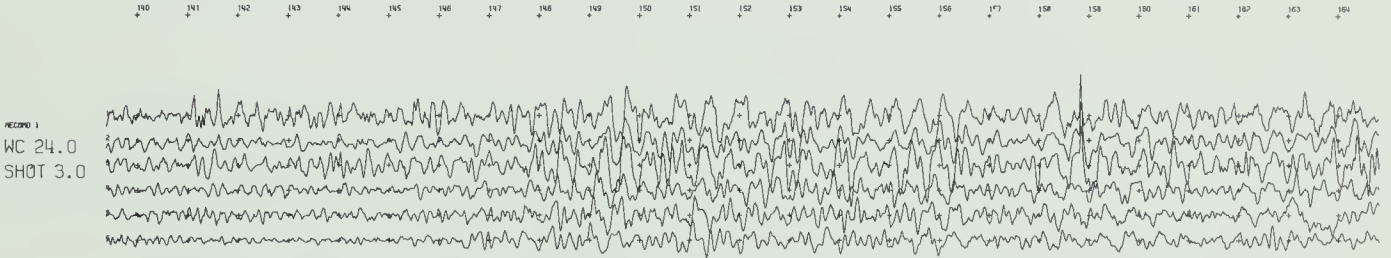
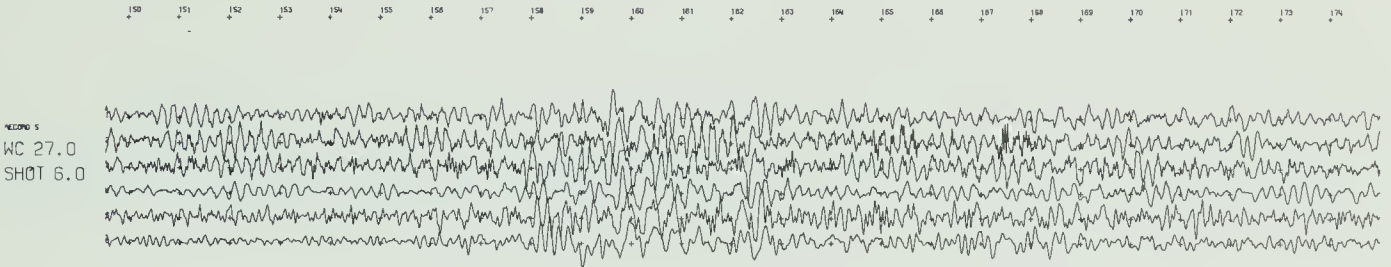
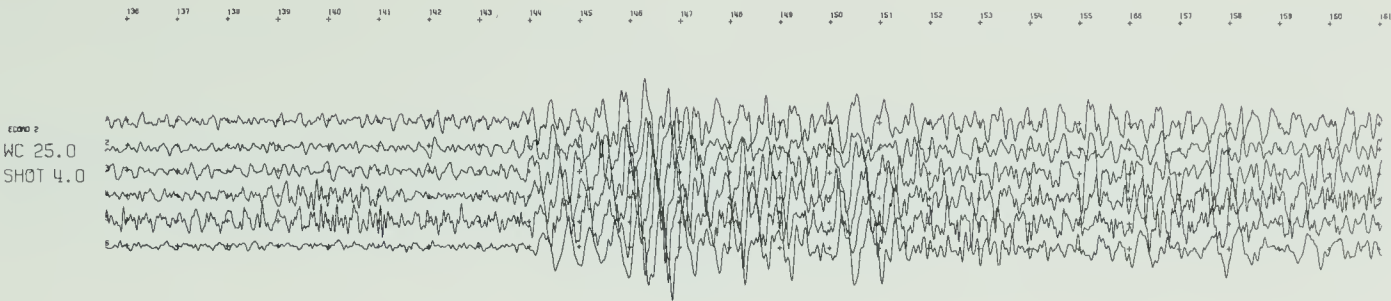
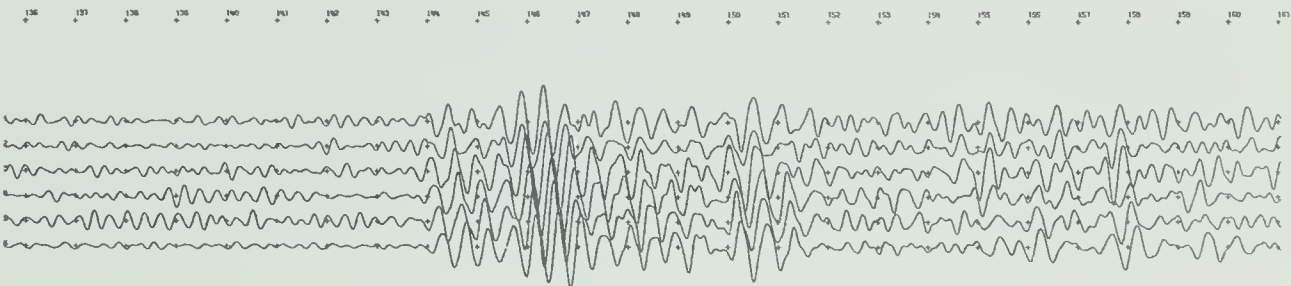
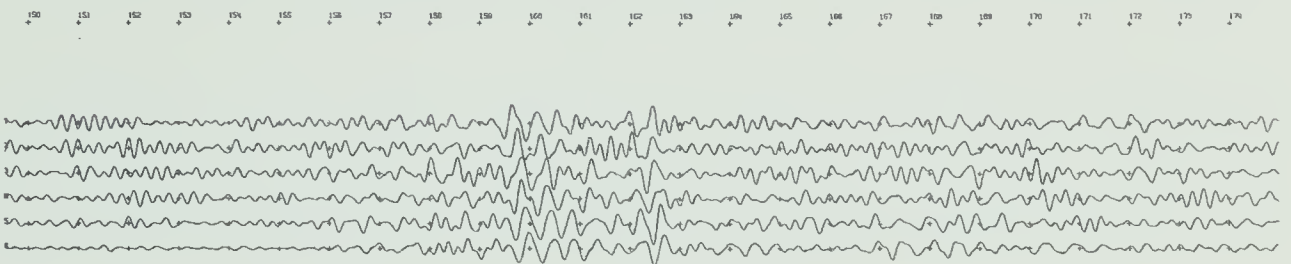


Figure 2.21. Four seismic records from Project Early Rise filtered by a zero phase shift band pass recursive digital Butterworth filter with cut-off frequencies at 1 c.p.s. and 5 c.p.s.

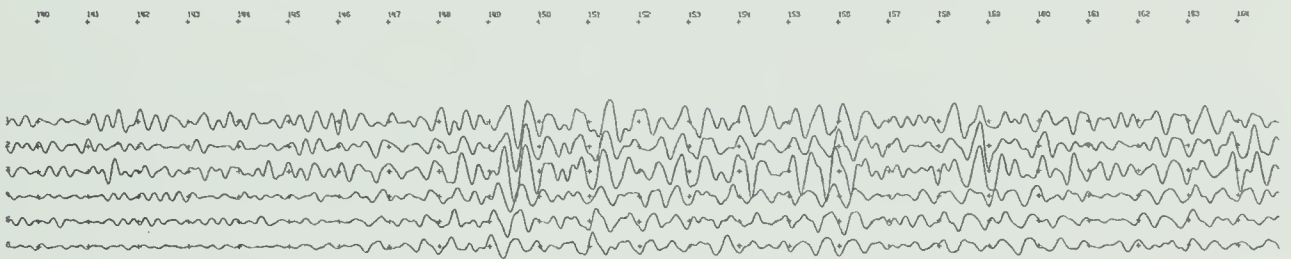
RECORD 2
WC 25.0
SHOT 4.0
BW FILTER
1.00 5.0



RECORD 5
WC 27.0
SHOT 6.0
BW FILTER
1.00 5.0



RECORD 1
WC 24.0
SHOT 3.0
BW FILTER
1.00 5.0



RECORD 15
WC 32.0
SHOT 16.0
BW FILTER
1.00 5.0

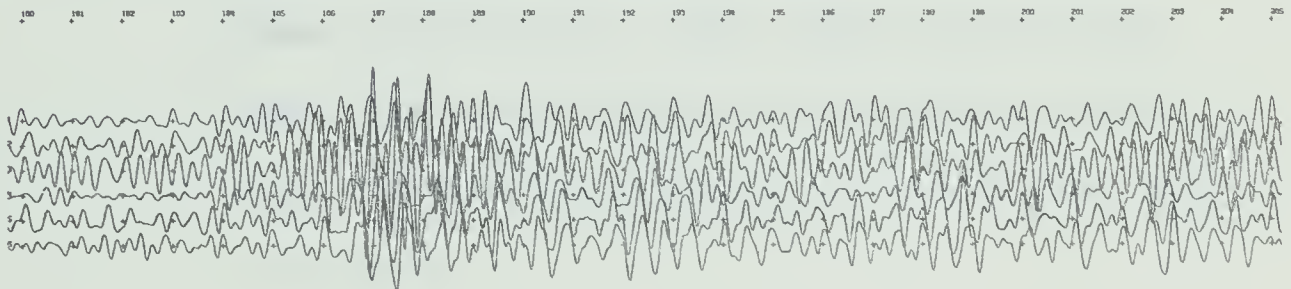
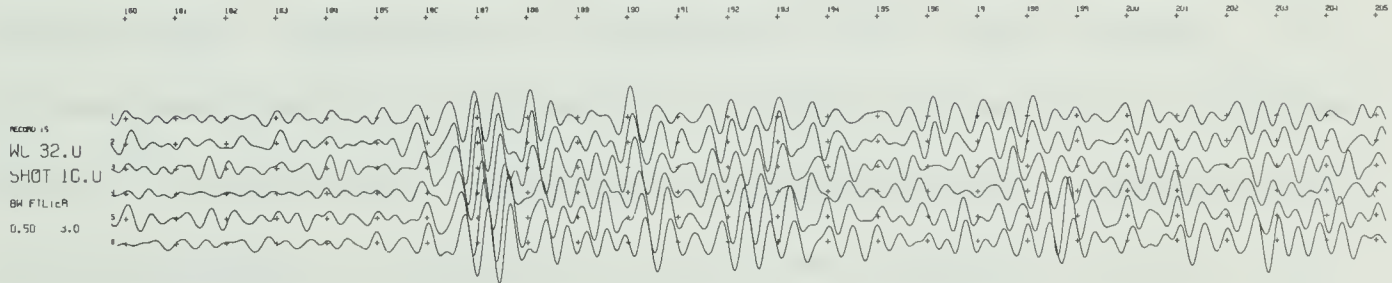
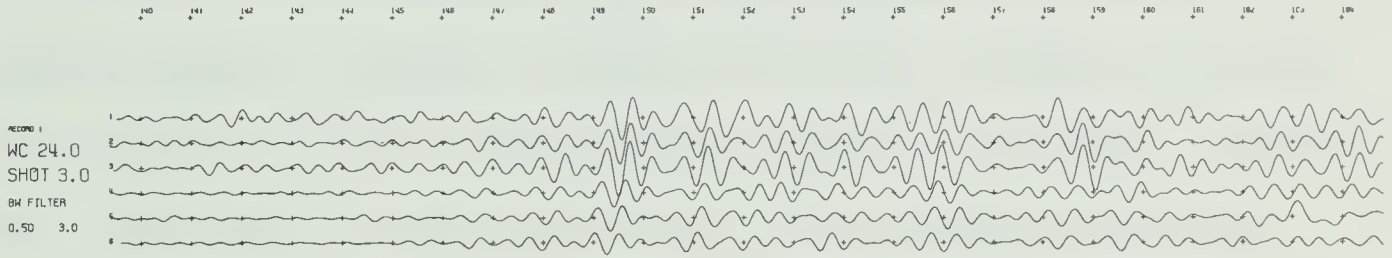
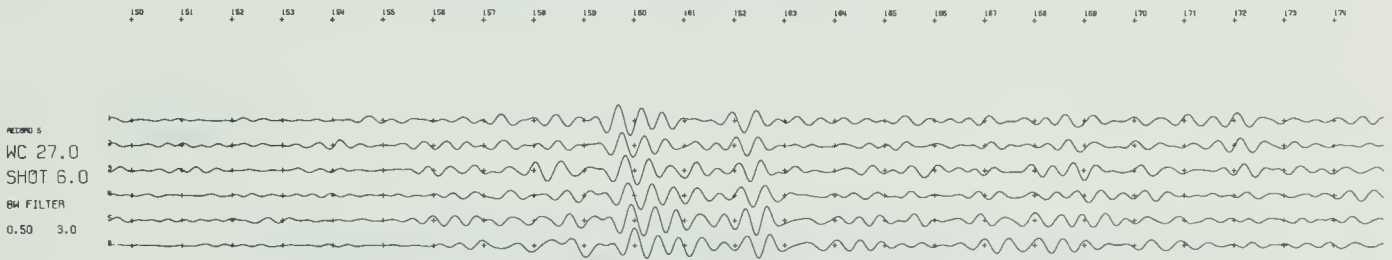
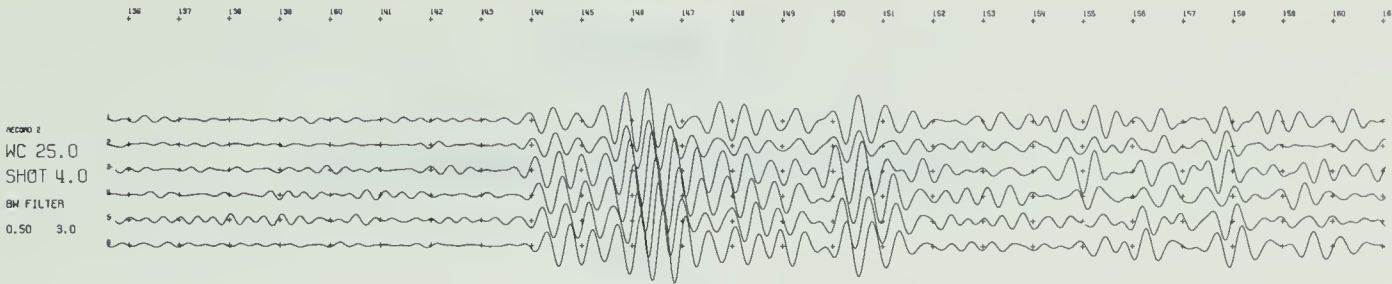


Figure 2.22. Four seismic records from Project Early Rise filtered by a zero phase shift band pass recursive digital Butterworth filter with cut-off frequencies at 0.5 c.p.s. and 3.0 c.p.s.



CHAPTER 3

THE CRUSTAL TRANSFER FUNCTION

AND

SPECTRAL RATIOS

3.1. Theory.

A solution of the boundary value problem for seismic waves transmitted in a layered medium by the Thomson-Haskell matrix formulation gives a rapid and exact calculation of the corresponding transfer function. Boundary conditions for the solution of the problem are the continuity of stress and displacement at each internal interface and vanishing of stresses at the free surface. It is assumed that for the earth's crust the ratio of longitudinal to shear wave velocity is approximately constant ($\sqrt{3}$), corresponding to a value of 0.25 for Poisson's ratio. It is also assumed that the density increases linearly with increasing seismic velocities (Birch, 1964).

The theory for obtaining the transfer function has been given by Haskell (1962), (see Appendix 1). The transfer functions for the horizontal and vertical components of ground motion at a given frequency for a plane P-waves which is incident at the bottom of the n^{th} layer are given by

$$TV_P(\omega) = \frac{2c^2(J_{42} - J_{32})}{\alpha_n^2 D} \quad 3.1$$

$$TW_P(\omega) = \frac{2c^2(J_{41} - J_{31})}{\alpha_n^2 D r_{\alpha_n}} \quad 3.2$$

where c is the apparent surface velocity,

$$r_{\alpha_n} = \sqrt{\frac{c^2}{\alpha_n^2} - 1} \quad c > \alpha_n$$

$$D = (J_{11} - J_{21})(J_{32} - J_{42}) - (J_{12} - J_{22})(J_{31} - J_{41}) \quad 3.3$$

and J_{ik} are the elements in the matrix

$$J = E_n^{-1} \cdot a_{n-1} \cdot a_{n-2} \cdots a_1 \quad 3.4$$

E_n^{-1} is a 4×4 matrix associated with the boundary condition between the half-space and the $n-1^{\text{th}}$ layer. This matrix is independent of frequency.

a_{n-1} is a 4×4 matrix associated with transmission across the $n-1^{\text{th}}$ layer and the boundary between the $n-1^{\text{th}}$ layer and $n-2^{\text{nd}}$ layer.

This matrix depends on the layer constants, the angle of incidence and the frequency of the input plane wave.

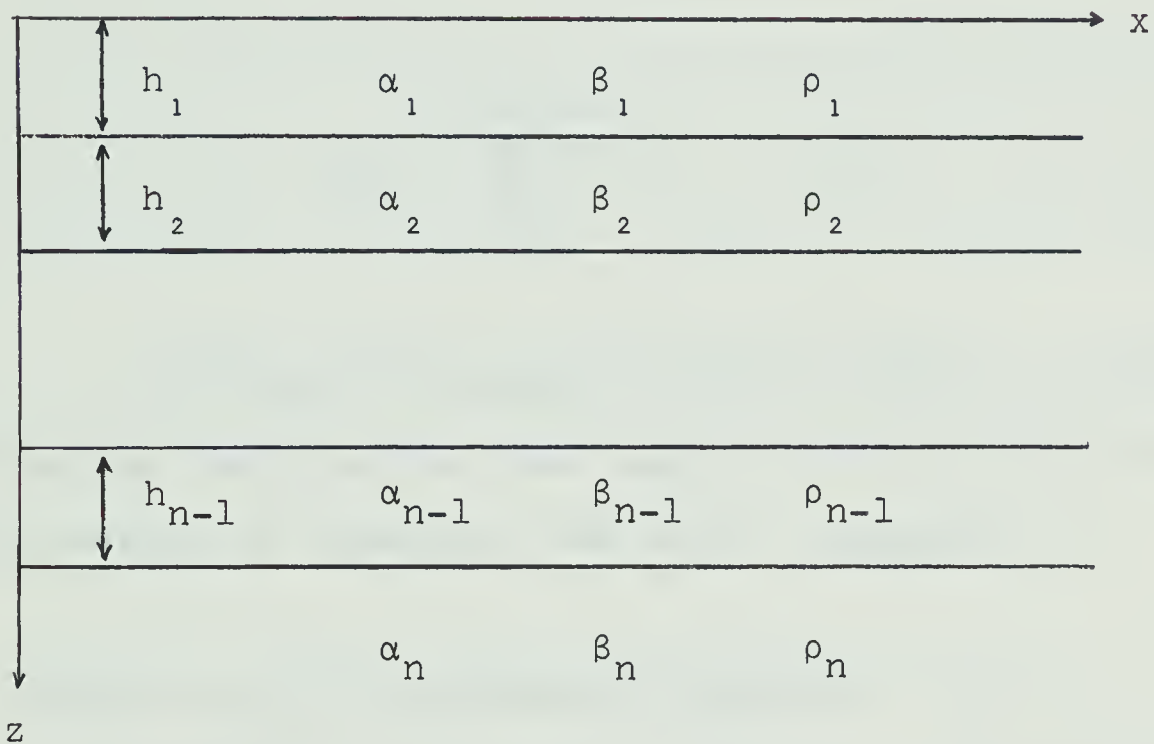


Figure 3.1. Notation used for a crustal system of n layers.

Similarly the horizontal and vertical component of ground motion for an incident S wave can be written as

$$TV_S(\omega) = \frac{2(J_{12} - J_{22})}{\gamma_n r_{\beta_n} D} \quad 3.5$$

$$TW_S(\omega) = \frac{2(J_{21} - J_{11})}{\gamma_n D} \quad 3.6$$

where

$$\gamma = \frac{2\beta^2}{c^2}$$

and

$$r_{\beta_n} = \sqrt{\frac{c^2}{\beta_n^2} - 1} \quad c > \beta_n$$

A fortran IV program written by Hanon to calculate the transfer function has been modified for operation on the University of Alberta's IBM 360/67 (Appendix 2).

3.2. Properties of the Transfer Function.

In order to investigate the crustal structure using the transfer function it is necessary to know how it behaves with variations in the crustal parameters. Hanon (1964) and Fernandez (1965) have studied the behavior of the crustal transfer function. It will be useful to review briefly some of Hanon's conclusions:

1. "Variations in the total thickness of the crust as small as one kilometer cause a noticeable shift in the position of the peaks and troughs of the transmission coefficients."

2. "For crustal models having the same total thickness, the main difference in the frequency variation of the transmission coefficients is in the character of the oscillations."

3. "The variation in the horizontal transmission coefficient is more irregular than that of vertical coefficient in the range of angles of incidence studied."

In this study a crustal model (Table 1.) obtained by Cumming and Kanasewich (1966) for southern Alberta is used.

TABLE I - CRUSTAL MODEL FOR SOUTHERN ALBERTA

Depth (km)	V_P (km/sec)	V_S (km/sec)	Density (gm/cc)
1.105	2.31	1.33	2.04
2.202	3.06	1.77	2.21
33.4	6.50	3.75	2.73
43.2	7.15	4.13	3.20
-	8.08	4.66	3.45

The transfer function and spectral ratios will be calculated for this model.

When the thickness of the third layer was increased by 3 kilometers this caused noticeable shifts in the

peaks of the transfer function (Figure 3.2). The sensitivity of the transfer function to variations in the P-wave velocity in the same layer was also tested by increasing the velocity by 1 km/sec. This introduced a change of amplitude in the transfer function as well as shift in the peaks (Figure 3.3). The above test is also performed for a different angle of incidence and as seen in figure 3.4 it is insensitive to variations in this parameter. The phase response of the transfer function of above model is almost linear as seen in figure 3.5.

3.3. Application of the Crustal transfer function.

A signal transmitted through the crust and recorded at the surface is modified in a manner depending on the density and elastic properties of the media. The spectrum of such a signal can be expressed as a convolution of a source function with the crustal transfer function:

$$R(f) = P(f) * H(f) \quad 3.7$$

where $P(f)$ is the spectrum of the incident pulse and $H(f)$ is the transfer function which depends upon the crustal parameters. Equation 3.7 can be written for both the vertical and horizontal components:

Figure 3.2. Modulus of transfer functions and their ratios for plane waves incident on a southern Alberta crustal section at an angle of incidence of 80° . The depth has been increased in the third layer by 3 kilometers. The crosses denote the thicker model

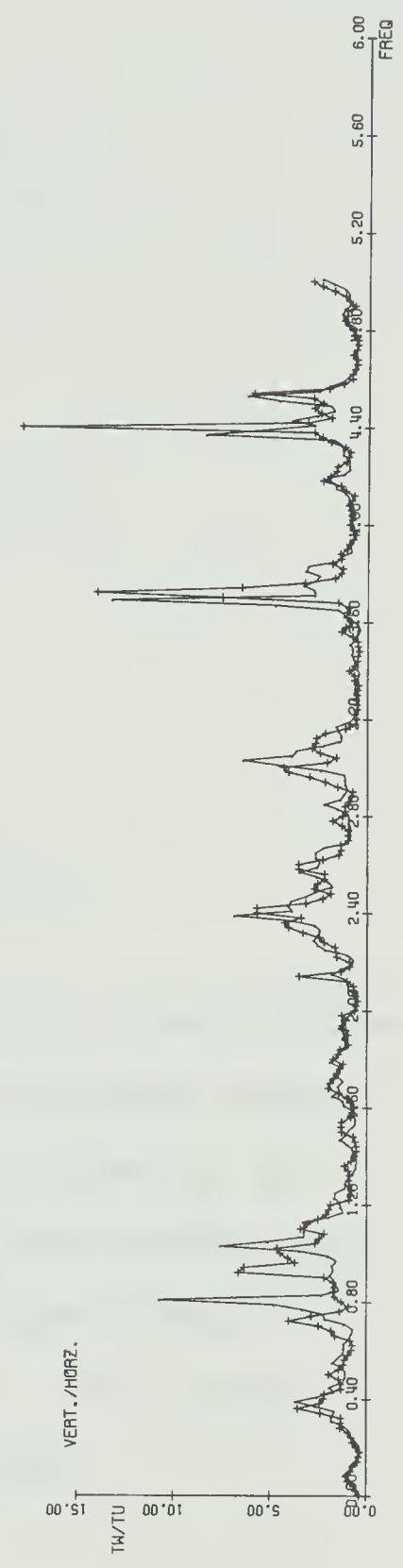
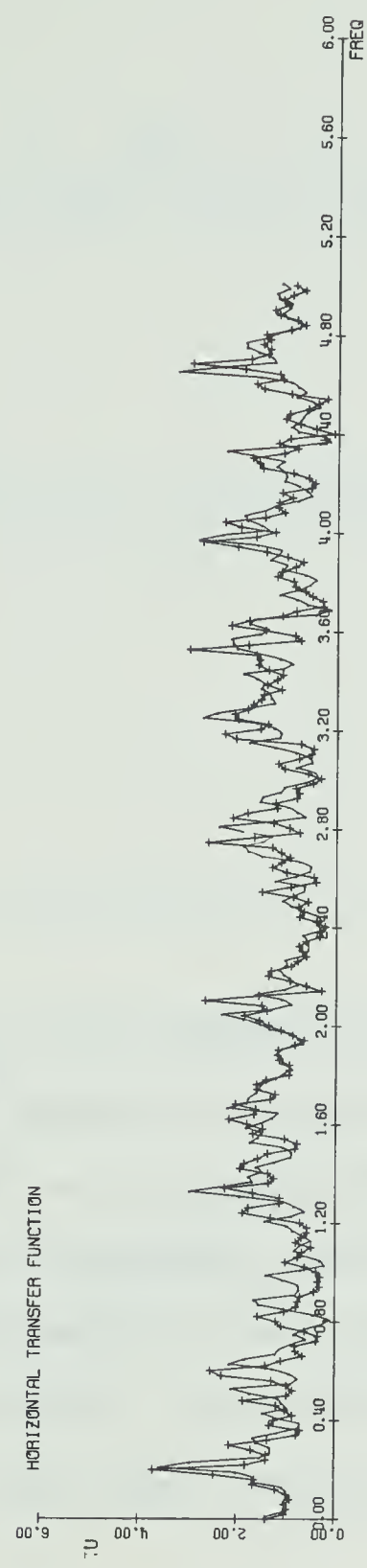
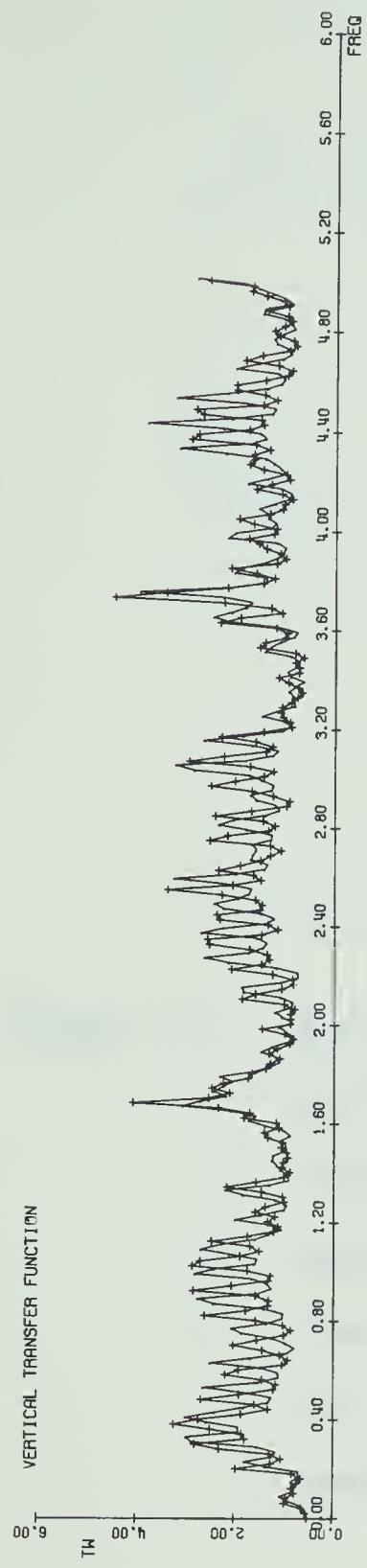




Figure 3.3. Modulus of the transfer function, their ratios and the phase of the ratios for plane waves incident on a southern Alberta model at an angle of incidence of 80° . The velocity has been increased in the third layer from 6.50 to 7.50 km/sec. (see table 1). The crosses denote the higher velocity model

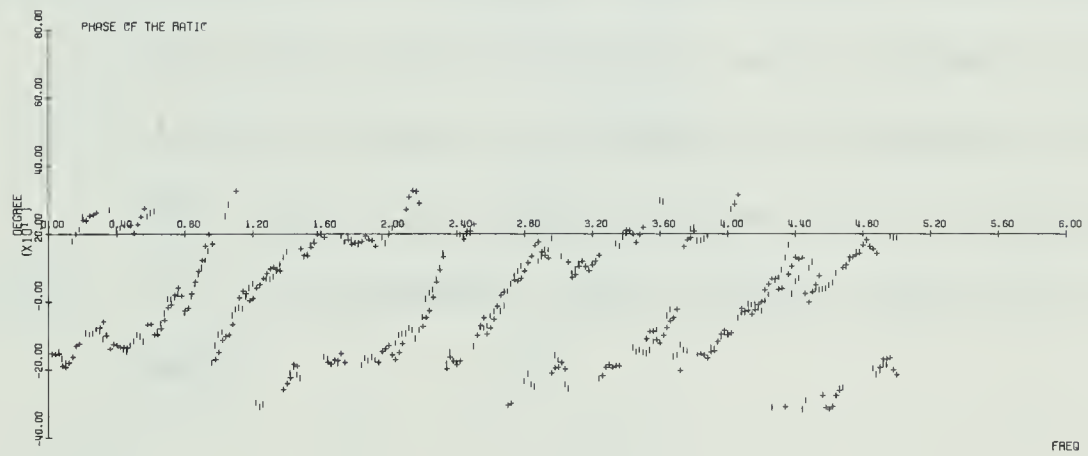
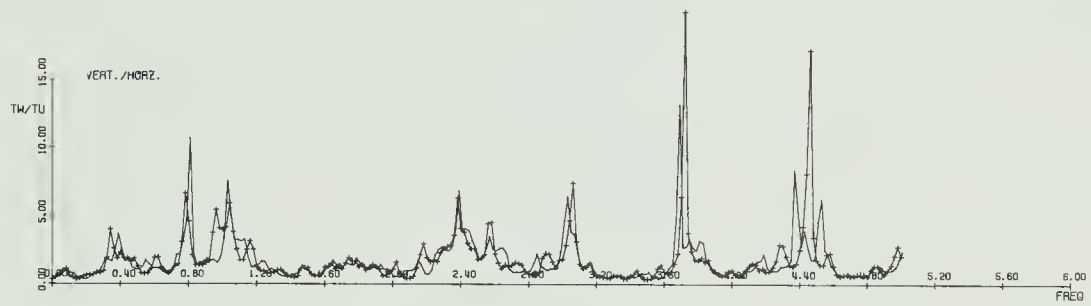
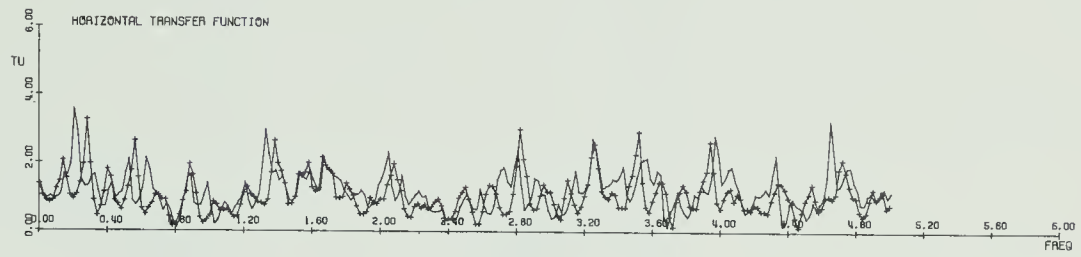
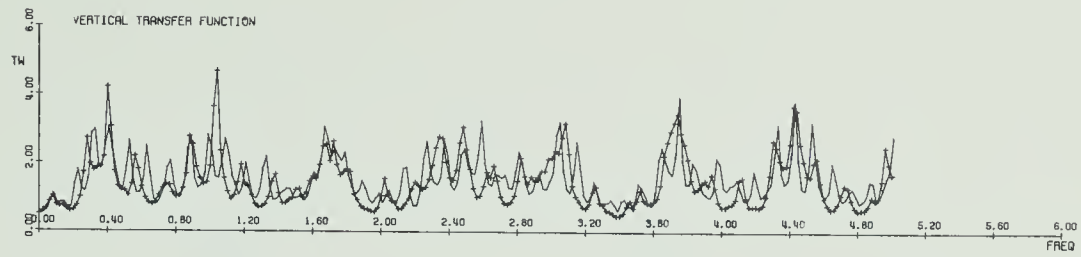
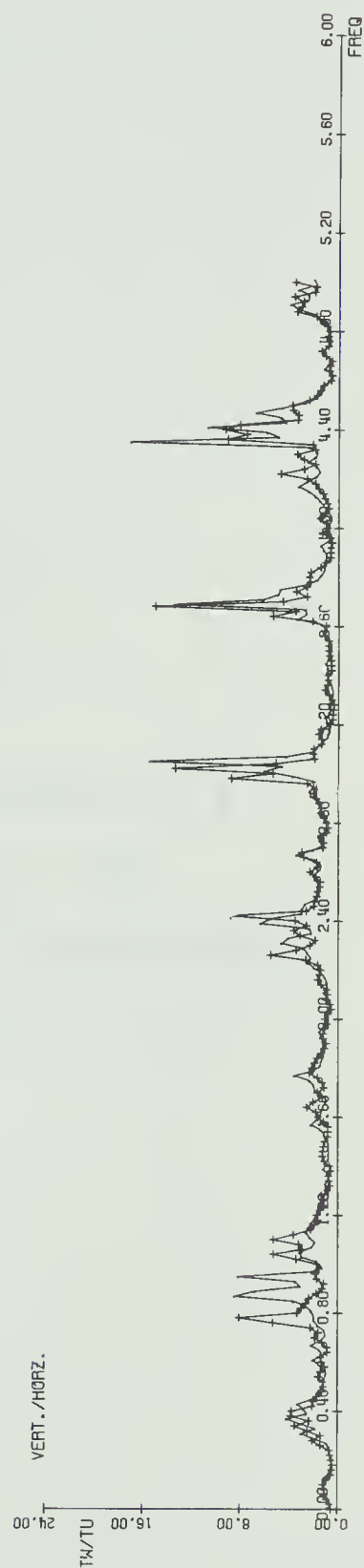
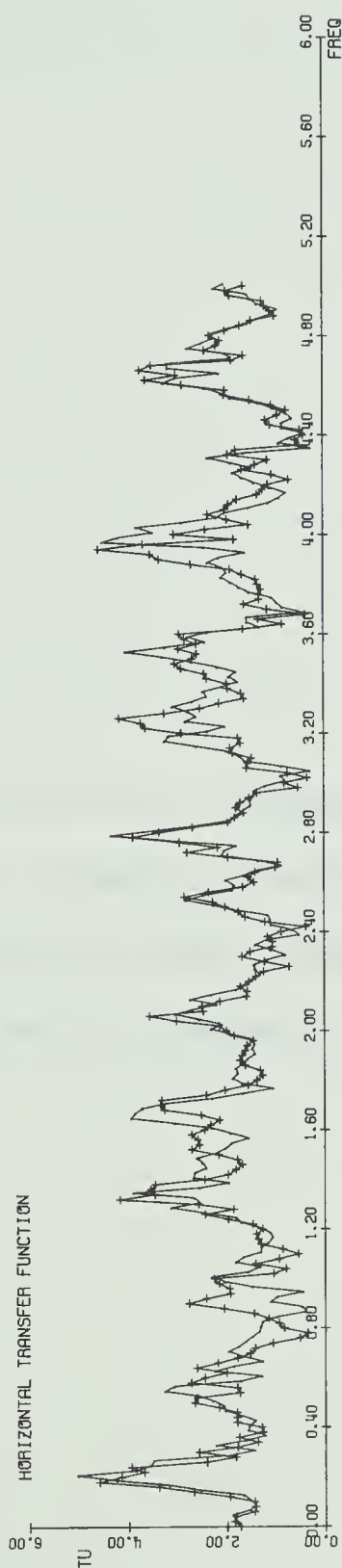
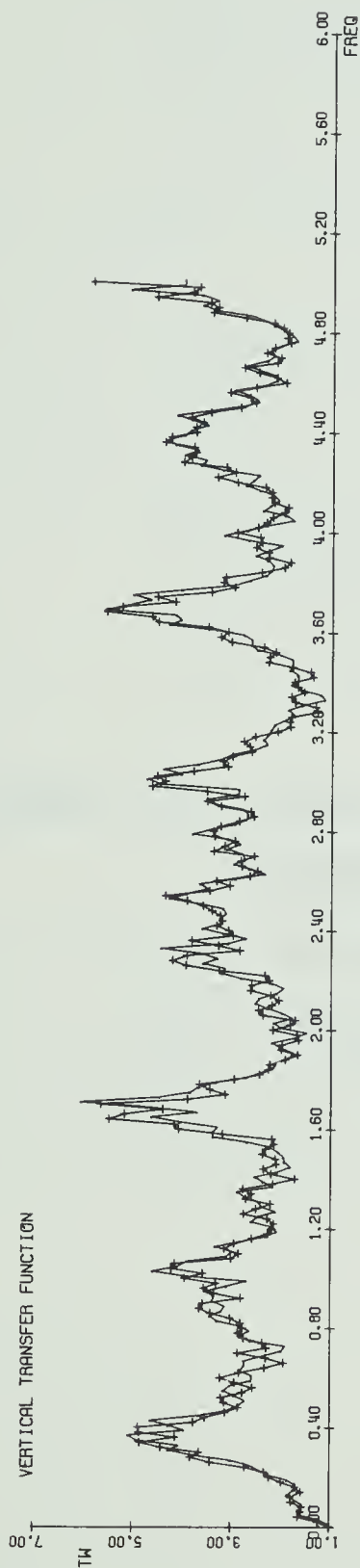


Figure 3.4. Modulus of transfer function and their ratios for plane waves incident on a southern Alberta crustal model at an angle of incidence of 60° . The depth has been increased in the third layer by 3 kilometers. The crosses denote the thicker model




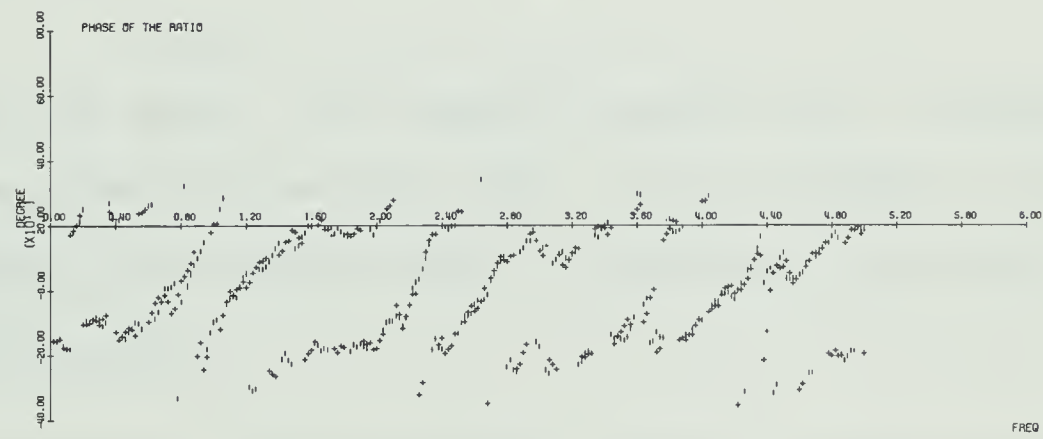
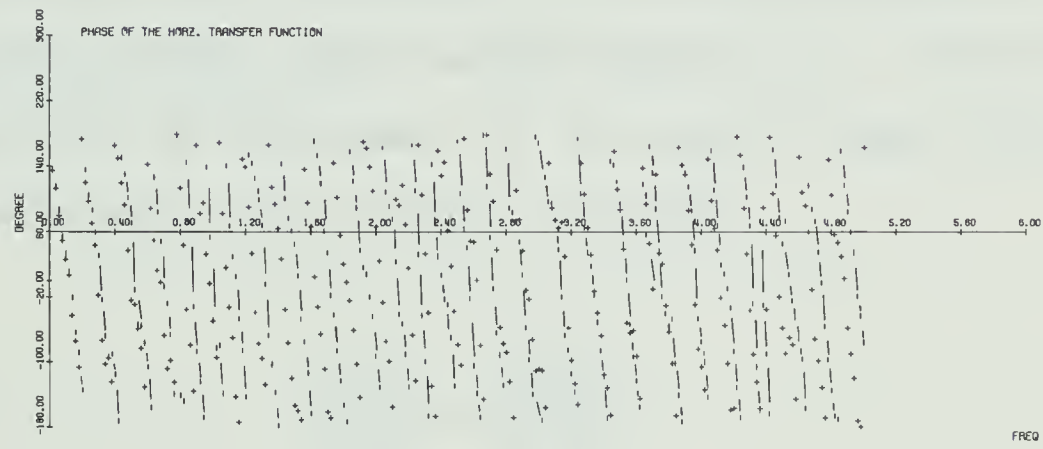
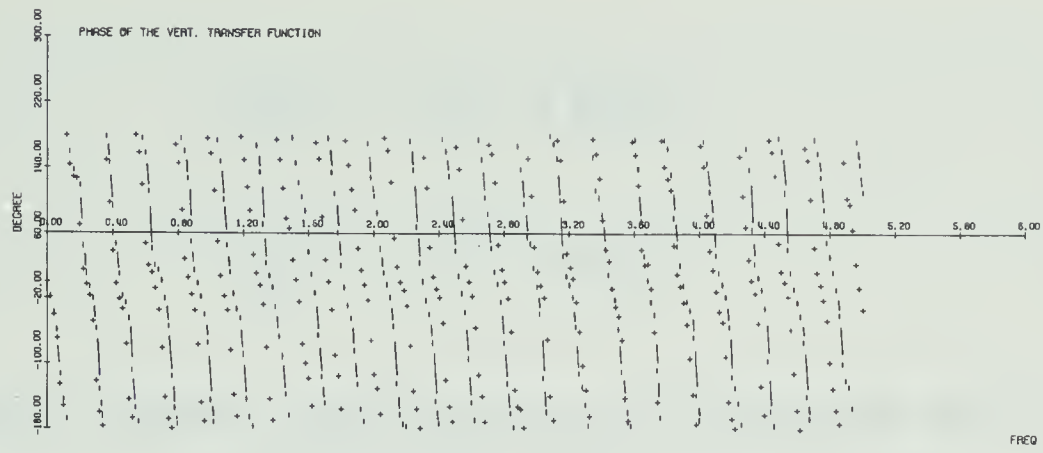


Figure 3.5. Phase curves for transfer functions of a southern Alberta crustal model. This corresponds to the modulus of transfer function shown in figure 3.2.



$$R_Z(f) = P(f) * H_Z(f) \quad 3.8$$

$$R_H(f) = P(f) * H_H(f) \quad 3.9$$

The crustal transfer function can be calculated and if one knows the source function, $P(f)$, it is possible to obtain the recorded signal using equation 3.7. Since the impulse, $P(f)$, is not known, it is usual to take the ratio of the horizontal and vertical spectrum:

$$\frac{R_Z(f)}{R_H(f)} = \frac{H_Z(f)}{H_H(f)} \quad 3.10$$

By taking the ratio, the unknown function $P(f)$ is eliminated. The observed spectral ratio can be matched to the theoretically calculated ratio of transfer functions for any crustal model.

Phinney (1964) was the first to use the ratio of the transfer functions to obtain crustal structure using long period data. Fernandez (1965) calculated master curves to determine the crustal structure from the spectrum of long period P waves in the United States. In their studies a time window applied to observed spectra was neglected because long period data was used. For short period data the

window must be short so that additional phases do not arrive and its effect cannot be neglected (Leblanc, 1966). A recorded seismogram seen through a window $W(f)$ can be expressed as:

$$R_T(f) = R(f) * W(f) \quad 3.11$$

or in the time domain

$$r_T(t) = r(t) \cdot W(t) = R(f) * W(f) \quad 3.12$$

using equation 3.7 in equation 3.11:

$$R_T(f) = [P(f) \cdot H(f)] * W(f) \quad 3.13$$

A difficulty arises in equation 3.13 because the convolution must be performed on two unknown functions. However Leblanc (1966) showed that the convolution can be done on one unknown only; e.g. on $H(f)$:

$$R_T(f) = [P(f) \cdot H(f)] * W(f) = P(f) \cdot [H(f) * W(f)] \quad 3.14$$

This convolution is valid under two conditions (Leblanc, 1966):

1. The transfer function in the time domain can be approximated by a sequence of weighted delayed delta functions.

2. The source function is assumed to be of finite duration and short compared to time duration of the record T , to prevent truncation of any sub-pulses by the window. Therefore equation 3.10 can be written as

$$\frac{R_{ZT}(f)}{R_{HT}(f)} = \frac{H_{ZT}(f)}{H_{HT}(f)} \quad 3.15$$

A convolution of the transfer function with a window can be performed by a method explained by Leblanc, 1966, but there are difficulties in the case of a rectangular window as indicated because of its slow convergence. In this study the truncation of the transfer function has been done by a double Fourier transform. A simple rectangular window $W(t)$ is used where

$$W(t) = 1 \quad 0 < t < T$$

$$= 0 \quad \text{elsewhere}$$

and T is the time duration of the signal. The steps used in truncation are:

1. The transfer function was calculated using the program listed in Appendix 2. The time synthesis of transfer function was obtained by a Fourier transformation using a Fast Fourier algorithm (Cooley and Tukey, 1965):

$$h(t) = \frac{1}{N} \sum_{T=0}^{N-1} H(f) e^{\frac{-2\pi i W T}{N}} \quad 3.17$$

In the expression above N is the total number of points calculated at intervals of Δf c.p.s. and W is the digital frequency index.

2. The desired length of $h(t)$ is generally chosen by a study of time synthesis of the transfer function. This time length must be equal or almost equal to the time duration of the seismic records under analysis but at the same time such that $h(t)$ has a value as near to zero as possible for $t = T$. Taking the Fourier transform of equation 3.17

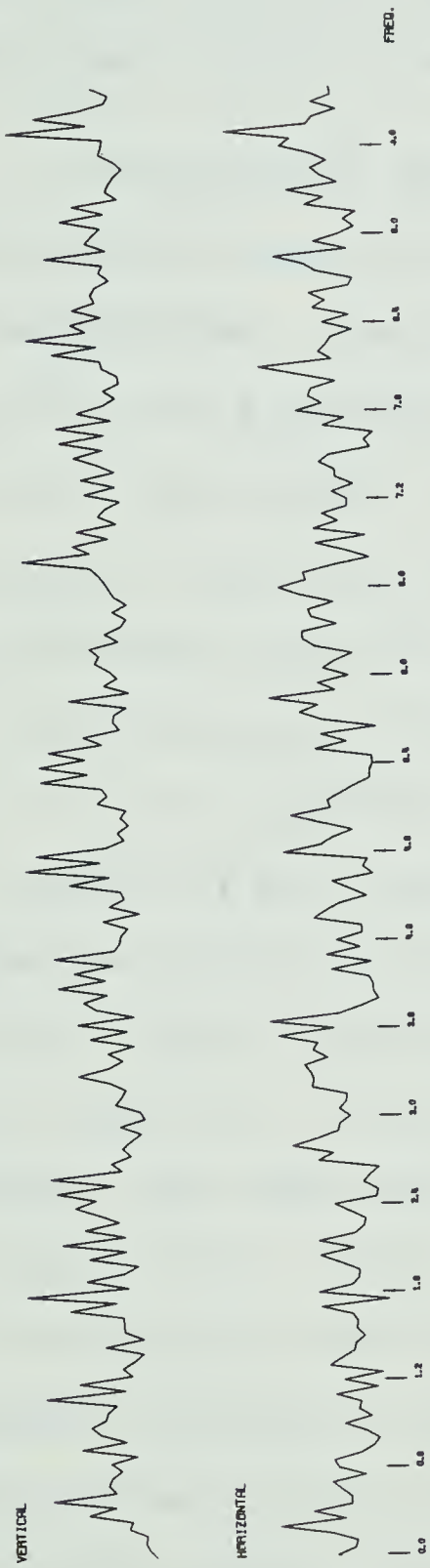
$$H(f) = \sum_{T=0}^{N-1} h(t) e^{\frac{-2\pi i W T}{N}} \quad 3.18$$

Figure 3.6 shows the steps described above. Here 4.34 seconds window was used since the major pulses have arrived at this time. A perfect time synthesis of the transfer function would be obtained using the full range of integration i.e., from $-\infty$ to $+\infty$. For a narrower range of frequency one must assure that the transfer function is not affected by the rejected frequencies. For this reason the stability of the truncated transfer function was tested with calculation using higher frequencies in the time synthesis. It was noted that when the synthetic seismogram was truncated over a constant time interval (4.34 seconds) that the truncated transfer function in the frequency range 0 - 10 c.p.s. was similar to the truncated transfer function with the frequency range 0 - 15 c.p.s.

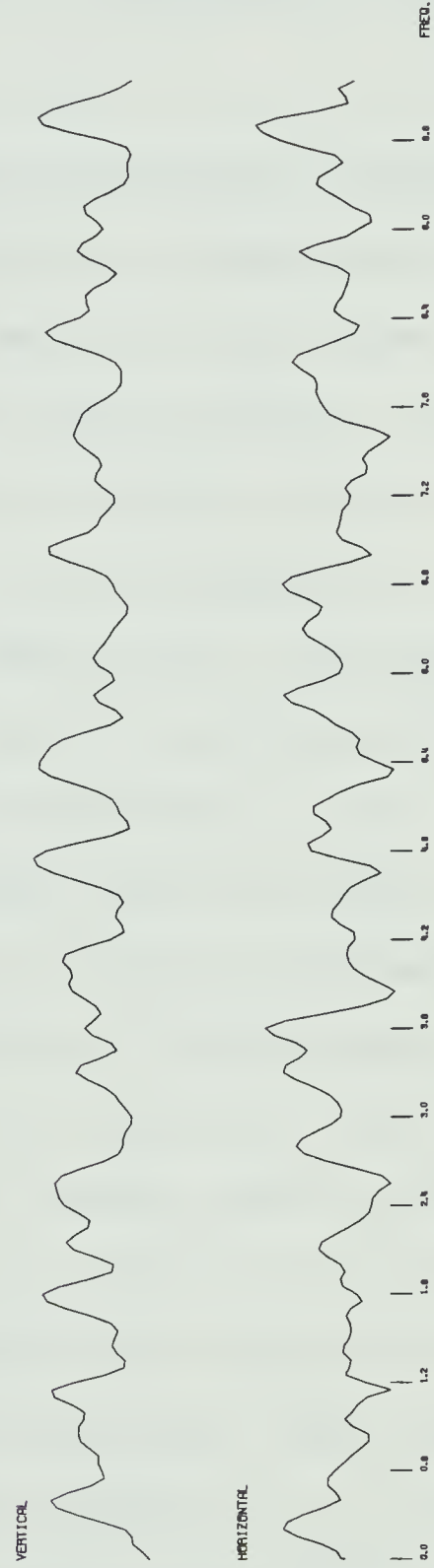
3.4. Analysis of data.

Power spectra of field records were computed by first calculating the autocorrelation function, this function was modified by a Daniell window whose length is 4.34 seconds and the power spectrum was obtained by a fast Fourier transform of the modified autocorrelation function. The field records were filtered with a Butterworth band-pass filter modified for zero phase shift, whose cut-off frequencies are 1 and 5 c.p.s. This filter reduced the noise background on the power spectrum (Figure 3.7). The

Figure 3.6. Truncation of transfer function for Alberta model using frequency interval of $\Delta f=0.05$ and time interval of $\Delta t=1/50$



NON-TRUNCATED TRANSFER FUNCTIONS
ANGLE OF INCIDENCE 80 DEGREES



TRUNCATED TRANSFER FUNCTIONS
ANGLE OF INCIDENCE 80 DEGREES

main peak is centered at about 2 c.p.s. , small peaks at higher frequencies on some records appear to represent mainly noise since the peaks are not consistent from trace to trace and record to record.

For Project Early Rise the vertical, horizontal and ratio spectrums were calculated at 9 locations in Alberta and Saskatchewan. Theoretical spectral ratios were also calculated for a southern Alberta model (Table 1) to compare with the field records. At location WC 25, which is the beginning of the line recorded by the University of Alberta, the theoretical spectral ratio obtained for this model agrees well with the spectral ratios from the field records (Figure 3.7). In this comparison one must make use of only the part around the mid-frequency rather than the higher or lower frequencies which are distorted by various instrumental effects. The last recording station in Saskatchewan, WC 34, did not agree with these theoretical spectral ratios and an attempt has been made to find a better model by changing the depths of the layers. After 11 trials, it was found that the spectral ratio for a model with the third layer thickness increased to about 36 kilometers, fits the spectral ratios of the field record better (Figure 3.8). In Alberta the spectral ratios for the field record at WC 39 was found to be similar to the theoretical spectral ratios when the third layer thickness was increased to about 41 kilometers

(Figure 3.9).

The spectral ratios for the field records were not very stable from one location to the other. The change in the spectral behavior can be explained by three effects: (1) variation in the source function, (2) upper mantle effects due to triplication in the travel time curve and (3) crustal effects such as non parallel layering or faulting. It is difficult to predict the pulse shape, however, the pulse can be approximated by various functions such as the $\sin X/X$ which was used. Since the charge was detonated in the water at a location which varied slightly from shot to shot it has been impossible to represent these variations in the pulse function. However the effect of the pulse can be eliminated to great extent by taking spectral ratios. One must also remember that the Lake Superior crustal structure where the source was generated can effect the spectrum of field records. The most likely explanation for the rapid changes in the character of the spectrum is the effect of the upper mantle. Body waves traveling from the shot point to the recording station are modified by mantle structure and in particular reflected waves are generated at second order discontinuities. Interference of one wavefront with another can produce minima and maxima. The observed spectrum was found to agree with the theoretical one obtained for a reasonable Earth model and seems that the technique can be

successful if used with discrimination.

3.5. Conclusion.

The transfer function calculated by the Thomson-Haskell matrix method has been found to be very sensitive to the variation of crustal parameters. Spectral ratios for field records were compared with the theoretical ones with the thicknesses of the layers being varied. It appears likely that the crustal thickness increases in the westward direction along the line of recording stations. However for a limited number of recordings, we could not find a plausible crustal model. One can get a better fit of the theoretical spectral ratios to the observed spectral ratios by changing parameters other than thickness but the amount of model computation can be very large. In general, it appears that the spectral ratios of short period body waves is very sensitive diagnostic for obtaining crustal structure if one can obtain a reasonable level of signal to noise from sources at distances where the upper mantle complications do not affect the crustal reverberations. It is also difficult, at this stage to determine if one has a unique model or only one of a family of possible ones. Recording of spectral ratios over a wider band of frequencies could resolve this ambiguity.

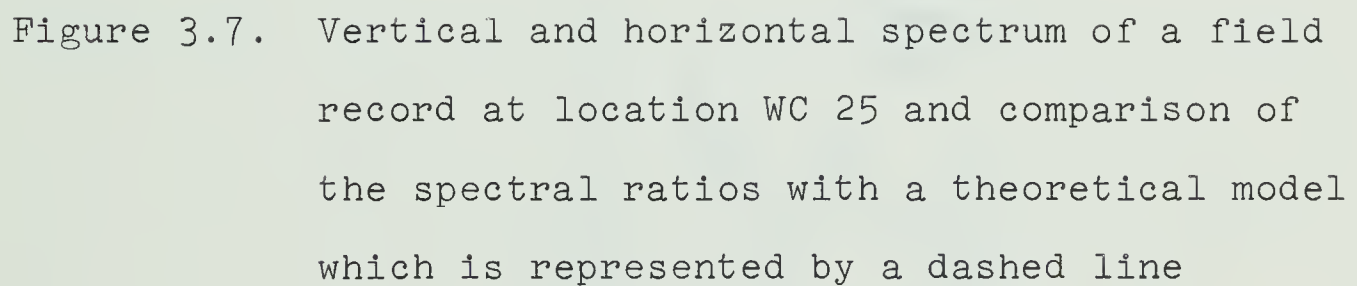
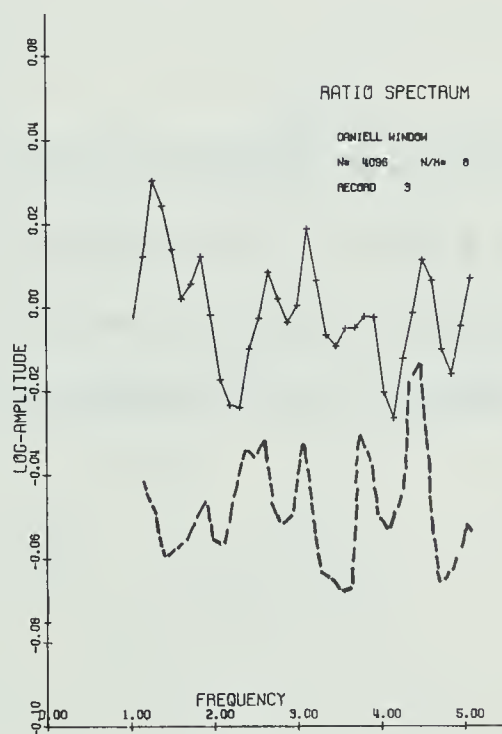
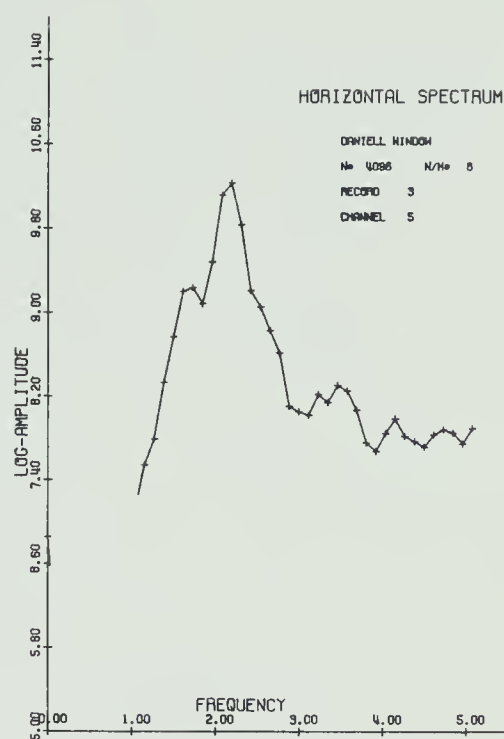
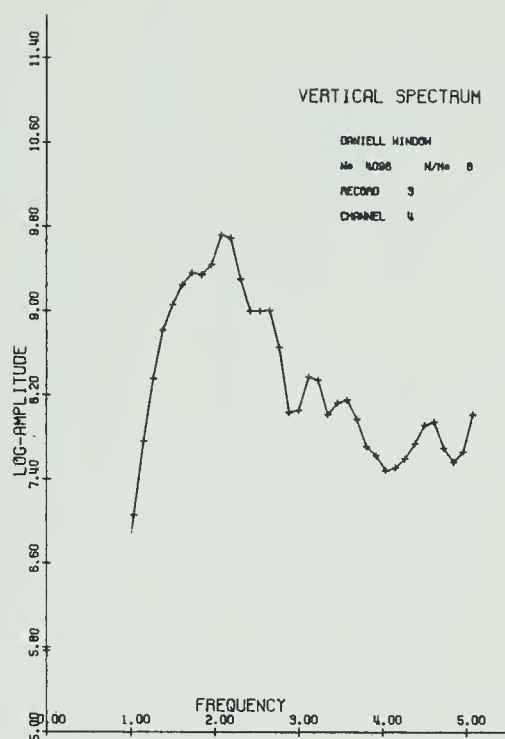


Figure 3.7. Vertical and horizontal spectrum of a field record at location WC 25 and comparison of the spectral ratios with a theoretical model which is represented by a dashed line






Figure 3.8. Vertical and horizontal spectrum of a field record at location WC 34 and a comparison of spectral ratios with the theoretical model which is represented by a dashed line

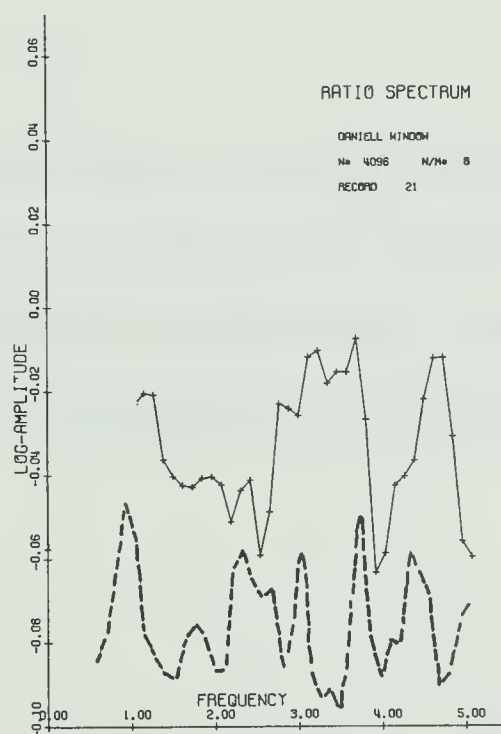
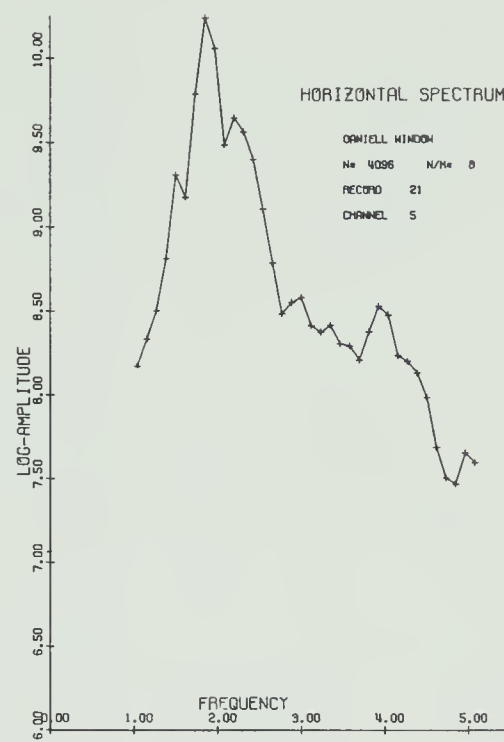
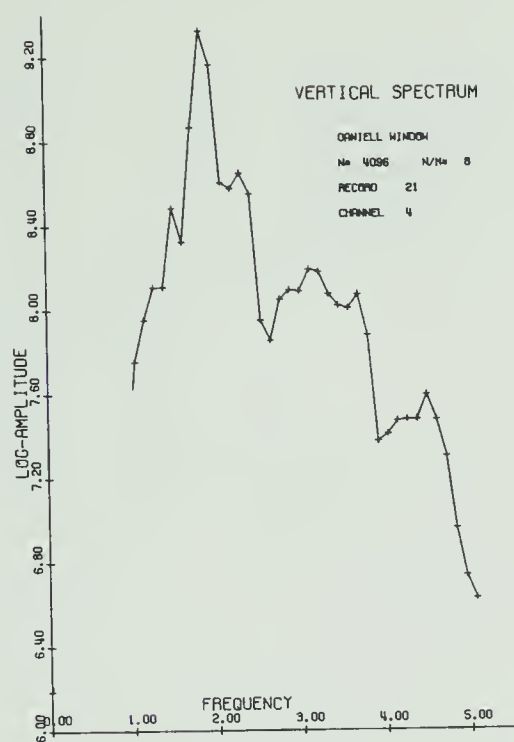
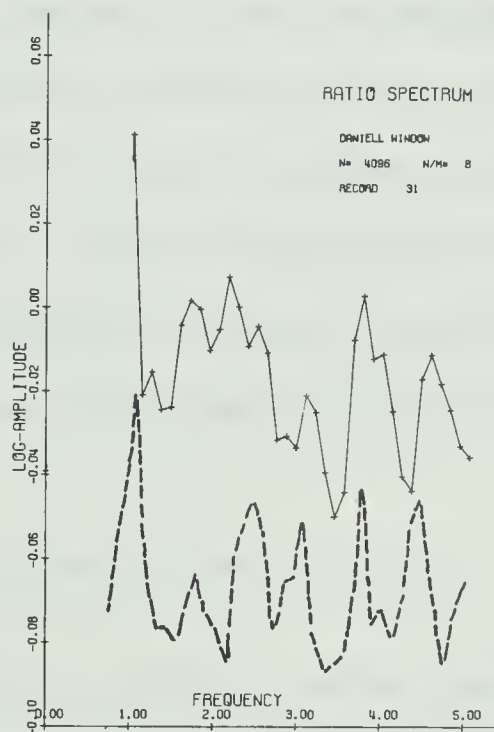
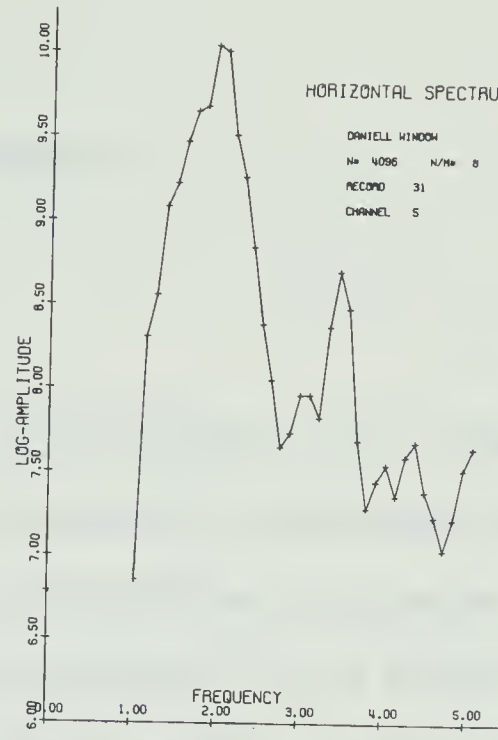
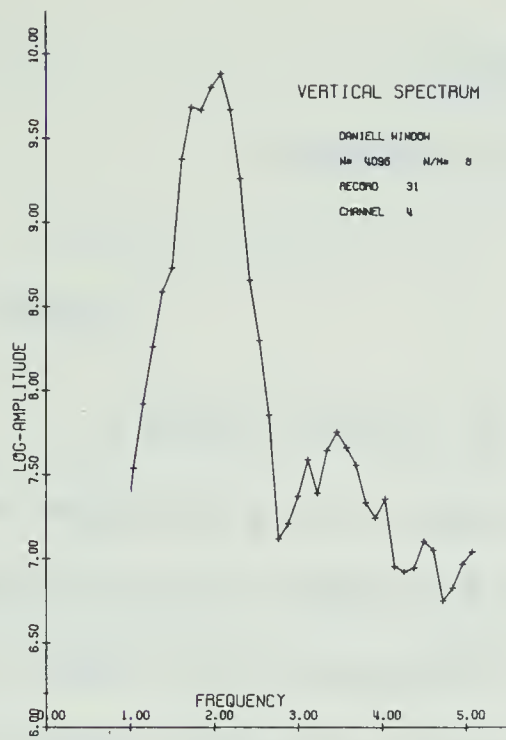


Figure 3.9. Vertical and horizontal spectrum of a field record at location WC 39 and a comparison of the spectral ratios with the theoretical model which is represented by a dashed line



CHAPTER 4

SYNTHETIC SEISMOGRAMS

4.1 Theory.

A time history of the surface motion of a layered system responding to a pulse is obtained by convolving the transfer function with a function simulating the pulse. Hanon (1964) first obtained a time synthesis for a number of plane layers using the Thomson-Haskell matrix. He studied the effects of the pulse frequency, angle of incidence, and layering of the system on the seismograms. McCamy (1967) made similar theoretical calculations but when he compared the results with actual field records he did not find many similarities. In this chapter synthetic seismograms will be calculated for a southern Alberta model of the crust and compared with field records from Project Early Rise.

4.2 Generation of synthetic seismograms.

In this study a simple pulse function (Figure 4.1) is used to calculate seismograms:

$$\begin{aligned}
 P(f) &= 1 & f < 10 \text{ c.p.s.} \\
 &= 0 & f > 10 \text{ c.p.s.}
 \end{aligned}$$

4.1

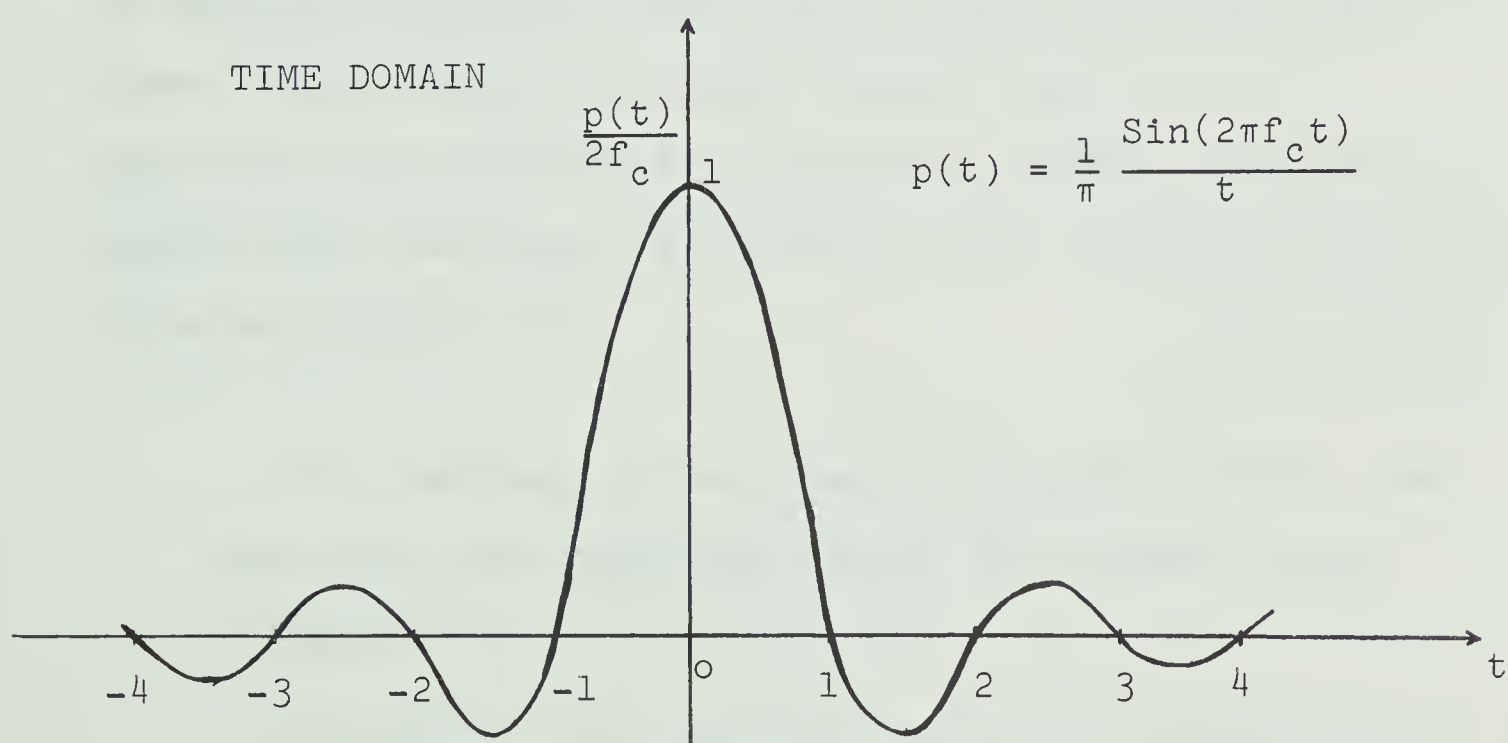
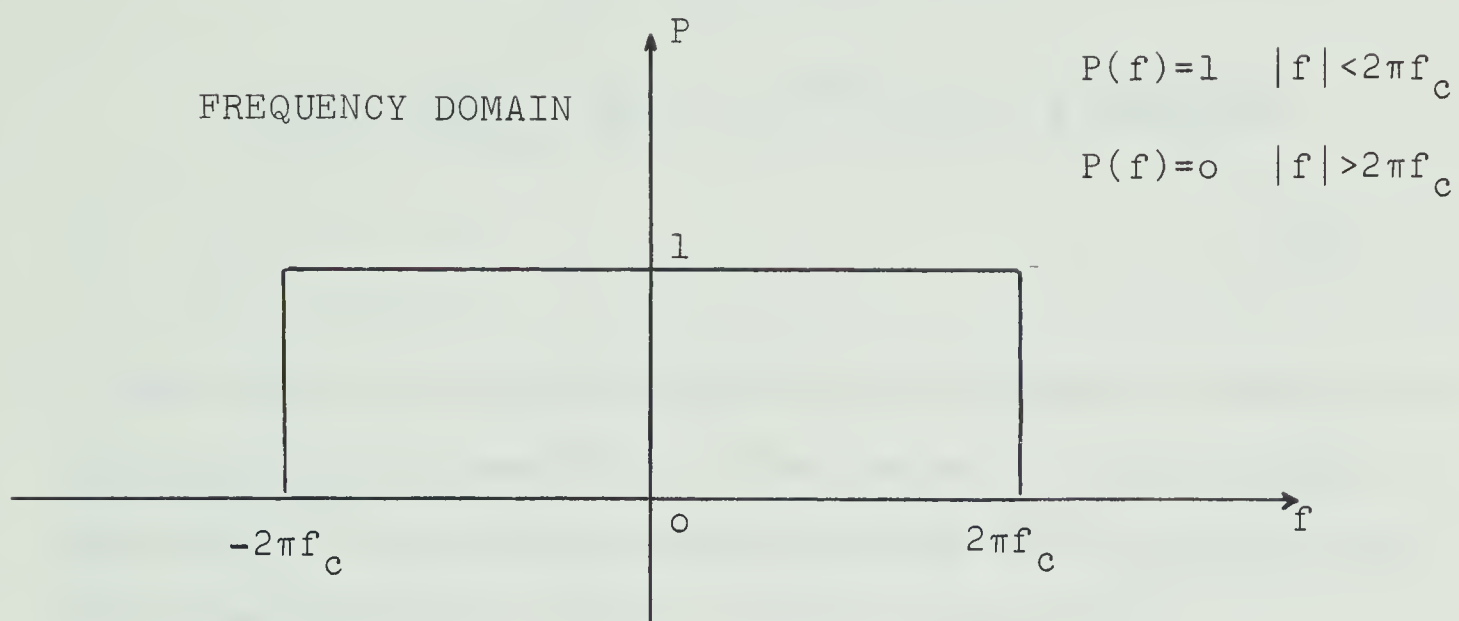


Figure 4.1. The source function.

The corresponding time function is

$$p(t) = \frac{1}{2\pi} \int_{-\infty}^{\infty} P(f) \cdot e^{i2\pi ft} df = \frac{1}{\pi} \frac{\sin 20\pi t}{t}$$

4.2

A time synthesis of ground motion is obtained by taking the inverse Fourier transform of the product of the transfer function of the layered crustal system, $H(f)$ obtained from the Thomson-Haskell matrix, and the pulse, $P(f)$:

$$r(t) = \frac{1}{2\pi} \int_{-\infty}^{\infty} H(f) \cdot P(f) e^{i2\pi ft} df \quad 4.3$$

An assumption has been made that we have plane waves and plane elastic layers in welded contact which do not attenuate the energy in any inelastic process. The seismograms were calculated according to the following steps (also see figure 4.2):

1. The modulus of the transfer function, $|H(f)|$, and the phase were calculated using the program listed in Appendix 2.
2. The real and imaginary part of the transfer function were calculated:

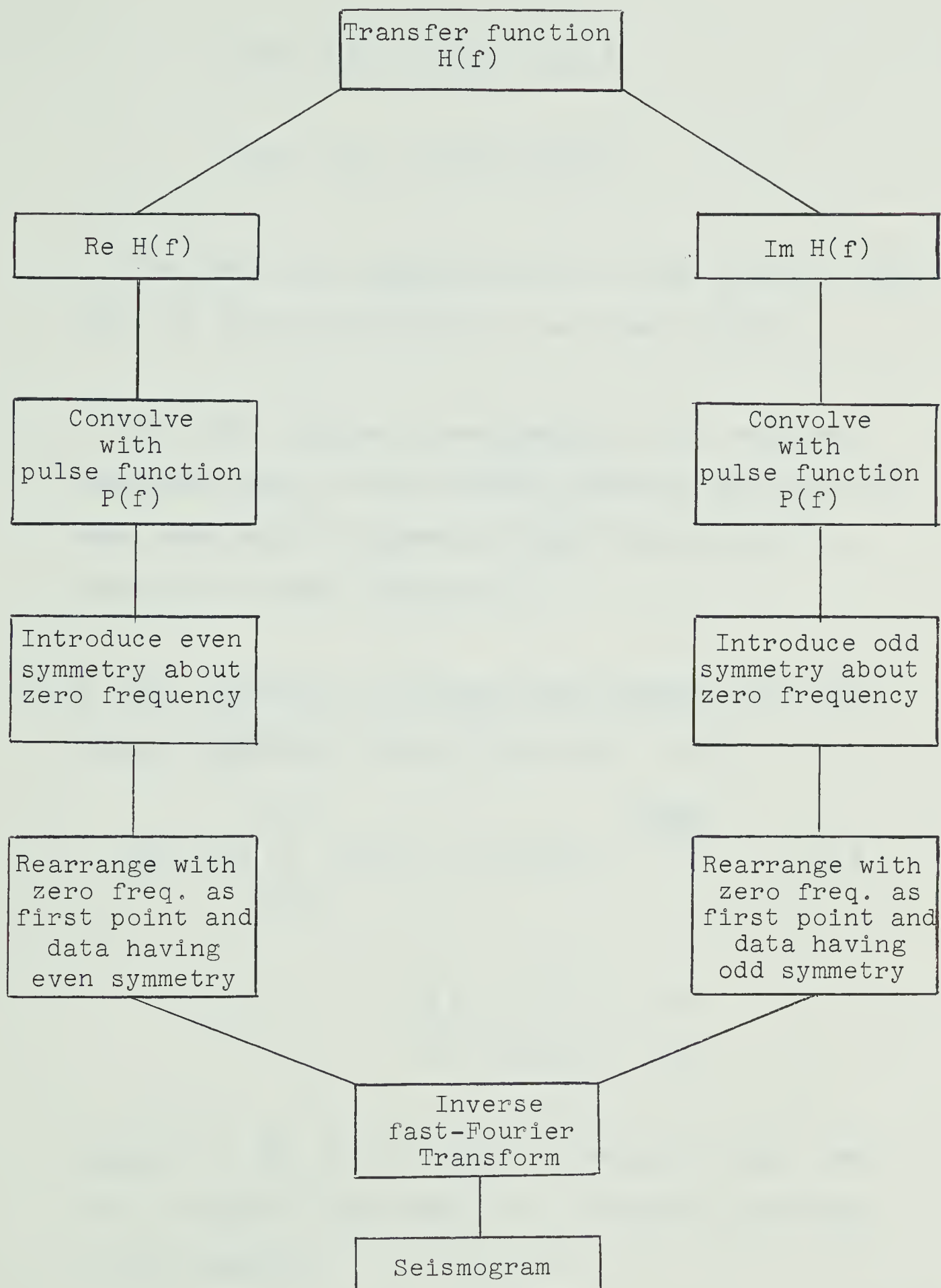


Figure 4.2. Calculation of theoretical seismogram using fast Fourier algorithm.

$$\text{Re } H = H_R = |H(f)| \cos \theta$$

$$\text{Im } H = H_I = |H(f)| \sin \theta$$

3. The real and imaginary parts of the transfer function, H , were multiplied by the pulse function.

4. For fast Fourier transformation, the real and imaginary part of the transfer function were made to have even and odd symmetry respectively about the mid-point or zero frequency.

5. The synthetic seismogram was obtained by a fast Fourier algorithm (Cooley and Tukey, 1965):

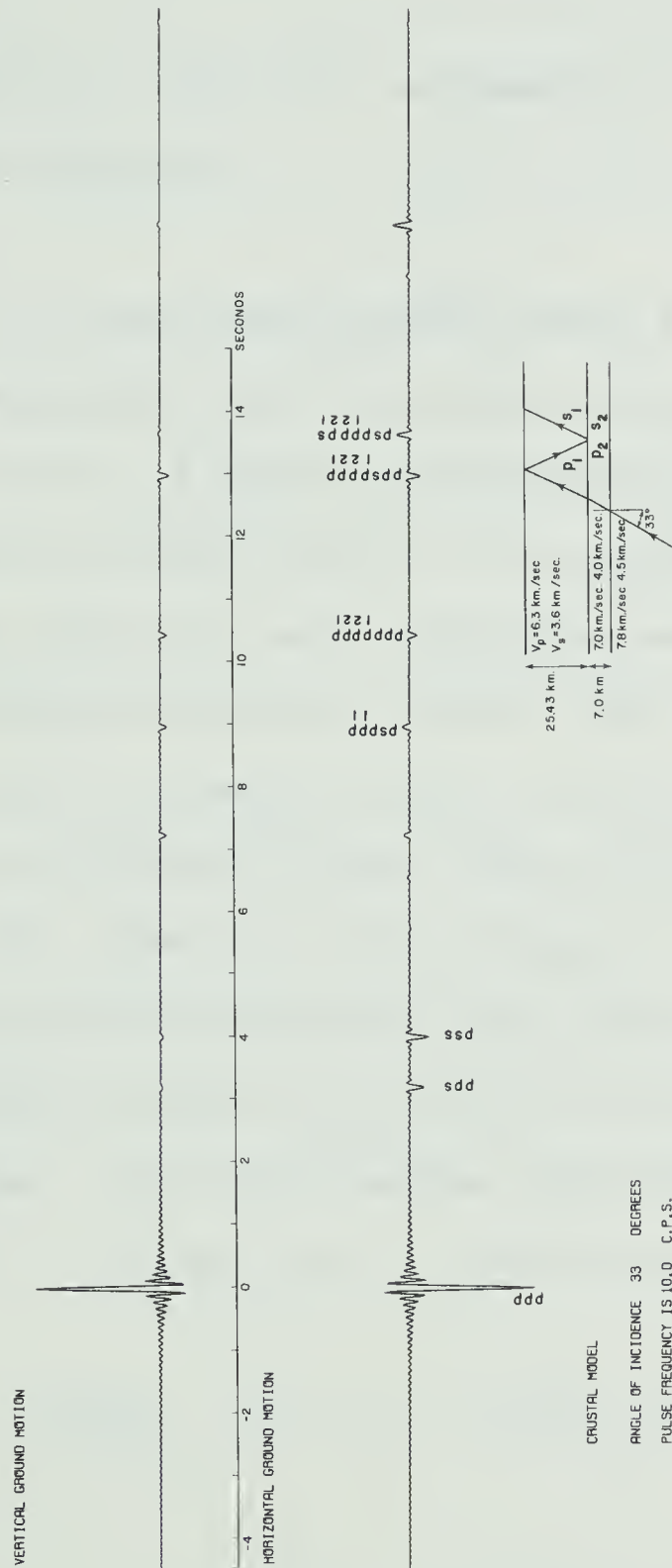
$$h(T) = \frac{1}{N} \sum_{W=0}^{N-1} (H_R(W) + i H_I(W)) e^{\frac{2\pi i WT}{N}} \quad 4.4$$

$$W = 0, 1, 2 \dots N-1$$

$$T = 0, 1, 2 \dots M-1$$

where $M \leq \frac{N}{2}$, W is a digital frequency index, and T is a digital time index. N is chosen according to the relation

Figure 4.3. Theoretical seismogram calculated for
Hanon's (1964) model



$$N = \frac{1}{\Delta t \cdot \Delta f}$$

where Δt and Δf are sampling intervals in time and frequency.

To check the program using a fast Fourier transform a seismogram was calculated using Hanon's (1964) crustal model. A comparison (Figure 4.3) shows that we can duplicate these results in a satisfactory manner. As a further check the same seismogram was calculated using another Fourier transform (Howe, 1956) with similar results. Another test is simply carried out for a simple layer model over an infinite half space using different angle of incidence. The converted phases (Figure 4.4) and multiple arrivals may be predicted by ray theory and these agree well in amplitude, phase and time with arrivals on the synthetic seismogram. For this case the difference in travel time between P arrival and S conversions is

$$\Delta t = \left(\frac{h_1}{\cos \phi_{1p}} \sin \phi_{1p} - \frac{h_1}{\cos \phi_{1s}} \sin \phi_{1s} \right) \frac{\sin \phi_{2p}}{\alpha_2} + \frac{h_1}{\beta_1 \cos \phi_{1s}} - \frac{h_1}{\alpha_1 \cos \phi_{1p}} \quad 4.5$$

where ϕ_{2p} is the angle of incidence below the interface for P waves.

ϕ_{1p} and ϕ_{1s} are the angles in the layer for P and converted S waves.

and α_i and β_i are P and S wave velocities in the i^{th} layer.

From Snell's law one can also write:

$$\frac{\alpha_1}{\sin \phi_{1p}} = \frac{\beta_1}{\sin \phi_{1s}} = \frac{\alpha_2}{\sin \phi_{2p}} \quad 4.6$$

Substituting equation 4.6 in equation 4.5 one can obtain

$$\Delta t = \frac{h_1}{\alpha_1} \left(\frac{\alpha_1}{\beta_1} \cos \phi_{1s} - \cos \phi_{1p} \right) \quad 4.7$$

Using the assumption, which was made in calculations of the transfer function, that Poisson's ratio is equal to 0.25 for the crust, equation 4.7 will have the form of

$$\Delta t = \frac{h_1}{\alpha_1} \left(\sqrt{3} \cos \phi_{1s} - \cos \phi_{1p} \right) \quad 4.8$$

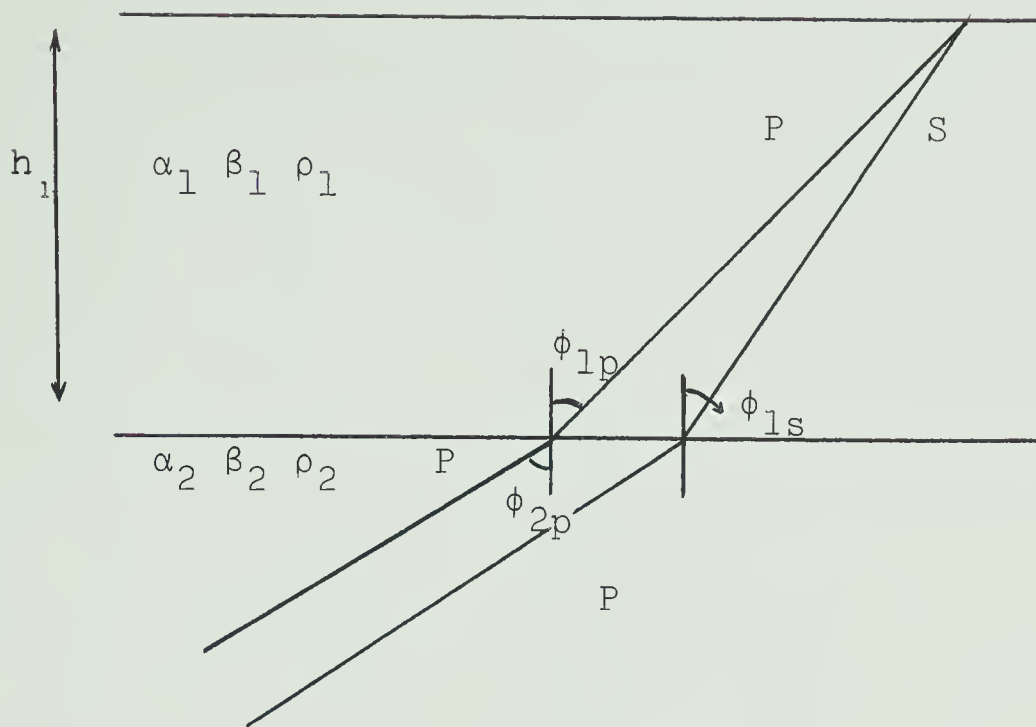


Figure 4.4. Conversion in a single layer model.

After assuring that the Fortran IV program designed to calculate synthesized ground motion worked properly, a theoretical seismogram was calculated (Figure 4.5) for a southern Alberta crustal model. The seismogram calculated is very complex because of arrivals of different converted phases from four interfaces, however, it is still possible to recognize and identify the late arriving converted phases. In calculating this seismogram the angle of incidence is taken to be 80° , this insures that the different phases are separated sufficiently in time and is a realistic approximation to field data at distances of 500 to 2000 km from the shot. A frequency interval of $\Delta f = 0.02$ c.p.s. and a time interval of $1/50$ second was

Figure 4.5. Theoretical ground motions for a southern Alberta model using a frequency interval $\Delta f = 0.02$ c.p.s.

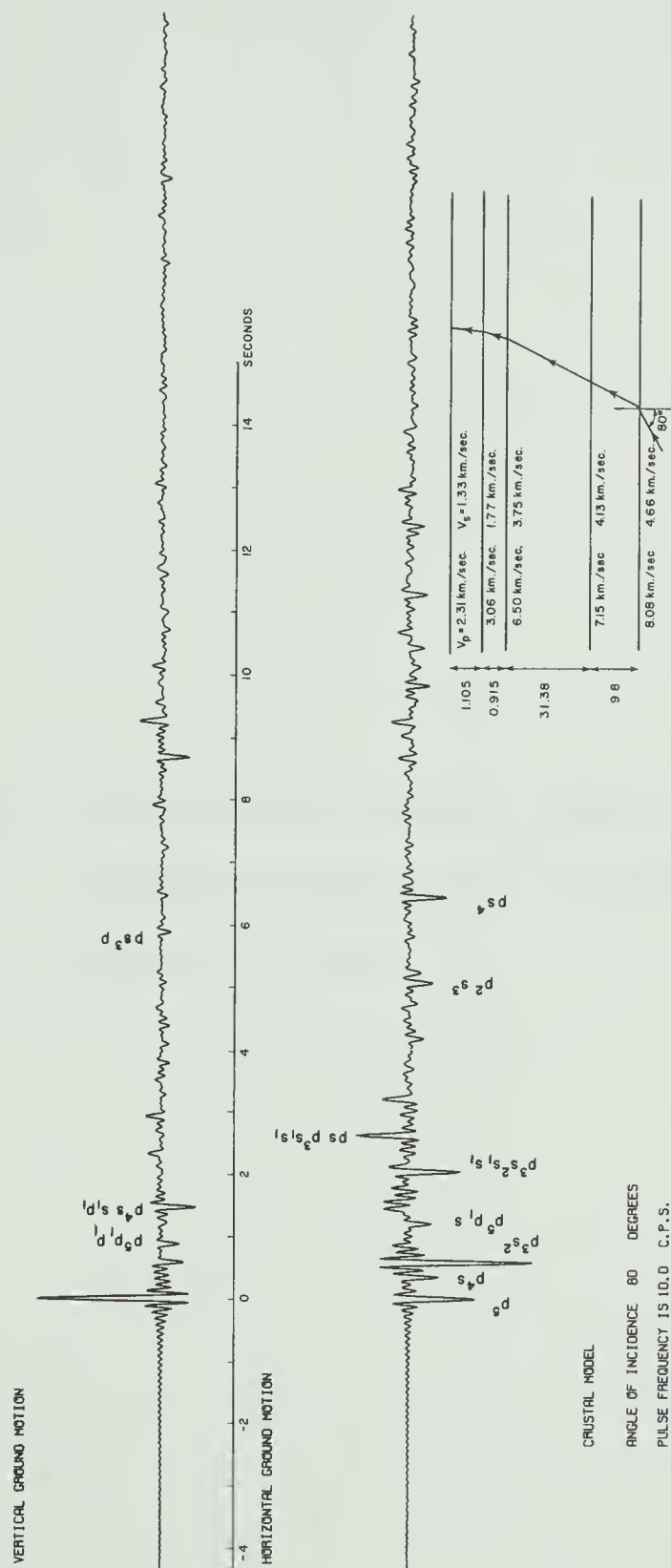
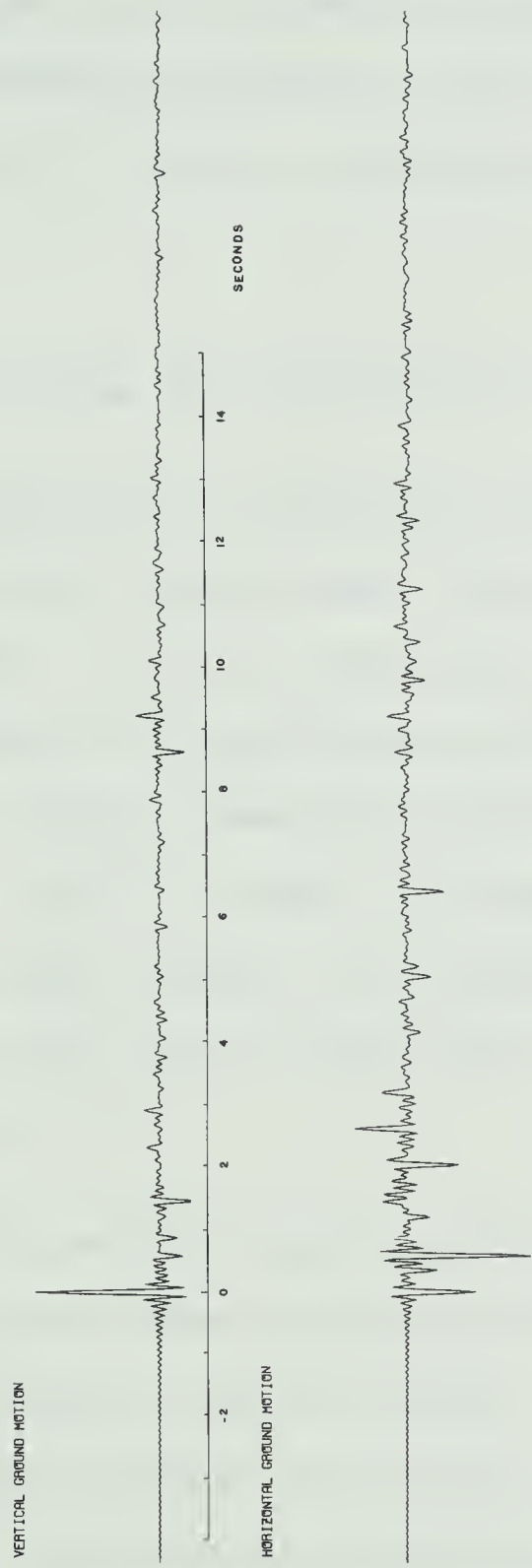


Figure 4.6. Theoretical ground motions for a southern Alberta model using a frequency interval $\Delta f = 0.005$ c.p.s.



CRUSTAL MODEL
ANGLE OF INCIDENCE 80 DEGREES
PULSE FREQUENCY IS 10.0 C.P.S.

used. The same seismogram was calculated using a frequency interval of $\Delta f = 0.005$ c.p.s. and a time interval of $1/40$ second (Figure 4.6), to check the stability of the seismogram. A frequency interval of $\Delta f = 0.02$ c.p.s. was found to sufficient to obtain a seismogram without any aliasing problems.

4.3 Field records and theoretical seismograms.

Theoretical seismograms obtained above for a southern Alberta crustal model (Table 1) are compared with field records. In this comparison, filtered field records were used since filtering enhanced the signals and removed much of the locally generated high frequency noise (Figure 2.20, 2.21, 2.22). To make the comparison of theoretical and observed data easier, the theoretically determined seismograms were also filtered with a Butterworth band pass filter (Figure 4.7).

The vertical and horizontal components of the field seismograms show similarities with the one obtained by the Thomson-Haskell matrix formula. Many field seismograms are complicated because of arrivals from the mantle. In figure 4.8, a theoretical seismogram compared with the field seismogram for two pulses of energy travelling by different paths in the upper mantle. The comparison for the two

arrivals show substantial agreement between the field data and the theoretical seismograms. The comparison is not very good at certain locations (Figure 4.9) which means that models must be modified using the results obtained in Chapter 3.

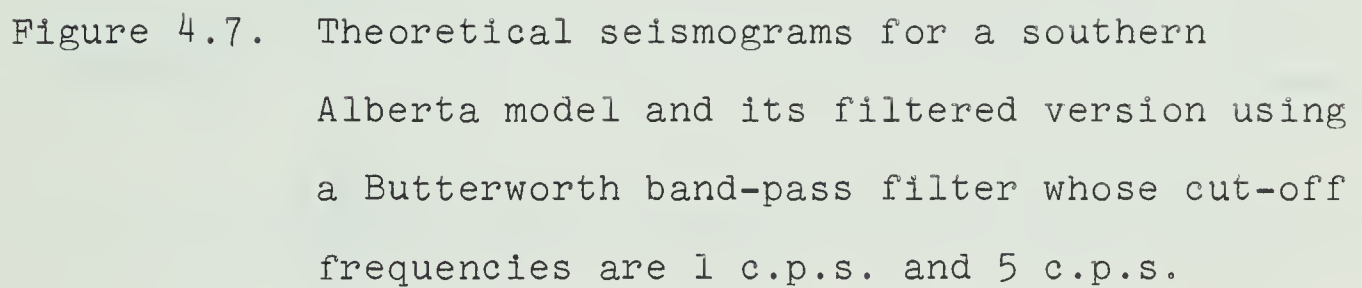
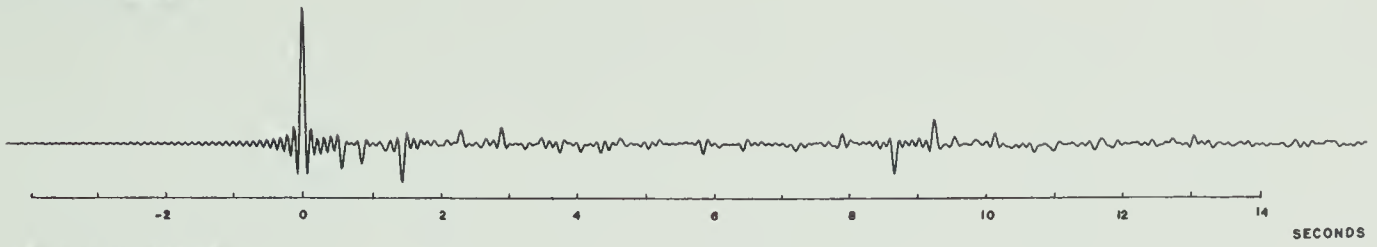


Figure 4.7. Theoretical seismograms for a southern Alberta model and its filtered version using a Butterworth band-pass filter whose cut-off frequencies are 1 c.p.s. and 5 c.p.s.

VERTICAL GROUND MOTION



HORIZONTAL GROUND MOTION

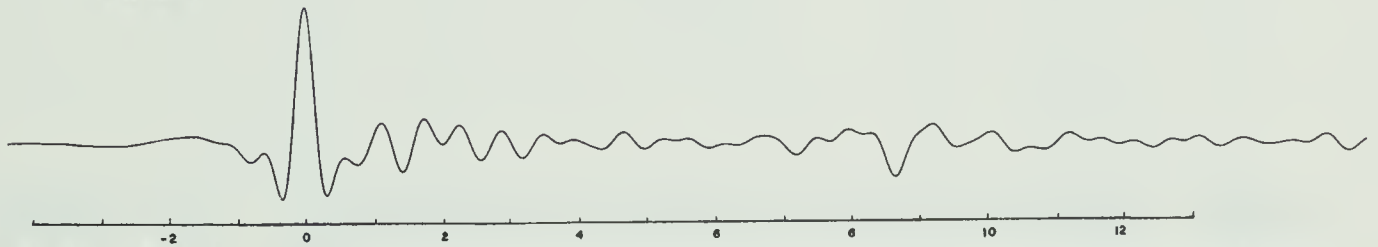


CRUSTAL MODEL

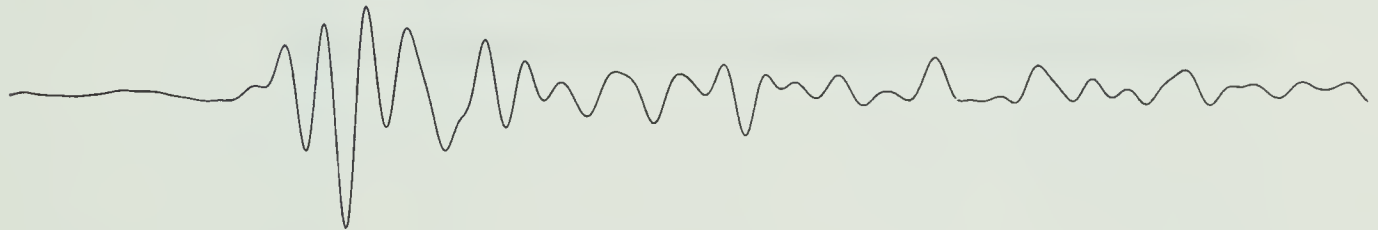
ANGLE OF INCIDENCE 80 DEGREES

PULSE FREQUENCY IS 10.0 C.P.S.

VERTICAL GROUND MOTION



HORIZONTAL GROUND MOTION



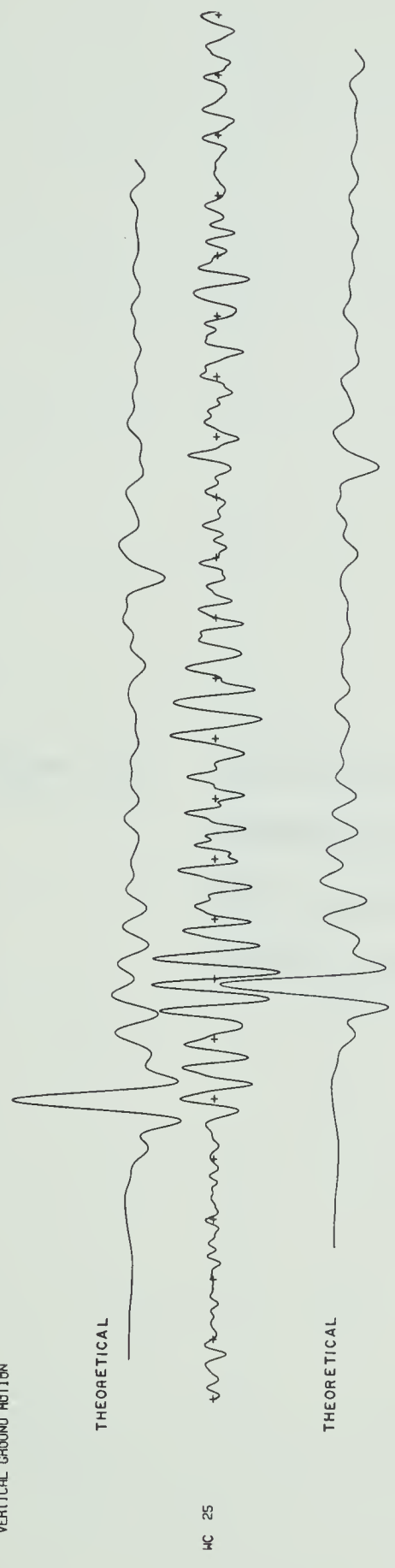
CRUSTAL MODEL

ANGLE OF INCIDENCE 80 DEGREES

PULSE FREQUENCY IS 10.0 C.P.S.

Figure 4.8. Comparison of vertical and horizontal components of a field record with the theoretical seismograms for a southern Alberta model

VERTICAL GROUND MOTION



CRUSTAL MODEL
ANGLE OF INCIDENCE 80 DEGREES
PULSE FREQUENCY IS 10.0 C.P.S.

HORIZONTAL GROUND MOTION



Figure 4.9. Additional comparison of vertical and horizontal components of a field record with the theoretical seismograms for a southern Alberta model

VERTICAL GROUND MOTION



CRUSTAL MODEL
ANGLE OF INCIDENCE 80 DEGREES
PULSE FREQUENCY IS 10.0 C.P.S.

HORIZONTAL GROUND MOTION



BIBLIOGRAPHY

- Baum, R.F., A contribution to the approximation problem,
Proc. I.R.E. Vol. 36, no. 7, July, 1948.
- Blackman, R.B. and Tukey, J.W., The measurement of power
spectra, Dower Publications, Inc., New York, 1958.
- Birch, F., Density and composition of mantle and core,
J. Geoph. Res., 69, 4377-4388, 1964.
- Butterworth, S., On the theory of filter amplifiers,
Wireless Engr. 1, 536-541, 1930.
- Cooley, J.W. and Tukey, J.W., An algorithm for the machine
calculation of complex Fourier series, 90, Mathematics
of computation, 19, 297-301, 1965.
- Constain, J.K., Robinson, E.S. and Cook, K.L., Ground motion
diagrams from pulse transmission through simple layered
structures, Jour. Geoph. Res., 72, 2577-2582, 1967.
- Cumming, G.L., and Kanasewich, E.R., Seismic arrivals from
the Earth's upper mantle, Nature, 206, 248-249, 1965.
- Cumming, G.L., and Kanasewich, E.R., Crustal structure in
Western Canada, final report, contract no. AF19(628)-
2835, 1966.

Dorman, J., Period equation for waves of Rayleigh type on a layered liquid-solid half-space, Bull. Seis. Soc. Am., 52, 389-397, 1962.

Dunkin, J.W., Computation of model solutions in layered, elastic media at high frequencies, Bull. Seis. Soc. Am., 55, 335-358, 1965.

Ewing, W.M., Jardetzky, W.S., and Press, F., Elastic waves in layered media, McGraw-Hill Book Comp. Inc., New York, 1957.

Fernandez, L.M., The determination of crustal thickness from the spectrum of P waves, Scientific report No. 13, Contract AF19(604)7399, Project 865201, 1965.

Ford, W.T. and Hearne, J.H., Least-squares inverse filtering, Geophysics, Vol. 31, No. 5, 917-926, 1966.

Golden, R.M. and Kaiser, J.B., Design of wideband sampled-data filter, the Bell System Tech. Jour., V. 43, P. 1533-1646, 1964.

Guillemin, E.A., Synthesis of passive networks, John Wiley and Sons, Inc., New York, 1957.

Gutenberg, B., Effects of ground on Earth's motion, Bull. Seis. Soc. Am., 47, 221-249, 1957.

Hanon, W.J., An application of the Haskell-Thomson matrix method to the synthesis of the surface motion due to dilatational waves, Bull. Seis. Soc. Am. 54, 2607-2079, 1964.

Hanon, W.J., Some effects of a layered system on dilatational wave, Tech. Report No. 3, St. Louis Univ. Contract AF19(604)-7399, 1964.

Haskell, N.A., The dispersion of surface waves in multilayered media, Bull, Seis. Soc. Am., 43, 17-34, 1953.

Haskell, N.A., Crustal reflection of plane SH waves, J. Geophy. Res., 65, 4147-4150, 1960.

Haskell, N.A., Crustal reflection of plane P and SV waves, Jour. Geophy. Res. 67, 4751-4767, 1962.

Holtz, H., and Leondes, C.T., The synthesis of recursive digital filters, Jour. ACM, V. 13, No. 2, 262-280, 1966.

Howe, H.S., Fourier analysis of non-periodic pulses on automatic computer, National Bureau of Standards Report 5018, 1956.

Imamura, A., On the Earth-vibrations induced in some localities at the arrival of seismic waves, Bull. Earthq. Res. Inst. (Tokyo) 7, 489-494, 1929.

- Jury, E.I., Theory and application of the z-transform method, John Wiley and Sons, Inc., New York, 1964.
- Kaiser, J.F., Design methods for sampled data filters, Proc. First Allerton Conference on circuit and system theory, Monticello, III; 221-236, 1963.
- Kaiser, J.F., Some practical considerations in the realization of linear digital filters, Proc. Third Allerton Conference on circuit and system theory, Monticello, III; 621-633, 1966.
- Kanai, K., Relation between the nature of surface layer and the amplitudes of earthquake motions, Bull. Earthq. Res. Ins. (Tokyo), 30, 30-39, 1952.
- Kanai, K., Relation between the nature of surface layer and the amplitudes of earthquake motions, part II, Bull. Earthq. Res. Inst. (Tokyo) 31, 219-226, 1953a.
- Kanai, K., Relation between the nature of surface layer and the amplitude of earthquake motions, part III, Bull. Earthq. Res. Inst. (Tokyo), 31, 275-279, 1953b.
- Leblanc, G., Spectral analysis of short-period first arrivals of the 13th of April 1963 Peruvian earthquake, Ph.D. thesis, The Pennsylvania State University, 143 pp., 1966.

- McCamy, K., An investigation and application of the crustal transfer ratio as a diagnostic for explosion seismology, Bull. Seis. Soc. Am., 57, 1409-1428, 1967.
- Nasu, N., Comparative studies of Earthquake motions above-ground and in a tunnel, Part I, Bull, Earthq. Res. Inst. (Tokyo), 9, 454-472, 1931.
- Nuttli, O., Some observations relating to the effect of the crust on long-period P wave motion, Bull. Seis. Soc. Am., 54, 141-149, 1964.
- Ormsby, J.F.A., Design of numerical filters with applications to missile data processing, J. Assoc. Computing Mach. 8(4), 440-466, 1961.
- Phinney, R.A., Structure of the Earth's crust from spectral behavior of long-period body waves. Jour. Geophys. Res. 69, 2997-3017, 1964.
- Robinson, E.A., Extremal properties of the world decomposition, Jour. Math. Analysis and Application, Vol. 6, No. 1, 75-85, 1963.
- Robinson, E.A. and Treitel, S., Principles of digital filtering, Geophy. Vol. 29, 3, 395-404, 1964.

- Robinson, E.A. and Treitel, S., Dispersive digital filters, Reviews of Geophysics, Vol. 3. No. 4, 433-461, 1965.
- Robinson, E.A., Multichannel z-transforms and minimum delay, Geophy. Vol. 31, No. 3, 482-500, 1966.
- Robinson, E.A. and Treitel, S., Principle of digital wiener filtering, Geophy. Pros. Vol. 15, No. 3, 311-333, 1967.
- Sezawa, K., Possibility of the free oscillations of the surface layer excited by the seismic waves, Bull. Earthq. Res. Inst. (Tokyo), 8, 1-11, 1930.
- Sezawa, K. and Kanai, K., Possibility of the free oscillations of strata excited by seismic waves, III, Bull. Earthq. Res. Inst. (Tokyo), 10, 1-18, 1932a.
- Sezawa, K. and Kanai, K., Possibility of free oscillations of strata excited by seismic waves, IV, Bull. Earthq. Res. Inst., 10, 273-298, 1932b.
- Sezawa, K., and Kanai, K., On the free vibrations of a surface layer due to an obliquely incident disturbance, Bull. Earthq. Res. Inst., (Tokyo), 15, 375-383, 1937.
- Shanks, J.L., Recursion filters for digital processing, Geophy. Vol. 32, No. 1, 33-51, 1967.

- Stallings, C.B., The use of semi-recursive polynomials in the design of numerical filters, Proc. AFIPS Conf. 29, 549-561, 1966.
- Suzuki, T., On the angle of incidence of the initial motion observed at Hongo and Mikita, Bull. Earthq. Res. Inst. (Tokyo), 10, 517-530, 1932.
- Thomson, W.T., Transmission of elastic waves through a stratified solid medium, J. Appl. Phys., 21, 89-93, 1950.
- Treitel, S. and Robinson, E.A., The stability of digital filters, Trans. Geoscience Electronics, V. 2, 1964.
- Treitel, S. and Robinson, E.A., The design of high resolution digital filters, Trans. Geoscience Electronics, V. 4, 25-38, 1966.
- Truxal, J.G., Automatic feedback control system synthesis, McGraw-Hill Book Co. Inc., New York, 531, 1955.
- Weinberg, L., Network Analysis and Synthesis, McGraw Hill Book Co. Inc., New York, 485-498, 1962.
- Wiener, N., Extrapolation and smoothing of stationary time series, Cambridge, M.I.T Press, 1949.
- Wood, L.C., A review of digital filtering, Reviews of Geophysics, Vol. 6, No. 1, 73-97, 1968.

APPENDIX 1

THOMSON-HASKELL MATRIX

FORMULATION

A.1.1. Introduction.

This appendix is the summary of following papers: Haskell (1953), Haskell (1960), Haskell (1962) Thomson (1950). The following notation is used in this section:

$$\Theta = \frac{\partial u}{\partial x} + \frac{\partial v}{\partial y} + \frac{\partial w}{\partial z} : \text{Cubical dilation}$$

$$\Omega_{ij} = 1/2 \left(\frac{\partial u_j}{\partial x_i} - \frac{\partial u_i}{\partial x_j} \right) : \text{Rotation vector (Anti-symmetric vector)}$$

$$\alpha = \sqrt{\frac{\lambda + 2\mu}{\rho}} : \text{Velocity of P waves.}$$

λ, μ, ρ are Lamé constants and density.

$$\beta = \sqrt{\frac{\mu}{\rho}} : \text{Velocity of S wave.}$$

$$k_\alpha = \frac{\omega}{\alpha} = \text{wave number} = \frac{2\pi}{\text{wavelength}}$$

$$k_\beta = \frac{\omega}{\beta} = \text{wave number.}$$

c = Apparent phase velocity measured along the surface.

$$k_c = \frac{\omega}{c} = \frac{2\pi}{\text{Horizontal wavelength}} = \frac{2\pi}{\lambda_H} : \text{ Apparent wave-}$$

number as measured along the surface.

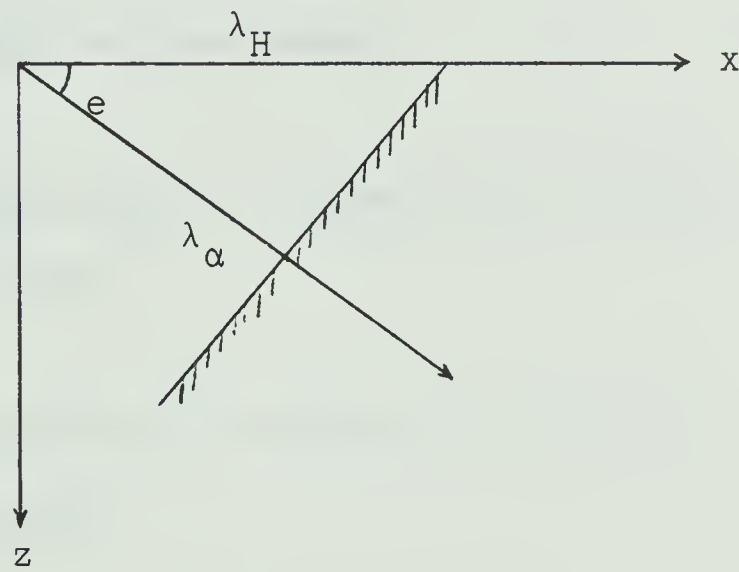


Figure A.1.1. Wavelength and wavefront of a wave propagating in z direction.

$$\cos e = \frac{\lambda_\alpha}{\lambda_H} \quad (\text{Figure A1.1}).$$

$$P_{ij} = \lambda \theta \delta_{ij} + \mu \left(\frac{\partial u_j}{\partial x_i} + \frac{\partial u_i}{\partial x_j} \right) = \text{stress tensor.}$$

$$\delta_{ij} = \begin{cases} 1 & i = j \quad \text{normal stress} \\ 0 & i \neq j \quad \text{shear stress} \end{cases}$$

$l_\alpha, m_\alpha, n_\alpha$ = Direction cosines of the normal to the advancing dilatation wave front with respect to x, y, z axes.

$l_\beta, m_\beta, n_\beta$ = Direction cosines of the normal to the rotational wave front with respect to x, y, z axes.

θ_o = Angle of incidence.

ϕ_i, ϕ_r, ϕ_t = Amplitude of incident, reflected, transmitted P waves.

$\Omega_i, \Omega_r, \Omega_t$ = Amplitude of incident, reflected, transmitted S waves.

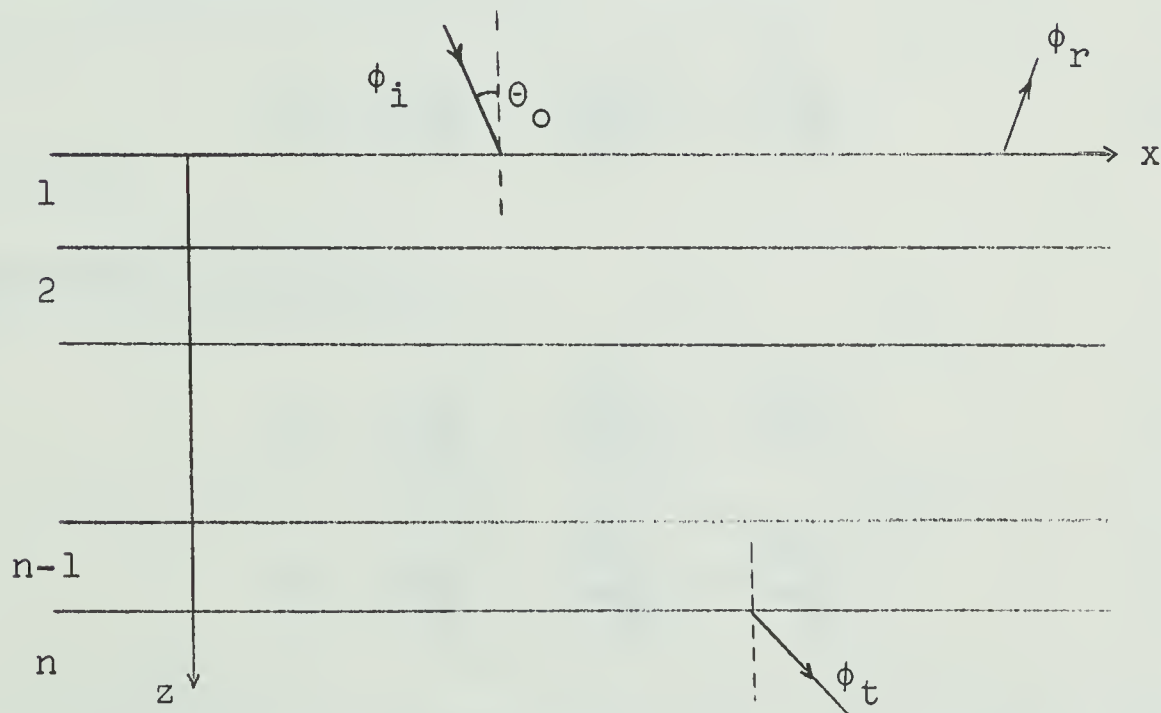


Figure A.1.2. Incident, reflected and transmitted waves in an n layer model.

A.1.2. Wave Equations and plane wave solution.

Differentiating cubical dilatational with respect to x :

$$\frac{\partial \Theta}{\partial x} = \frac{\partial^2 u}{\partial x^2} + \frac{\partial^2 v}{\partial x \partial y} + \frac{\partial^2 \omega}{\partial x \partial z} \quad \text{A.1.1}$$

adding and subtracting the term $[\pm(\frac{\partial^2 u}{\partial y^2} + \frac{\partial^2 u}{\partial z^2})]$:

$$\frac{\partial \Theta}{\partial x} = \left(\frac{\partial^2 u}{\partial x^2} + \frac{\partial^2 u}{\partial y^2} + \frac{\partial^2 u}{\partial z^2} \right) + \frac{\partial}{\partial y} \left(\frac{\partial v}{\partial x} - \frac{\partial u}{\partial y} \right) - \frac{\partial}{\partial z} \left(\frac{\partial u}{\partial z} - \frac{\partial \omega}{\partial x} \right) \quad \text{A.1.2}$$

Since $\Omega_z = \frac{\partial v}{\partial x} - \frac{\partial u}{\partial y}$ and $\Omega_y = \frac{\partial u}{\partial z} - \frac{\partial \omega}{\partial x}$

And rearranging equation A.1.2 we get

$$\nabla^2 u = \frac{\partial \Theta}{\partial x} - 2 \frac{\partial \Omega_z}{\partial y} + 2 \frac{\partial \Omega_y}{\partial z} \quad \text{A.1.3}$$

Similarly we can write

$$\nabla^2 v = \frac{\partial \Theta}{\partial y} - 2 \frac{\partial \Omega_x}{\partial z} + 2 \frac{\partial \Omega_z}{\partial x} \quad \text{A.1.4}$$

$$\nabla^2 \omega = \frac{\partial \Theta}{\partial z} - 2 \frac{\partial \Omega_y}{\partial x} + 2 \frac{\partial \Omega_x}{\partial y} \quad \text{A.1.5}$$

A plane dilatational and rotational wave will have the form:

$$\Theta = e^{i\{\omega t - k_{\alpha}(\ell_{\alpha}x + m_{\alpha}y + \eta_{\alpha}z)\}} \quad A.1.6$$

$$\Omega = e^{i\{\omega t - k_{\beta}(\ell_{\beta}x + m_{\beta}y + \eta_{\beta}z)\}} \quad A.1.7$$

Displacement can be written as

$$u_{\theta} = e^{i\{\omega t - k_{\alpha}(\ell_{\alpha}x + m_{\alpha}y + \eta_{\alpha}z)\}} \quad A.1.8$$

Substituting into A.1.3 the equation of wave will be

$$\nabla^2 u_{\theta} = -k_{\alpha}^2(\ell_{\alpha}^2 + m_{\alpha}^2 + \eta_{\alpha}^2)u_{\theta} = -k_{\alpha}^2 u_{\theta} \quad A.1.9$$

The solution of equation A.1.3 can be written as

$$u = -\frac{1}{k_{\alpha}^2} \frac{\partial \Theta}{\partial x} + \frac{2}{k_{\beta}^2} \frac{\partial \Omega_z}{\partial y} - \frac{2}{k_{\beta}^2} \frac{\partial \Omega_x}{\partial z} \quad A.1.10$$

Similarly

$$v = -\frac{1}{k_{\alpha}^2} \frac{\partial \Theta}{\partial y} + \frac{2}{k_{\beta}^2} \frac{\partial \Omega_x}{\partial z} - \frac{2}{k_{\beta}^2} \frac{\partial \Omega_z}{\partial x} \quad A.1.11$$

$$w = -\frac{1}{k_{\alpha}^2} \frac{\partial \Theta}{\partial z} + \frac{2}{k_{\beta}^2} \frac{\partial \Omega_y}{\partial x} - \frac{2}{k_{\beta}^2} \frac{\partial \Omega_x}{\partial y} \quad A.1.12$$

It is assumed that a plane wave is propagating in the positive x and z directions with the amplitude diminish-

ing exponentially in the positive direction. The plane wave solution is then

$$\theta = e^{i(\omega t - k_\alpha \ell_\alpha x)} \{ \theta_t e^{i\eta_\alpha k_\alpha z} + \theta_r e^{i\eta_\alpha k_\alpha z} \} \quad A.1.13$$

$$\Omega_y = e^{i(\omega t - k_\beta \ell_\beta x)} \{ \Omega_t e^{-i\eta_\alpha k_\alpha z} + \Omega_r e^{i\eta_\beta k_\beta z} \} \quad A.1.14$$

For a two dimensional plane wave the cubical dilatational only components of the rotation vector are

$$\theta = \frac{\partial u}{\partial x} + \frac{\partial \omega}{\partial z} \quad A.1.15$$

$$\Omega_y = 1/2 \left(\frac{\partial u}{\partial z} - \frac{\partial \omega}{\partial x} \right) \quad A.1.16$$

By substituting in equations A.1.10, A.1.11, A.1.12 the partial velocities are found to be

$$\dot{u} = \frac{-\omega \ell_\alpha \theta}{k_\alpha} - \frac{2\omega \eta_\beta}{k_\beta} e^{i(\omega t - k_\beta \ell_\beta x)} \{ \Omega_t e^{-i\eta_\beta k_\beta z} - \Omega_r e^{i\eta_\beta k_\beta z} \} \quad A.1.17$$

$$\dot{\omega} = - \frac{\omega \eta_\alpha}{k_\alpha} e^{i(\omega t - k_\alpha \ell_\alpha x)} \{ \theta_t e^{-i\eta_\alpha k_\alpha z} - \theta_r e^{i\eta_\alpha k_\alpha z} \} + \frac{2\ell_\beta \omega}{k_\beta} \Omega_y \quad A.1.18$$

Dropping the term $e^{i\omega t}$ in equations A.1.17 and A.1.18 and letting $x = 0$,

$$\begin{aligned} P &= \eta_{\alpha} k_{\alpha} z \\ Q &= \eta_{\beta} k_{\beta} z \end{aligned} \quad \text{A.1.19}$$

the equations become

$$\begin{aligned} \dot{u} = & -\frac{\omega \ell_{\alpha}}{k_{\alpha}} \cos P \{\theta_t + \theta_r\} + \frac{i\omega \ell_{\alpha}}{k_{\alpha}} \sin P \{\theta_t - \theta_r\} - \\ & \frac{2\omega \eta_{\beta}}{k_{\beta}} \cos Q \{\Omega_t - \Omega_r\} + \frac{i2\omega \eta_{\beta}}{k_{\beta}} \sin Q \{\Omega_t + \Omega_r\} \end{aligned} \quad \text{A.1.20}$$

and

$$\begin{aligned} \dot{\omega} = & \frac{-\omega \eta_{\alpha}}{k_{\alpha}} \cos P \{\theta_t - \theta_r\} + \frac{i\omega \eta_{\alpha}}{k_{\alpha}} \sin P \{\theta_t + \theta_r\} + \\ & + \frac{2\omega \ell_{\beta}}{k_{\beta}} \cos Q \{\Omega_t + \Omega_r\} - \frac{i2\omega \ell_{\beta}}{k_{\beta}} \sin Q \{\Omega_t - \Omega_r\} \end{aligned} \quad \text{A.1.21}$$

The P wave velocity can be written as

$$\alpha = \frac{\omega}{k_{\alpha}} \quad \text{A.1.22}$$

and the horizontal phase velocity as

$$c = \frac{\omega}{k} \quad \text{A.1.23}$$

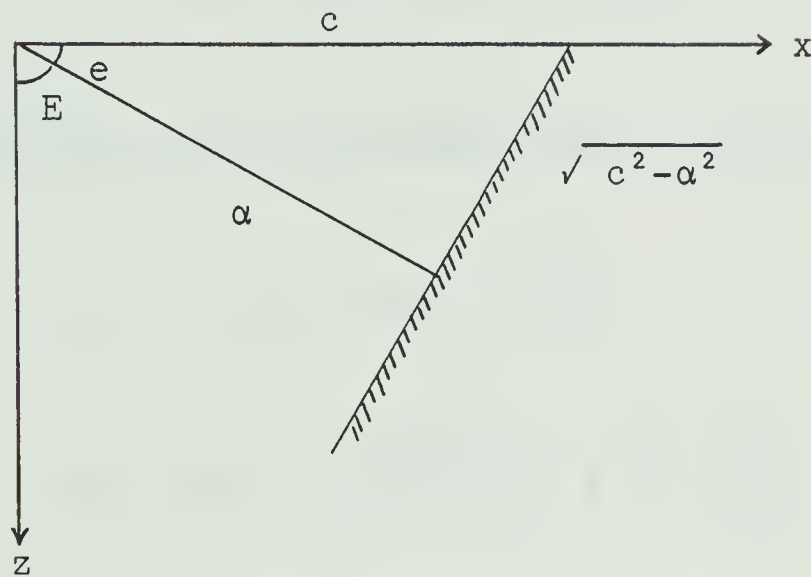


Figure A.1.3

$$k_{\alpha} = \frac{c k}{\alpha} \quad \text{A.1.24}$$

From figure A.1.3 the following relations are evident:

$$l_{\alpha} = \cos e = \frac{\alpha}{c} \quad \text{A.1.25}$$

$$\eta_{\alpha} = \cos E = \frac{\sqrt{c^2 - \alpha^2}}{c} = \sqrt{1 - \frac{\alpha^2}{c^2}} \quad \text{A.1.26}$$

$$r_{\alpha} = \tan e = \frac{\sqrt{c^2 - \alpha^2}}{\alpha} = \sqrt{\frac{c^2}{\alpha^2} - 1} \quad c > \alpha \quad \text{A.1.27}$$

Similarly S wave velocity can be written as:

$$\beta = \frac{\omega}{k_{\beta}} \quad \text{A.1.28}$$

$$k_{\beta} = \frac{c k}{\beta} \quad \text{and} \quad c = \frac{\omega}{k} \quad \text{A.1.29}$$

From figure A.1.4 the following relations also hold:

$$l_{\beta} = \cos f = \frac{\beta}{c} \quad \text{A.1.30}$$

$$\eta_{\beta} = \cos F = \frac{\sqrt{c^2 - \beta^2}}{c} = \sqrt{1 - \frac{\beta^2}{c^2}} \quad \text{A.1.31}$$

$$r_{\beta} = \operatorname{tg} f = \frac{\sqrt{c^2 - \beta^2}}{\beta} = \sqrt{\frac{c^2}{\beta^2} - 1} \quad c > \beta \quad \text{A.1.32}$$

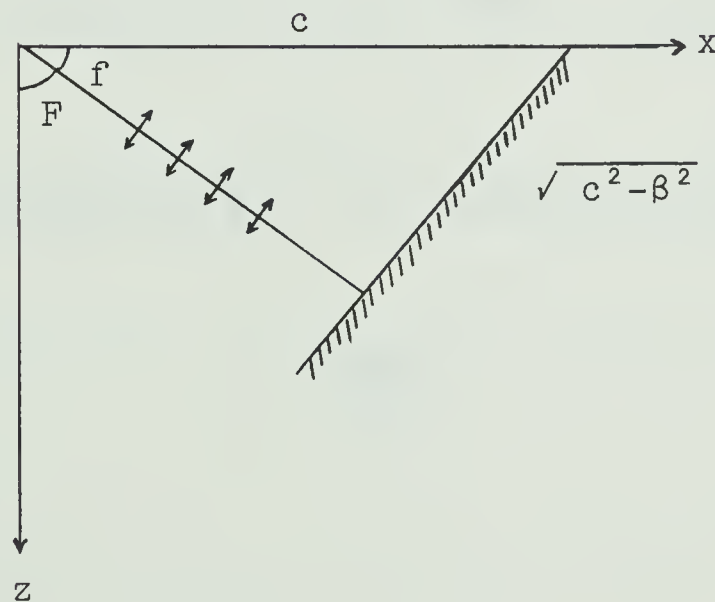


Figure A.1.4.

In equations A.1.20 and A.1.21 using the relations:

$$\frac{\omega}{k_\alpha} \ell_\alpha \cos(\eta_\alpha k_\alpha z) = c \frac{\alpha^2}{c^2} \cos(kr_\alpha z) \quad \text{A.1.33}$$

and

$$\frac{2\omega\eta_\beta}{k_\beta} \cos(\eta_\beta k_\beta z) = \frac{2c\beta^2}{c^2} r_\beta \cos(kr_\beta z) \quad \text{A.1.34}$$

It can be written as

$$\begin{aligned} \frac{\dot{u}}{c} = & - \frac{\alpha^2}{c^2} \cos(kr_\alpha z) \{\theta_t + \theta_r\} + \frac{i\alpha^2}{c^2} \sin(kr_\alpha z) \{\theta_t - \theta_r\} \\ & - \gamma r_\beta \cos(kr_\beta z) \{\Omega_t - \Omega_r\} + i\gamma r_\beta \sin(kr_\beta z) \{\Omega_t - \Omega_r\} \end{aligned} \quad \text{A.1.35}$$

$$\begin{aligned} \frac{\dot{w}}{c} = & - \frac{\alpha^2}{c^2} r_\alpha \cos(kr_\alpha z) \{\theta_t - \theta_r\} + \frac{i\alpha^2}{c^2} r_\alpha \sin(kr_\alpha z) \{\theta_t + \theta_r\} + \\ & + \gamma \cos(kr_\beta z) \{\Omega_t + \Omega_r\} - i\gamma \sin(kr_\alpha z) \{\Omega_t - \Omega_r\} \end{aligned} \quad \text{A.1.36}$$

where

$$\gamma = \frac{2\beta^2}{c^2}$$

A.1.3. Equations of stress.

Normal stress can be written as

$$P_{zz} = \lambda \theta + 2\mu \left\{ -\frac{1}{k_{\alpha}^2} \frac{\partial^2 \theta}{\partial z^2} + \frac{2}{k_{\beta}} \frac{\partial^2 \Omega_y}{\partial x \partial z} - \frac{2}{k_{\beta}^2} \frac{\partial^2 \Omega_x}{\partial y \partial z} \right\} \quad A.1.37$$

and shear stress:

$$\begin{aligned} P_{xz} = 2\mu \left\{ -\frac{1}{2k_{\alpha}^2} \frac{\partial^2 \theta}{\partial x \partial z} + \frac{1}{k_{\beta}^2} \frac{\partial^2 \Omega_z}{\partial y \partial z} - \frac{1}{k_{\beta}^2} \frac{\partial^2 \Omega_y}{\partial z^2} - \frac{1}{k_{\alpha}^2} \frac{\partial^2 \theta}{\partial z \partial x} \right. \\ \left. + \frac{1}{k_{\beta}^2} \frac{\partial^2 \Omega_y}{\partial x^2} + \frac{1}{k_{\beta}^2} \frac{\partial^2 \Omega_x}{\partial y \partial x} \right\} \quad A.1.38 \end{aligned}$$

Using the equations A.1.13 and A.1.14 and arranging terms, the equation A.1.37 can be written as

$$\begin{aligned} P_{zz} = -\rho \alpha^2 (\gamma - 1) \cos P \{ \theta_t + \theta_r \} + i \rho \alpha^2 (\gamma - 1) \sin P \{ \theta_t - \theta_r \} \\ - \rho c^2 \gamma^2 r_{\beta} \cos Q \{ \Omega_t - \Omega_r \} + i \rho c^2 \gamma^2 r_{\beta} \sin Q \{ \Omega_t + \Omega_r \} \end{aligned}$$

A.1.39

Similarly

$$\begin{aligned}
P_{xz} = & \rho\gamma\alpha^2 r_\alpha \cos P \{ \theta_t - \theta_r \} - i\rho\gamma\alpha^2 r_\alpha \sin P \{ \theta_t + \theta_r \} \\
& - \rho c^2 \gamma(\gamma-1) \cos Q \{ \Omega_t + \Omega_r \} + i\rho c^2 \gamma(\gamma-1) \sin Q \{ \Omega_t - \Omega_r \}
\end{aligned}$$

A.1.40

A.1.4. Matrix formulation and transfer functions.

Equation A.1.35, A.1.36, A.1.39 and A.1.40 can be written at the m^{th} interface.

$$\begin{aligned}
\frac{\dot{u}}{c} = & - \frac{\alpha_m^2}{c^2} \cos P_m \{ \theta_{t_m} + \theta_{r_m} \} + \frac{i\alpha_m^2}{c^2} \sin P_m \{ \theta_{t_m} - \theta_{r_m} \} \\
& - \gamma_m r_{\beta_m} \cos Q \{ \Omega_{t_m} - \Omega_{r_m} \} + i\gamma_m r_{\beta_m} \sin Q_m \{ \Omega_{t_m} - \Omega_{r_m} \}
\end{aligned}$$

A.1.41

$$\begin{aligned}
\frac{\dot{\omega}_m}{c} = & \frac{i\alpha_m^2}{c^2} r_{\alpha_m} \sin P_m \{ \theta_{t_m} + \theta_{r_m} \} - \frac{\alpha_m^2}{c^2} r_{\alpha_m} \cos P_m \{ \theta_{t_m} - \theta_{r_m} \} \\
& - i\gamma_m \sin Q_m \{ \Omega_{t_m} - \Omega_{r_m} \} + \gamma_m \cos Q_m \{ \Omega_{t_m} + \Omega_{r_m} \}
\end{aligned}$$

A.1.42

$$\begin{aligned}
P_{zz} = & - \rho_m \alpha_m^2 (\gamma_m - 1) \cos P_m \{ \theta_{t_m} + \theta_{r_m} \} + i\rho_m \alpha_m^2 (\gamma_m - 1) \sin P_m \{ \theta_{t_m} - \theta_{r_m} \} \\
& - \rho_m c^2 \gamma_m^2 r_{\beta_m} \cos Q_m \{ \Omega_{t_m} - \Omega_{r_m} \} + i\rho_m c^2 \gamma_m r_{\beta_m} \sin Q_m \{ \Omega_{t_m} + \Omega_{r_m} \}
\end{aligned}$$

A.1.43

A.13

$$\begin{aligned}
P_{xz} = & -i\rho_m\gamma_m\alpha_m^2r_{\alpha_m}\sin P_m\{\theta_t+\theta_r\} + \rho_m\gamma_m\alpha_m^2r_{\alpha_m}\cos P_m\{\theta_{t_m}-\theta_{r_m}\} \\
& - \rho_mc^2\gamma_m(\gamma_m-1)\cos Q_m\{\Omega_{t_m}+\Omega_{r_m}\} + i\rho_mc^2\gamma_m(\gamma_m-1)\sin Q_m\{\Omega_{t_m}-\Omega_{r_m}\}
\end{aligned}$$

A.1.44

Equations A.1.41, A.1.42, A.2.43, A.1.44 can be expressed in matrix form:

$$\begin{bmatrix} \frac{\dot{u}_m}{c} \\ \frac{\dot{\omega}_m}{c} \\ P_{zz_m} \\ P_{xz_m} \end{bmatrix} = D_m \begin{bmatrix} \theta_{t_m} + \theta_{r_m} \\ \theta_{t_m} - \theta_{r_m} \\ \Omega_{t_m} - \Omega_{r_m} \\ \Omega_{t_m} + \Omega_{r_m} \end{bmatrix}$$

A.1.45

where the elements of the matrix D_m are

$$(d_m)_{11} = -\frac{\alpha_m^2}{c} \cos P_m$$

$$(d_m)_{12} = \frac{i\alpha_m^2}{c^2} \sin P_m$$

$$(d_m)_{13} = -\gamma_m r_{\beta_m} \cos Q_m$$

$$(d_m)_{14} = i\gamma_m r_{\beta_m} \sin Q_m$$

$$(d_m)_{21} = \frac{i\alpha_m^2}{c^2} r_{\alpha_m} \sin P_m$$

$$(d_m)_{22} = \frac{-\alpha_m^2}{c^2} r_{\alpha_m} \cos P_m$$

$$(d_m)_{23} = -i\gamma_m \sin Q_m$$

$$(d_m)_{24} = \gamma_m \cos Q_m$$

$$(d_m)_{31} = -\rho_m \alpha_m^2 (\gamma_m - 1) \cos P_m$$

$$(d_m)_{32} = i\rho_m \alpha_m^2 (\gamma_m - 1) \sin P_m$$

$$(d_m)_{33} = -\rho_m c^2 \gamma_m^2 r_{\beta_m} \cos Q_m$$

$$(d_m)_{34} = i\rho_m c^2 \gamma_m^2 r_{\beta_m} \sin Q_m$$

$$(d_m)_{41} = -i\rho_m \gamma_m \alpha_m^2 r_{\alpha_m} \sin P_m$$

$$(d_m)_{42} = \rho_m \gamma_m \alpha_m^2 r_{\alpha_m} \cos P_m$$

$$(d_m)_{43} = i\rho_m c^2 \gamma_m (\gamma_m - 1) \sin Q_m$$

$$(d_m)_{44} = -\rho_m c^2 \gamma_m (\gamma_m - 1) \cos Q_m \quad \text{A.1.46}$$

Equation A.1.45 can be written for reflected and incident waves which is incident from the bottom of the n^{th} layer (Figure A.1.5):

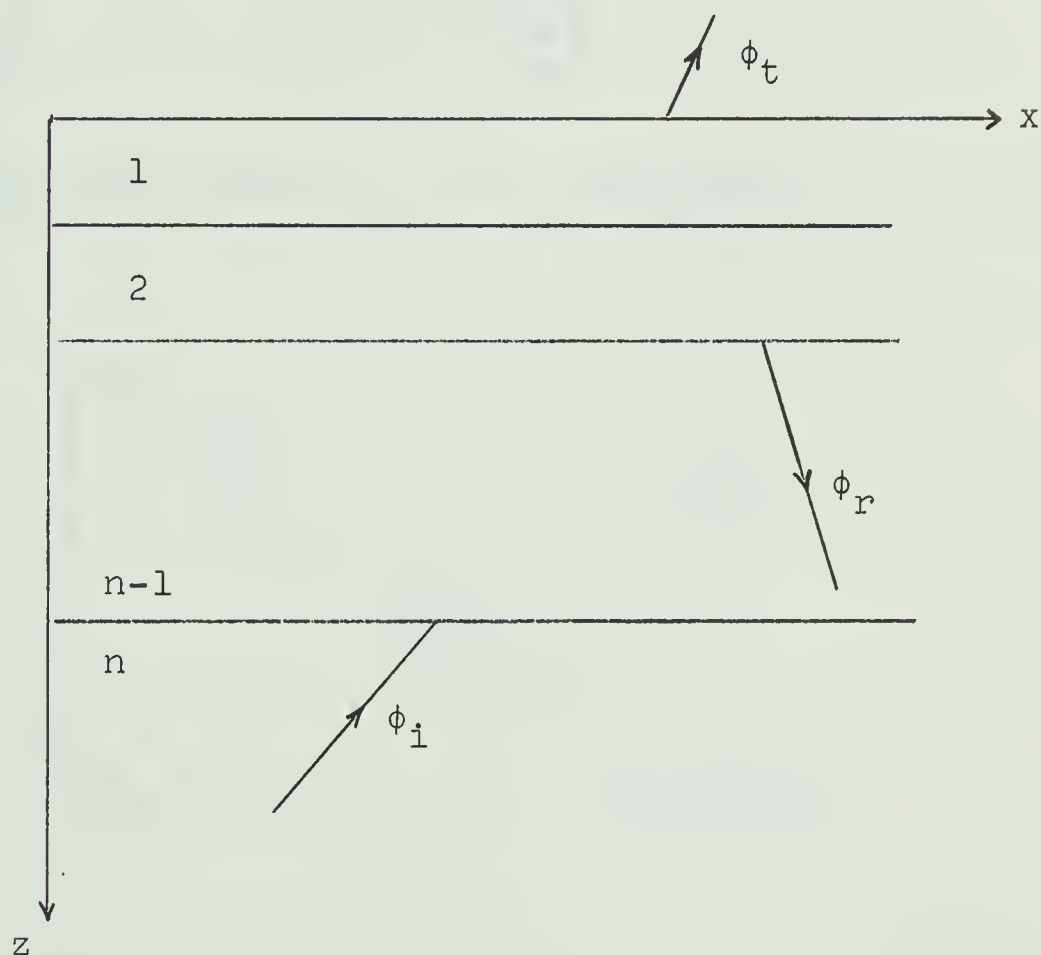


Figure A.1.15. Direction of axis and numbering of layers.

$$\begin{bmatrix} \frac{\dot{u}_m}{c} \\ \frac{\dot{\omega}_m}{c} \\ P_{zz_m} \\ P_{xz_m} \end{bmatrix} = D_m \begin{bmatrix} \Theta_{r_m} + \Theta_{i_m} \\ \Theta_{r_m} - \Theta_{i_m} \\ \Omega_{r_m} - \Omega_{i_m} \\ \Omega_{r_m} + \Omega_{i_m} \end{bmatrix} \quad \text{A.1.47}$$

At the top of the layer, $d_m = 0$ and equation A.1.47 will be

$$\begin{bmatrix} \frac{\dot{u}_{m-1}}{c} \\ \frac{\dot{\omega}_{m-1}}{c} \\ P_{zz_{m-1}} \\ P_{xz_{m-1}} \end{bmatrix} = \begin{bmatrix} -\frac{\alpha_m^2}{c^2} & 0 & -\gamma_m r \beta_m & 0 \\ 0 & \frac{-\alpha_m^2}{c^2} r \alpha_m & 0 & \gamma_m \\ -\rho_m \alpha^2 (\gamma_m - 1) & 0 & -\rho_m c^2 \gamma_m^2 r \beta_m & 0 \\ 0 & \rho_m \gamma_m \alpha_m^2 r \alpha_m & 0 & -\rho_m c^2 \gamma_m (\gamma_m - 1) \end{bmatrix} \cdot B_m$$

A.1.48a

where B_m is

$$B_m = \begin{bmatrix} \Theta_{r_m} + \Theta_{i_m} \\ \Theta_{r_m} - \Theta_{i_m} \\ \Omega_{r_m} - \Omega_{i_m} \\ \Omega_{r_m} + \Omega_{i_m} \end{bmatrix} \quad \text{A.1.48b}$$

or

$$\begin{bmatrix} \frac{\dot{u}_{m-1}}{c} \\ \frac{\dot{\omega}_{m-1}}{c} \\ P_{zz_{m-1}} \\ P_{xz_{m-1}} \end{bmatrix} = E_m \begin{bmatrix} \Theta_{r_m} + \Theta_{i_m} \\ \Theta_{r_m} - \Theta_{i_m} \\ \Omega_{r_m} - \Omega_{i_m} \\ \Omega_{r_m} + \Omega_{i_m} \end{bmatrix} \quad \text{A.1.49}$$

It can be written as

$$\begin{bmatrix} \Theta_{r_m} + \Theta_{i_m} \\ \Theta_{r_m} - \Theta_{i_m} \\ \Omega_{r_m} - \Omega_{i_m} \\ \Omega_{r_m} + \Omega_{i_m} \end{bmatrix} = E_m^{-1} \begin{bmatrix} \frac{\dot{u}_{m-1}}{c} \\ \frac{\dot{\omega}_{m-1}}{c} \\ P_{zz_{m-1}} \\ P_{xz_{m-1}} \end{bmatrix} \quad \text{A.1.50}$$

where E_m^{-1} is given by

$$E_m^{-1} = \begin{bmatrix} -2 \frac{\beta_m^2}{\alpha_m^2} & 0 & \frac{1}{\rho_m \alpha_m^2} & 0 \\ 0 & \frac{c^2 (\gamma_m - 1)}{\alpha_m^2 r \alpha_m} & 0 & \frac{1}{\rho_m \alpha_m^2 r \alpha_m} \\ \frac{\gamma_m - 1}{\gamma_m r \beta_m} & 0 & - \frac{1}{\rho_m c^2 \gamma_m r \beta_m} & 0 \\ 0 & 1 & 0 & \frac{1}{\rho_m c^2 \gamma_m} \end{bmatrix}$$

From Equations A.1.48 and A.1.49

$$\begin{bmatrix} \frac{\dot{u}_m}{c} \\ \frac{\dot{\omega}_m}{c} \\ P_{zz_m} \\ P_{xz_m} \end{bmatrix} = D_m E_m^{-1} \begin{bmatrix} \frac{\dot{u}_{m-1}}{c} \\ \frac{\dot{\omega}_{m-1}}{c} \\ P_{zz_{m-1}} \\ P_{xz_{m-1}} \end{bmatrix} \quad \text{A.1.52}$$

Matrix $a_m = D_m E_m^{-1}$ can be calculated from equations A.1.48 and A.1.51:

$$(a_m)_{11} = \gamma_m \cos P_m - (\gamma_m - 1) \cos Q_m$$

$$(a_m)_{12} = i[(\gamma_m - 1) \frac{1}{r_{\alpha_m}} \sin P_m + \gamma_m r_{\beta_m} \sin Q_m]$$

$$(a_m)_{13} = -(\rho_m c^2)^{-1} (\cos P_m - \cos Q_m)$$

$$(a_m)_{14} = i(\rho_m c^2)^{-1} (r_{\alpha_m}^{-1} \sin P_m + r_{\beta_m} \sin Q_m)$$

$$(a_m)_{21} = -i[\gamma_m r_{\alpha_m} \sin P_m + (\gamma_m - 1) r_{\beta}^{-1} \sin Q_m]$$

$$(a_m)_{22} = -(\gamma_m - 1) \cos P_m + \gamma_m \cos Q_m$$

$$(a_m)_{23} = i(\rho_m c^2)^{-1} (r_{\alpha_m} \sin P_m + r_{\beta_m}^{-1} \sin Q_m)$$

$$(a_m)_{24} = (a_m)_{13}$$

$$(a_m)_{31} = \rho_m c^2 \gamma_m (\gamma_m - 1) (\cos P_m - \cos Q_m)$$

$$(a_m)_{32} = i\rho_m c^2 [(\gamma_m - 1)^2 r_{\alpha_m}^{-1} \sin P_m + \gamma_m^2 r_{\beta_m} \sin Q_m]$$

$$(a_m)_{33} = (a_m)_{22}$$

$$(a_m)_{34} = (a_m)_{12}$$

$$(a_m)_{41} = i\rho c^2 [\gamma_m^2 r_{\alpha_m} \sin P_m + (\gamma_m - 1)^2 r_{\beta_m}^{-1} \sin Q_m]$$

$$(a_m)_{42} = (a_m)_{31}$$

$$(a_m)_{43} = (a_m)_{21}$$

$$(a_m)_{44} = (a_m)_{11}$$

A.1.53

Repeating equation A.1.52 for each interface, displacement at the surface can be found in terms of displacement at the bottom of the layers:

$$\begin{bmatrix} \frac{\dot{u}_m}{c} \\ \frac{\dot{\omega}_m}{c} \\ P_{zz_m} \\ P_{xz_m} \end{bmatrix} = \begin{bmatrix} a_m \end{bmatrix} \begin{bmatrix} a_{m-1} \end{bmatrix} \cdots \begin{bmatrix} a \end{bmatrix} \begin{bmatrix} \frac{\dot{u}_0}{c} \\ \frac{\dot{\omega}_0}{c} \\ P_{zz_0} \\ P_{xz_0} \end{bmatrix} \quad \text{A.1.54}$$

From equation A.1.50 and letting $P_{zz} = P_{xz} = 0$ at the free surface, we can write

$$\begin{bmatrix} \theta_{r_m} + \theta_{i_m} \\ \theta_{r_m} - \theta_{i_m} \\ \Omega_{r_m} - \Omega_{i_m} \\ \Omega_{r_m} + \Omega_{i_m} \end{bmatrix} = E_m^{-1} \begin{bmatrix} a_{m-1} \end{bmatrix} \begin{bmatrix} a_{m-2} \end{bmatrix} \cdots \begin{bmatrix} a_1 \end{bmatrix} \begin{bmatrix} \frac{\dot{u}_0}{c} \\ \frac{\dot{\omega}_0}{c} \\ 0 \\ 0 \end{bmatrix} \quad \text{A.1.55}$$

Substituting

$$J = E_m^{-1} a_{m-1} a_{m-2} \dots a_1 \quad A.1.56$$

we can write

$$\begin{aligned} \Theta_{r_m} + \Theta_{i_m} &= J_{11} \frac{\dot{u}_o}{c} + J_{12} \frac{\dot{\omega}_o}{c} \\ \Theta_{r_m} - \Theta_{i_m} &= J_{21} \frac{\dot{u}_o}{c} + J_{22} \frac{\dot{\omega}_o}{c} \\ \Omega_{r_m} - \Omega_{i_m} &= J_{31} \frac{\dot{u}_o}{c} + J_{32} \frac{\dot{\omega}_o}{c} \\ \Omega_{r_m} + \Omega_{i_m} &= J_{41} \frac{\dot{u}_o}{c} + J_{42} \frac{\dot{\omega}_o}{c} \end{aligned} \quad A.1.57$$

In the case of P waves of unit dilatational amplitude in the m^{th} layer, setting $\Theta_{i_m} = 1$ and $\Omega_{i_m} = 0$ in equations A.1.57, and solving:

$$\Theta_{r_m} = D^{-1} [(J_{11} + J_{21})(J_{32} - J_{42}) - (J_{12} + J_{22})(J_{31} - J_{41})] \quad A.1.58$$

$$\Omega_{r_m} = 2D^{-1} (J_{32} J_{41} - J_{31} J_{42}) \quad A.1.59$$

$$\frac{\dot{u}_o}{c} = 2D^{-1}(J_{32} - J_{42}) \quad A.1.60$$

$$\frac{\dot{w}_o}{c} = 2D^{-1}(J_{41} - J_{31}) \quad A.1.61$$

where

$$D = (J_{11} - J_{21})(J_{32} - J_{42}) - (J_{12} - J_{22})(J_{31} - J_{41}) \quad A.1.62$$

From equation A.2.48, at the top of the m^{th} layer

$$\frac{\dot{u}_{m-1}}{c} = - \left(\frac{\alpha_m}{c}\right)^2 (\theta_{r_m} + \theta_{i_m}) - \gamma_m r_{\beta_m} (\Omega_{r_m} - \Omega_{i_m}) \quad A.1.63$$

$$\frac{\dot{w}_{m-1}}{c} = - \left(\frac{\alpha_m}{c}\right)^2 r_{\alpha_m} (\theta_{r_m} - \theta_{i_m}) + \gamma_m (\Omega_{r_m} + \Omega_{i_m}) \quad A.1.64$$

Taking the ratios of component in equations A.1.60, A.1.61, A.1.63 and A.1.64, we get Horizontal and Vertical transfer functions at a given frequency:

$$TV_P(\omega) = \frac{2c^2(J_{42} - J_{32})}{\alpha_m^2 D} \quad A.1.65$$

$$TW_P(\omega) = \frac{2c^2(J_{41} - J_{31})}{\alpha_m^2 D r_{\alpha_m}} \quad A.1.66$$

Equations A.1.65 and A.1.66 are the complex functions of frequency.

To normalize surface amplitudes to unit total amplitude in the incident wave, equation A.1.65 should be multiplied by

$$\frac{\alpha_m}{c} = \sin \phi_o \quad \text{A.1.67}$$

and equation A.1.66 should be multiplied by

$$\frac{\alpha_m}{c} r_{\alpha_m} = \cos \phi_o \quad \text{A.1.68}$$

In the case of S incident wave in A.1.57 setting $\theta_{i_m} = 0$ and $\Omega_{i_m} = 1$, we find

$$\Omega_{r_{ms}} = 2D^{-1}(J_{12}J_{21} - J_{11}J_{22}) \quad \text{A.1.69}$$

$$\omega_{r_{ms}} = D^{-1}[(J_{12} - J_{22})(J_{31} + J_{41}) - (J_{11} - J_{21})(J_{32} + J_{42})] \quad \text{A.1.70}$$

$$\frac{\dot{\omega}_{os}}{c} = 2D^{-1}(J_{12} - J_{22}) \quad \text{A.1.71}$$

$$\frac{\dot{\omega}_{os}}{c} = 2D^{-1}(J_{21} - J_{11}) \quad \text{A.1.72}$$

Using equations A.1.63 and A.1.64, transfer functions are found:

$$TV_S(\omega) = 2(J_{12} - J_{22})/\gamma_m r_{\beta_m} D \quad A.1.73$$

$$TW_S(\omega) = 2(J_{21} - J_{11})/\gamma_m D \quad A.1.74$$

For normalization equation A.1.73 should be multiplied by

$$\frac{\beta_m^r \beta_m}{c} = \cos \phi_o \quad A.1.75$$

and equation A.1.74 should be multiplied by

$$\frac{\beta_m}{c} = \sin \phi_o \quad A.1.76$$

APPENDIX 2
LISTING OF COMPUTER PROGRAMS

This appendix contains the Fortran IV programs developed using the theory in the text.

FORTRAN IV
THE BUTTERWORTH LOW-PASS
FILTER SUBROUTINES

SUBROUTINE FILCO

C.....
 C THIS SUBROUTINES CALCULATES BUTTERWORTH LOW PASS FILTER COEFFICIENTS
 C

COMMON/FIL/F(4)/INT/AT/CUT/FREQ
 REAL COEF(4)
 COMPLEX S(4),M(4)

C FREQ. IS CUT OFF FREQUENCY
 C

52 FORMAT(1H1,5X,22HCORRECTED CUT OF FREQ.,F6.3)
 99 FORMAT(1H1,17HCUT OFF FREQUENCY,F6.3//)
 100 FORMAT(F6.3)
 101 FORMAT(F6.3)
 102 FORMAT(2X,19HDIGITIZING INTERVAL,F8.3//)
 103 FORMAT(1H1,38HS-PLANE POLES FOR UNIT LOW PASS FILTER//)
 104 FORMAT(1X,F9.4,F9.4)
 105 FORMAT(1H1,17HS-PLANE POLES FOR,F6.3,18HHZ LOW PASS FILTER//)
 106 FORMAT(1H1,16HCOEFF. OF POLYN.//)
 107 FORMAT(1X,2(I5,F17.5))
 108 FORMAT(1H1,38HFILTER COEFFICIENTS FOR LOW PASS FREQ.,F6.3//)

C
 READ(5,100) FREQ
 WRITE(6,101) FREQ
 READ(5,101) AT
 T=1./AT
 WRITE(6,102) T

C
 S(1)=(-0.9229,0.3827)
 S(2)=(-0.9229,-0.3827)
 S(3)=(-0.3827,0.9229)
 S(4)=(-0.3827,-0.9229)

C
 WRITE(6,103)
 WRITE(6,104)(S(I),I=1,4)
 W=FREQ*6.2831853

C
 C FREQ. CORRECTION
 C

X=W*T/2.
 A=(2.0/T)*TAN(X)
 WRITE(6,52) A

C
 DO 1 I=1,4
 M(I)=S(I)*A
 1 CONTINUE
 WRITE(6,105) FREQ
 WRITE(6,104)(M(I),I=1,4)

C
 I=1
 20 COEF(I)=-(M(I)+M(I+1))
 COEF(I+1)=M(I)*M(I+1)
 I=I+2


```
      IF(I.EQ.5) GO TO 30
      GO TO 20
30  WRITE(6,106)
      WRITE(6,107)(I,COFF(I),I=1,4)
C   TRANSFORM IN TO Z-PLANE
C
      K=1
110  REP=2*COFF(K+1)-8./(T**2)
      ALP=(4./(T**2))-(2*COFF(K))/T+COFF(K+1)
      CAK=(4./(T**2))+(2*COFF(K))/T+COFF(K+1)
      F(K)=REP/CAK
      F(K+1)=ALP/CAK
      K=K+2
      IF(K.EQ.5) GO TO 109
      GO TO 110
109  WRITE(6,108) FREQ
      WRITE(6,107)(I,F(I),I=1,4)
      RETURN
      END
```



```
SUBROUTINE FILTER(NG)
COMMON/HOLD/P(1000),SR(1000)/FIL/F(4)
DIMENSION C(1000)
C(1)=P(1)
C(2)=P(2)+P(1)-F(1)*C(1)
SR(1)=C(1)
SR(2)=C(2)+C(1)-F(3)*SR(1)
DO 10 I=3,NG
C(I)=P(I)+P(I-1)-F(1)*C(I-1)-F(2)*C(I-2)
SR(I)=C(I)+C(I-1)-F(3)*SR(I-1)-F(4)*SR(I-2)
10 CONTINUE
RETURN
END
```


FORTRAN IV
THE BUTTERWORTH HIGH-PASS
FILTER SUBROUTINES

SUBROUTINE FILCO

```

C .....
C
C THIS SUBROUTINE CALCULATES BUTTERWORTH HIGH PASS FILTER COEFFICIENTS
C
C     COMMON/FIL/F(4)/INT/AT/CUT/FREQ
C     REAL COFF(4)
C     COMPLEX S(4),M(4)
C
C FREQ. IS THE CUT OFF FREQ.
C
C 52 FORMAT(1H1,5X,22HCORRECTED CUT OF FREQ.,F6.3)
C 99 FORMAT(1H1,17HCUT OFF FREQUENCY,F6.3/)
C 100 FORMAT(F6.3)
C 101 FORMAT(F8.3)
C 102 FORMAT(2X,19HDIGITIZING INTERVAL,F8.2/)
C 103 FORMAT(1H1,38HS-PLANE POLES FOR UNIT LOW PASS FILTER//)
C 104 FORMAT(1X,F9.4,F9.4)
C 105 FORMAT(1H1,17HS-PLANE POLES FOR,F6.3,19PHZ.HIGH PASS FILTER//)
C 106 FORMAT(1H1,16HCOEFF. OF POLYN.//)
C 107 FORMAT(1X,2(15,F17.5))
C 108 FORMAT(1H1,39HFILTER COEFFICIENTS FOR HIGH PASS FREQ.,F6.3//)
C
C     READ(5,100) FREQ
C     WRITE(6,99) FREQ
C
C     READ(5,101) AT
C     T=1.0/AT
C     WRITE(6,102) T
C
C     S(1)=(-0.9229,0.3827)
C     S(2)=(-0.9229,-0.3827)
C     S(3)=(-0.3827,0.9229)
C     S(4)=(-0.3827,-0.9229)
C
C     WRITE(6,103)
C     WRITE(6,104)(S(I),I=1,4)
C     W=FREQ*6.2831853
C
C FREQ. CORRECTION
C
C     X=W*T/2.
C     A=(2.0/T)*TAN(X)
C     WRITE(6,52) A
C
C     DO 1 I=1,4
C     M(I)=A/S(I)
C 1 CONTINUE
C     WRITE(6,105) FREQ
C     WRITE(6,104)(M(I),I=1,4)
C
C     I=1
C 20 COFF(I)=- (M(I)+M(I+1))
C     COFF(I+1)=M(I)*M(I+1)
C     I=I+2

```



```

      IF(I.EQ.5) GO TO 30
      GO TO 20
30  WRITE(6,106)
      WRITE(6,107)(I,COFF(I),I=1,4)
C
C  TRANSFORM IN TO Z-PLANE
C
      K=1
110  PEP=((T**2)/2)*COFF(K+1)-2.
      ALP=1.-(T/2)*COFF(K)+((T**2)/4)*COFF(K+1)
      CAK=(T/2)*COFF(K)+((T**2)/4)*COFF(K+1)+1
      F(K)=PEP/CAK
      F(K+1)=ALP/CAK
      K=K+2
      IF(K.EQ.5) GO TO 109
      GO TO 110
109  WRITE(6,108) FREQ
      WRITE(6,107)(I,F(I),I=1,4)
      RETURN
      END

```



```
SUBROUTINE FILTER(NG)
COMMON/HOLD/P(1000),SR(1000)/FIL/F(4)
DIMENSION C(1000)
C(1)=P(1)
C(2)=P(2)-2*P(1)-F(1)*C(1)
SR(1)=C(1)
SR(2)=C(2)-2*C(1)-F(2)*SR(1)
DO 10 I=3,NG
C(I)=P(I)-2*P(I-1)+P(I-2)-F(1)*C(I-1)-F(2)*C(I-2)
SR(I)=C(I)-2*C(I-1)+C(I-2)-F(2)*SR(I-1)-F(4)*SR(I-2)
10 CONTINUE
RETURN
END
```


FORTRAN IV
THE BUTTERWORTH BAND-PASS
FILTER SUBROUTINES

SUBROUTINE FILCO

```

C .....
C THIS SUBROUTINE CALCULATES BUTTERWORTH BAND PASS FILTER COEFFICIENTS
C
COMMON/FIL/FI(8)/INT/AT/CUT/A1,A2
COMPLEX S(4),M(8)
REAL COEFF(8)

C
C A1,A2 ARE LOW AND HIGH CUT-OFF FREQUENCIES
C 1/AT=T DIGITIZING INTERVAL
C S... IS S-PLANE POLES OF LOW PASS BUTTERWORTH FILTER
C FI(8)... ARE FILTER COEFFICIENTS
C COEFF. OF POLYN.... ARE COEFFICIENT OF POLYNOMIAL OF TRANSFER
C FUNCTION IN S-PLANE
C
100 FORMAT(2F8.2)
101 FORMAT(1H1,23HZ-PLANE POLES FOR LOW PASS FILTER//)
102 FORMAT(1X,F7.4,F7.4)
103 FORMAT(1H1,5X,23HCORRECTED CUT OFF FREQ.//)
104 FORMAT(10X,2F10.2)
105 FORMAT(1H1,1X,13HS PLANE POLES//)
106 FORMAT(1X,1(I5,F12.4,F12.4))
107 FORMAT(1H1,5X,16HCOEFF. OF POLYN.//)
108 FORMAT(1H1,5X,20HFILTER COEFF. FOR...,F5.2,1X,F5.2//)
109 FORMAT(1X,2(I5,1X,F12.6))

C
S(1)=(-0.0239,0.3827)
S(2)=(-0.0239,-0.3827)
S(3)=(-0.3827,0.0239)
S(4)=(-0.3827,-0.0239)

C
READ(5,100) A1,A2
WRITE(6,101)
WRITE(6,102)(S(I),I=1,4)

C
T=1.0/AT
W1=A1*6.2831852
W2=A2*6.2831852

C
X=W1*T/2.
Y=W2*T/2.

C
A=(2./T)*TAN(X)
B=(2./T)*TAN(Y)
WRITE(6,103)
WRITE(6,104) A,B
AA=B-A
BB=A*B

C
DO 70 I=1,4
M(I)=(S(I)*AA)/2.-CSQRT(((AA*S(I)/2.)*2)-BB)
M(I+4)=(S(I)*AA)/2.+CSQRT(((AA*S(I)/2.)*2)-BB)
70 CONTINUE

```


C

```
WRITE(6,105)
WRITE(6,106)((I,M(I)),I=1,8)
```

C

```
      I=1
20  COEFF(I)=- (M(I)+M(I+1))
      COEFF(I+1)=M(I)*M(I+1)
      I=I+2
      IF(I.EQ.9) GO TO 30
      GO TO 20
30  WRITE(6,107)
      WRITE(6,109)((I,COEFF(I)),I=1,8)
```

C

```
      K=1
50  ALP=(COEFF(K+1)*T)/2.-COEFF(K)+2./T
      REP=COEFF(K+1)*T-4./T
      CAK=(COEFF(K+1)*T)/2.+COEFF(K)+2./T
      FI(K)=REP/CAK
      FI(K+1)=ALP/CAK
      K=K+2
      IF(K.EQ.9) GO TO 40
      GO TO 50
40  WRITE(6,108) A1,A2
      WRITE(6,109)(K,FI(K),K=1,9)
      RETURN
      END
```



```
SUBROUTINE PEVERS(N)  
COMMON/TUM/SB(6300)  
NN=N/2  
DO 10 I=1,NN  
  J=N-I  
  TEMP=SB(I)  
  SB(I)=SB(J+1)  
  SB(J+1)=TEMP  
10 CONTINUE  
RETURN  
END
```



```
SUBROUTINE SKIP(N)  
DO 5 K=1,N  
5 READ(4)  
RETURN  
END
```



```
SUBROUTINE REMOVE(NN,NG,NNN,NZ)
COMMON/HOLD/P(6,6200)
DO 1 L=1,NN
  SUM=0.0
  DO 2 I=1,NG
2  SUM=SUM+P(L,I)
  AV=SUM/FLOAT(NNN)
  WRITE(6,3)
  WRITE(6,4) AV
  DO 5 K=1,NNN
    P(L,K)=P(L,K)-AV
5  CONTINUE
1  CONTINUE
2  FORMAT(10X,13H AVERAGE VALUE/)
4  FORMAT(10X,F20.2)
  RETURN
END
```



```

SUBROUTINE FILTER(L,NG)
  DIMENSION C(3),D(3),F(3)
  COMMON/HOLD/P(6,6300)/TUM/SR(6300)/FIL/FI(8)
  MOD3(INDEX)=INDEX-((INDEX-1)/3)*3
  C(1)=P(L,1)
  C(2)=P(L,2)-FI(1)*C(1)
  C(3)=P(L,3)-P(L,1)-FI(1)*C(2)-FI(2)*C(1)
  D(1)=C(1)
  D(2)=C(2)-FI(3)*D(1)
  D(3)=C(3)-C(1)-FI(3)*D(2)-FI(4)*D(1)
  F(1)=D(1)
  F(2)=D(2)-FI(5)*F(1)
  F(3)=D(3)-D(1)-FI(5)*F(2)-FI(6)*F(1)
  SR(1)=F(1)
  SR(2)=F(2)-FI(7)*SR(1)
  SR(3)=F(3)-F(1)-FI(7)*SR(2)-FI(8)*SR(1)
  DO 10 I=4,NG
    IL=MOD3(I)
    IM1L=MOD3(I-1)
    IM2L=MOD3(I-2)
    C(IL)=P(L,I)-P(L,I-2)-FI(1)*C(IM1L)-FI(2)*C(IM2L)
    D(IL)=C(IL)-C(IM2L)-FI(3)*D(IM1L)-FI(4)*D(IM2L)
    F(IL)=D(IL)-D(IM2L)-FI(5)*F(IM1L)-FI(6)*F(IM2L)
    SR(I)=F(IL)-F(IM2L)-FI(7)*SR(I-1)-FI(8)*SR(I-2)
10 CONTINUE
  RETURN
  END

```



```
SUBROUTINE READ(LREC)  
COMMON/HOLD/P(6,6300)  
COMMON/TUM/IA(1200)  
INDEX=0  
DO 10 J=1,LREC  
  READ(4) IA  
  DO 20 LB=1,6  
    INDEX=200*(J-1)  
    DO 20 LRB=LB,1200,6  
      INDEX=INDEX+1  
20  P(LB,INDEX)=- (IA(LRB))  
10  CONTINUE  
  RETURN  
END
```



```

SUBROUTINE DPLOT(NN,NNN,RUE,IFIL,IREF)
COMMON/HOLD/P(6,6300)/TIM/SR(6300)/FIL/FI(8)
COMMON/CONST/TIN,UNIT,AMP,AMPMAX,CSEP,SHOT,TCOR,R/INT/T/CUT/A1,A2
RFC=FLOAT(IREF)
XSCALE=AMP/AMPMAX
YSCALE=TIN/UNIT
CALL PLOT(0.0,0.0,3)
CALL SYMBOL(0.50,-0.30,0.20,12HRECORD      A ,0.0,12)
CALL NUMBER(1.7,-0.30,0.20,REC,0.0,-1)
CALL NUMBER(2.5,-0.30,0.20,B,0.0,-1)
CALL SYMBOL(0.50,-1.00,0.20,4HSHOT,0.0,4)
CALL NUMBER(1.5,-1.00,0.20,SHOT,0.0,1)
CALL SYMBOL(0.50,-1.60,0.15,10HTIME CORR.,0.0,10)
CALL NUMBER(1.9,-1.60,0.10,TCOR,0.0,2)
CALL SYMBOL(0.50,-2.10,0.15,10HDIGIT.INT.,0.0,10)
CALL NUMBER(2.0,-2.10,0.10,T,0.0,4)
CALL SYMBOL(0.50,-2.60,0.15,8HARC LINE,0.0,8)
CALL SYMBOL(0.50,-3.10,0.15,9HPROJECT 9,0.0,9)
CALL SYMBOL(0.50,-3.50,0.15,10HEARLY RISE,0.0,10)
IF(IFIL.EQ.1) GO TO 10
CALL SYMBOL(0.50,-4.10,0.15,10HEFILTER BW.,0.00,10)
CALL SYMBOL(0.50,-4.60,0.15,15H          HZ.,0.00,15)
CALL NUMBER(0.50,-4.60,0.15,A1,0.0,2)
CALL NUMBER(1.20,-4.60,0.15,A2,0.0,2)
10 CONTINUE
IUNIT=IFIX(UNIT)
DO 1 J=1,NN
DO 2 I=1,NNN,IUNIT
CALL SYMBOL(((FLOAT(I-1)*YSCALE)+3.0),0.0,0.12,3,0.0,-1)
CALL PLOT(((FLOAT(I-1)*YSCALE)+3.0),P(J,I)*XSCALE,3)
JSTOP=I+IUNIT
IF(JSTOP.GT.NNN) GO TO 4
DO 3 II=I,JSTOP
CALL PLOT(((FLOAT(II-1)*YSCALE)+3.0),P(J,II)*XSCALE,2)
3 CONTINUE
2 CONTINUE
4 KK=JSTOP-IUNIT
CALL PLOT(((FLOAT(KK-1)*YSCALE)+3.0),P(J,KK)*XSCALE,3)
DO 5 K=KK,NNN
CALL PLOT(((FLOAT(K-1)*YSCALE)+3.0),P(J,K)*XSCALE,2)
5 CONTINUE
CALL PLOT(0.0,CSEP,-3)
1 CONTINUE
CALL PLOT(0.0,-0.5,-3)
DO 6 I=1,NNN,IUNIT
CALL SYMBOL(((FLOAT(I-1)*YSCALE)+3.0),0.0,0.30,13,0.0,-1)
A=FLOAT(I-1)/117.
CALL NUMBER(((FLOAT(I-1)*YSCALE)+2.9),-0.30,0.09,A,0.0,0)
6 CONTINUE
CALL PLOT(0.0,4*CSEP,-3)
RETURN
END

```


FORTRAN IV
THE BUTTERWORTH BAND-PASS
FILTER PROGRAM


```

C.....
C
C BUTTERWORTH BAND PASS FILTER.....
C
C THIS PROGRAM CALCULATES FILTER COEFFICIENTS AND FILTER ANY
C DIGITIZED IN PUT . CONSTANTS TO BE READ ARE ON COMMENT CARDS
C IN EACH SUBROUTINE.
C
C
C ND...NUMBER OF BLOCKS TO BE SKIPPED ON TAPE
C NF...NUMBER OF BLOCKS TO READ
C NF...NUMBER OF RECORDS TO BE PROCESSED
C NG...NUMBER OF WORDS PER CHANNEL
C MAXIMUM ALLOWABLE NG IS 6300
C NN...NUMBER OF CHANNELS TO BE FILTERED
C NNN...NUMBER OF WORDS, EXCLUSIVE OF LEADING AND TERMINATING ZEROS
C NZ...NUMBER OF ZEROS AFTER BLOCK OF WORDS
C IPLOT=1 PLOT THE DATA BEFORE FILTER
C      =0 DO NOT PLOT THE DATA BEFORE FILTER
C IW=1 WRITE FILTERED OUT PUT
C      =0 DO NOT WRITE FILTERED OUT PUT
C KLIST=0 DO NOT WRITE INPUT DATA
C      =1 WRITE THE INPUT DATA
C.....
C
C COMMON/HOLD/P(6,6300)/TUN/SP(6300)/FIL/FI(P)
C COMMON/CONST/TIN,UNIT,AMP,AMPMAX,CSEP,SHOT,TCOR,P/INT/T
C REAL*4 BUF(500)
C KK=4*500
C SET THE WORK AREA FOR PLOTTING
C CALL PLOTS(BUF(1),KK)
C CALL PLOT(00.0,27.0,-3)
C READ CONSTANTS
C
C READ(5,100) ND,NF,NF,NN,IPLOT,IW,KLIST,NNN,NZ
C READ(5,102) GAIN
C WRITE(6,199)
C WRITE(6,196) GAIN
C READ(5,105) TIN,UNIT,AMP,AMPMAX,CSEP
C WRITE(6,104)
C WRITE(6,105) TIN,UNIT,AMP,AMPMAX,CSEP
C NG=NNN+NZ
C WRITE(6,202)
C WRITE(6,203)(ND,NF,NF,NG,NN,IPLOT,IW,KLIST,NNN,NZ)
C
C
C CALCULATE FILTER COEFFICIENTS
C
C CALL FILCO
C

```



```

      IF(ND.EQ.0) GO TO 15
      CALL SKIP(ND)
15  CONTINUE

```

```

      DO 250 IL=1,NF

```

```

C  READ RECORD PARAMETER

```

```

C  SHOT IS SHOT NUMBER

```

```

C  TCOR IS TIME CORRECTION

```

```

C  B IS APC LINE NUMBER

```

```

      READ(5,103) SHOT,TCOR,B

```

```

      IREC=(ND+NE+(IL-1)*20)/30

```

```

      IF(IREC.EQ.0) IREC=1

```

```

      IF(NF.LT.30) IREC=(ND/30)+1

```

```

C  PUT ZEROS

```

```

      DO 1 L=1,NN

```

```

      DO 2 J=1,NG

```

```

      P(L,J)=0.0

```

```

      2 CONTINUE

```

```

      1 CONTINUE

```

```

      CALL READ(NE)

```

```

      WRITE(6,204)

```

```

      WRITE(6,204)

```

```

      CALL REMOVE(NN,NG,NNN,NZ)

```

```

      IF(KLIST.EQ.0) GO TO 22

```

```

      DO 40 LF=1,NN

```

```

      WRITE(6,1007) LF

```

```

40  WRITE(6,1006)(P(LF,LF),LF=1,NG)

```

```

22  IF(IPLT.EQ.0) GO TO 3

```

```

      IFIL=1

```

```

      CALL DPLOT(NN,NNN,BUF,IFIL,IREC)

```

```

      WRITE(6,1000)

```

```

      WRITE(6,1000)

```

```

      3 CONTINUE

```

```

      DO 25 L=1,NN

```

```

      FILTER((((((((((((((((((((((((((((((((

```

```

      CALL FILTER(L,NG)

```

```

      CALL REVERS(NG)

```


FORTRAN IV
FILTER IMPULSE AND
AMPLITUDE RESPONSE PROGRAM


```

C THIS PROGRAM CALCULATES IMPULSE AND AMPLITUDE RESPONSE OF BUTTERWORTH
C FILTER
C
C NOPTS...NUMBER OF POINTS
C NP...NUMBER OF POINTS TO PLOT
C
C     DIMENSION AY(1000),CX(1000),CY(1000),RX(102),RY(102),RUF(2000)
C     COMMON/HOLD/P(1000),SR(1000)/INT/AT/CONST/NOPTS
C     COMMON/DAT/X(480),Y(480)
C
C
C     99 FORMAT(1H1,10X,16HIMPULSE RESPONSE//)
C     100 FORMAT(2I6,F8.1)
C     102 FORMAT(1H1,19HREAL AND IMAG PARTS//)
C     103 FORMAT(1X,6(I5,1X,F15.2))
C     104 FORMAT(1H1,9HFILTER 1//)
C     105 FORMAT(1H1,9HFILTER 2//)
C     106 FORMAT(1X,4(I5,1X,F12.2,1X,F12.2))
C     107 FORMAT(1H1,10X,9HAMPLITUDE//)
C     108 FORMAT(1X,6(I5,1X,F15.1))
C     109 FORMAT(1H1,5X,4HGAIN//)
C     110 FORMAT(5X,F20.2)
C
C     READ(5,100) NOPTS,NP,AT
C
C     KK=2000*4
C     CALL PLOTS(RUF(1),KK)
C
C     CALL FILCO
C     CALL ZERO(NOPTS,P)
C
C     P(241)=1.0
C     CALL FILTER(NOPTS)
C
C     WRITE(6,104)
C     WRITE(6,103)((I,SR(I)),I=1,NOPTS)
C
C     CALL REVERS(NOPTS,SR)
C     CALL MOVE(NOPTS,SR,P)
C
C     CALL FILTER(NOPTS)
C     WRITE(6,105)
C     WRITE(6,103)((I,SR(I)),I=1,NOPTS)
C
C     CALL REVERS(NOPTS,SR)
C
C     WRITE(6,99)
C     WRITE(6,103)((I,SR(I)),I=1,NOPTS)
C
C PLOT IMPULSE RESPONSE
C

```



```

DO 450 I=1,NOPTS
CY(I)=SR(I)
CX(I)=FLOAT(I-1)/(AT-1)
450 CONTINUE
C
CALL MPLOT(CX,CY,NOPTS,BUF)
C
C FOURIER TRANSFORM
C
CALL MOVE(NOPTS,SR,X)
CALL ZERO(NOPTS,Y)
C
K=NOPTS/2+1
L=NOPTS/2-1
C
DO 15 I=1,L
X(I+K)=X(K-I)
15 CONTINUE
C
CALL FOUR 10
CALL SORT 10
C
WRITE(6,102)
WRITE(6,106)((JT,X(JT),Y(JT)),JT=1,NOPTS)
C
C
DO 30 JT=1,NOPTS
AY(JT)=SORT(X(JT)**2+Y(JT)**2)
30 CONTINUE
WRITE(6,107)
WRITE(6,108)((JT,AY(JT)),JT=1,NOPTS)
C
CALL MAX(NOPTS,AY,XMAX)
WRITE(6,109)
WRITE(6,110) XMAX
C
C
DO 170 I=1,100
RY(I)=AY(I)
SEC=AT/FLOAT(NOPTS)
PX(I)=SEC*FLOAT(I-1)
170 CONTINUE
C
CALL APLOT(PX,RY,BUF,ND)
C
CALL PLOT(0.0,0.0,0.0,999)
C
STOP
END

```



```
SUBROUTINE ZERO(LX,X)
  DIMENSION X(10)
  IF(LX) 30,30,10
10 DO 20 I=1,LX
  X(I)=0.0
20 CONTINUE
30 RETURN
  END
```



```
SUBROUTINE MOVE(LX,C,D)
  DIMENSION C(10),D(10)
  DO 10 I=1,LX
    D(I)=C(I)
10 CONTINUE
  RETURN
  END
```



```
SUBROUTINE REVERS(N,X)
  DIMENSION X(NOPTS)
  NN=N/2
  DO 10 I=1,NN
    J=N-I
    TEMP=X(I)
    X(I)=X(J+1)
    X(J+1)=TEMP
  10 CONTINUE
  RETURN
  END
```



```

SUBROUTINE FILTER(NG)
  DIMENSION C(3),D(3),F(3)
  COMMON/HOLD/P(1000),SB(1000)/FIL/FI(8)
  MOD3(INDEX)=INDEX-((INDEX-1)/3)*3
  C(1)=P(1)
  C(2)=P(2)-FI(1)*C(1)
  C(3)=P(3)-P(1)-FI(1)*C(2)-FI(2)*C(1)
  D(1)=C(1)
  D(2)=C(2)-FI(3)*D(1)
  D(3)=C(3)-C(1)-FI(3)*D(2)-FI(4)*D(1)
  F(1)=D(1)
  F(2)=D(2)-FI(5)*F(1)
  F(3)=D(3)-D(1)-FI(5)*F(2)-FI(6)*F(1)
  SB(1)=F(1)
  SB(2)=F(2)-FI(7)*SB(1)
  SB(3)=F(3)-F(1)-FI(7)*SB(2)-FI(8)*SB(1)
  DO 10 I=4,NG
    IL=MOD3(I)
    IM1L=MOD3(I-1)
    IM2L=MOD3(I-2)
    C(IL)=P(I)-P(I-2)-FI(1)*C(IM1L)-FI(2)*C(IM2L)
    D(IL)=C(IL)-C(IM2L)-FI(3)*D(IM1L)-FI(4)*D(IM2L)
    F(IL)=D(IL)-D(IM2L)-FI(5)*F(IM1L)-FI(6)*F(IM2L)
    SB(I)=F(IL)-F(IM2L)-FI(7)*SB(I-1)-FI(8)*SB(I-2)
10 CONTINUE
  RETURN
  END

```



```

SUBROUTINE MPLOT(CX,CY,N,BUF)
DIMENSION CX(1000),CY(1000)
COMMON/CUT/A1,A2/CONST/NORTS/INT/AT

```

C

```

CALL PLOT(0.0,0.0,3)
CALL PLOT(0.0,6.5,2)
CALL PLOT(10.0,6.5,2)
CALL PLOT(10.0,0.0,2)
CALL PLOT(0.0,0.0,2)
CALL SYMBOL(1.0,6.0,2.12,48HIMPULSE RESPONSE OF BUTTERWORTH BAND P
PASS FILTER,0.0,48)
CALL SYMBOL(5.0,5.0,0.10,17HIN PUT PARAMETERS,0.0,17)
CALL SYMBOL(5.0,4.6,0.08,2HVM=1,0.0,3)
CALL SYMBOL(6.5,4.6,0.08,8HLCF=      ,0.0,8)
CALL NUMBER(6.9,4.6,0.08,A1,0.0,1)
CALL SYMBOL(5.0,4.3,0.08,8HT=      ,0.0,8)
T=1./AT
CALL NUMBER(5.2,4.3,0.08,T,0.0,4)
CALL SYMBOL(6.5,4.3,0.08,8HCF=      ,0.0,8)
CALL NUMBER(6.9,4.3,0.08,A2,0.0,1)
P=FLOAT(NORTS)
CALL SYMBOL(5.0,4.0,0.08,5HNM=      ,0.0,5)
CALL NUMBER(5.2,4.0,0.08,P,0.0,1)
CALL PLOT(0.5,0.5,23)
CALL SCALE(CX,9.0,N,1,10.0)
CALL SCALE(CY,5.5,N,1,10.0)
IL=N+2
IK=N+1
CALL AXIS(0.0,0.0,9HAMPLITUDE,9.5,5,90.0,CY(IK),CY(IL),10.0)
CALL AXIS(0.0,0.0,6HSECOND,6.9,0,0.0,CX(IK),CX(IL),10.0)
CALL LINE(CX,CY,N,1,0,0)
CALL PLOT(0.0,10.0,-3)
WRITE(6,2)
WRITE(6,2)
2 FORMAT(1X,27HPLOTTING HAS BEEN COMPLETED)
RETURN
END

```



```
SUBROUTINE APLOT(RX,RY,RUF,NP)
```

```
C.....
```

```
C
C   DIMENSION RX(102),RY(102)
C   COMMON/CUT/A1,A2
```

```
C
C   DRAW THE OUT LINE OF THE PAGE
```

```
C
C   CALL PLOT(0.0,0.0,3)
C   CALL PLOT(0.0,6.5,2)
C   CALL PLOT(10.0,6.5,2)
C   CALL PLOT(10.0,0.0,2)
C   CALL PLOT(0.0,0.0,2)
C   CALL SYMBOL(1.0,6.0,0.12,68AMPLITUDE RESPONSE OF BUTTERWORTH BAND
C   . PASS FILTER FOR      -      HZ,0.0,68)
C   CALL NUMBER(6.7,6.0,0.12,A1,0.0,1)
C   CALL NUMBER(7.3,6.0,0.12,A2,0.0,1)
```

```
C
C   CALL PLOT(0.5,0.5,22)
```

```
C
C   CALL SCALE(RX,9.0,NP,1,40.0)
C   CALL SCALE(RY,5.5,NP,1,40.0)
```

```
C
C   CALL AXIS(0.0,0.0,9AMPLITUDE,9,5.5,90.0,RY(101),RY(102),40.0)
C   CALL AXIS(0.0,0.0,9FREQUENCY,9,9.0,90.0,RX(101),RX(102),40.0)
C   CALL LINE(RX,RY,NP,1,0,0)
```

```
WRITE(6,2)
```

```
WRITE(6,2)
```

```
2 FORMAT(1X,27HPLOTTING HAS BEEN COMPLETED)
```

```
RETURN
```

```
END
```



```

C      SUBROUTINE FOUR 1D
C      ONE DIMENSIONAL FOURIER TRANSFORM
C
C      COMMON/CONST/NOPTS
C      COMMON/DAT/X(480),Y(480)
C
C      INTEGER J,K,M,MP,J1,J2,J3,J4,J5,JT
C      REAL I1,I2,I3,I4,I5
C      INTEGER P,PMAX,U,V
C
C      NEEDS SORT 1D TO RECOVER UNSCRAMBLED FOURIER COEFFICIENTS
C
C      THIS SUBROUTINE REPLACES X + I Y BY ITS FOURIER TRANSFORM WHERE
C       $X(F) + IY(F) = \sum_{T=0, (NOPTS-1)} (X(T) + IY(T)) * \exp(-F * T / NOPTS)$ .
C
C      REAL I (PMAX), R (PMAX), C (PMAX,PMAX), S (PMAX,PMAX),
C      .A ((PMAX-1)**2+1), B ((PMAX-1)**2+1)
C
C      REAL I (13), R (13), C (13,13), S (13,13), A (145), B (145)
C
C      PMAX=13
C
C      TWOPI=6.283185307
C      M=NOPTS
100 CONTINUE
      IF (M.NE.(M/4)*4) GO TO 400
C
C      FACTORS OF FOUR
C
C      MR=M
C      M=M/4
C      DO 300 J=1,M
C      ARG=TWOPI*FLOAT(J-1)/FLOAT(MP)
C      C1=COS(ARG)
C      S1=SIN(ARG)
C      C2=COS(2.0*ARG)
C      S2=SIN(2.0*ARG)
C      C3=COS(3.0*ARG)
C      S3=SIN(3.0*ARG)
C      DO 200 K=MR,NOPTS,MP
C      J1=J+K-MP
C      J2=J1+M
C      J3=J2+M
C      J4=J3+M
C      R1=X(J1)+X(J3)
C      R2=X(J1)-X(J3)
C      I1=Y(J1)+Y(J3)
C      I2=Y(J1)-Y(J3)
C      R3=X(J2)+X(J4)
C      R4=X(J2)-X(J4)
C      I3=Y(J2)+Y(J4)
C      I4=Y(J2)-Y(J4)
C      X(J1)=R1+R3
C      Y(J1)=I1+I3

```



```

      X(J2)=(R2+I4)*C1+(I2-R4)*S1
      Y(J2)=(I2-R4)*C1-(R2+I4)*S1
      X(J2)=(R1-R3)*C2+(I1-I3)*S2
      Y(J2)=(I1-I3)*C2-(R1-R3)*S2
      X(J4)=(R2-I4)*C3+(I2+R4)*S3
      Y(J4)=(I2+R4)*C3-(R2-I4)*S3
200  CONTINUE
300  CONTINUE
      GO TO 100
400  CONTINUE
      IF (M.NE.(M/2)*2) GO TO 700

```

C
C
C

FACTORS OF TWO

```

      MR=M
      M=M/2
      DO 600 J=1,M
      ARG=TWOPI*FLOAT(J-1)/FLOAT(MR)
      C1=COS(ARG)
      S1=SIN(ARG)
      DO 500 K=MR,NPTS,MR
      J1=J+K-MR
      J2=J1+M
      R1=X(J1)+X(J2)
      R2=X(J1)-X(J2)
      I1=Y(J1)+Y(J2)
      I2=Y(J1)-Y(J2)
      X(J1)=R1
      Y(J1)=I1
      X(J2)=R2*C1+I2*S1
      Y(J2)=I2*C1-R2*S1
500  CONTINUE
600  CONTINUE
      GO TO 400
700  CONTINUE
      IF (M.NE.(M/3)*3) GO TO 1000

```

C
C
C

FACTORS OF THREE

```

      MR=M
      M=M/3
      A1=COS(TWOPI/3.0)
      R1=SIN(TWOPI/3.0)
      A2=COS(2.0*TWOPI/3.0)
      R2=SIN(2.0*TWOPI/3.0)
      DO 900 J=1,M
      ARG=TWOPI*FLOAT(J-1)/FLOAT(MR)

```

C
C
C

ABSORB TWIDDLE FACTOR INTO ANALYSIS COEFFICIENTS

```

      C21=COS(ARG)
      S21=SIN(ARG)
      C22=C21*A1-S21*B1

```



```

S22=C21*B1+S21*A1
C23=C21*A2-S21*B2
S23=C21*B2+S21*A2
C31=COS(2.0*ARG)
S31=SIN(2.0*ARG)
C32=C31*A2-S31*B2
S32=C31*B2+S31*A2
C33=C31*A1-S31*B1
S33=C31*B1+S31*A1
DO 800 K=NR,NORTS,MR

```

```

J1=J+K-MR

```

```

J2=J1+M

```

```

J3=J2+M

```

```

R1=X(J1)

```

```

I1=Y(J1)

```

```

R2=X(J2)

```

```

I2=Y(J2)

```

```

R3=X(J3)

```

```

I3=Y(J3)

```

```

X(J1)=R1+R2+R3

```

```

Y(J1)=I1+I2+I3

```

```

X(J2)=R1*C21+I1*S21+R2*C22+I2*S22+R3*C23+I3*S23

```

```

Y(J2)=I1*C21-R1*S21+I2*C22-R2*S22+I3*C23-R3*S23

```

```

X(J3)=R1*C31+I1*S31+R2*C32+I2*S32+R3*C33+I3*S33

```

```

Y(J3)=I1*C31-R1*S31+I2*C32-R2*S32+I3*C33-R3*S33

```

```

800 CONTINUE

```

```

900 CONTINUE

```

```

GO TO 700

```

```

1000 CONTINUE

```

```

IF (M.NE.(M/5)*5) GO TO 1300

```

```

C

```

```

C

```

```

C

```

```

MR=M

```

```

M=M/5

```

```

A1=COS(TWOPI/5.0)

```

```

R1=SIN(TWOPI/5.0)

```

```

A2=COS(2.0*TWOPI/5.0)

```

```

R2=SIN(2.0*TWOPI/5.0)

```

```

A3=COS(3.0*TWOPI/5.0)

```

```

R3=SIN(3.0*TWOPI/5.0)

```

```

A4=COS(4.0*TWOPI/5.0)

```

```

R4=SIN(4.0*TWOPI/5.0)

```

```

DO 1200 J=1,M

```

```

ARG=TWOPI*FLOAT(J-1)/FLOAT(MR)

```

```

C

```

```

C

```

```

C

```

```

ABSORB TWIDDLE FACTOR INTO ANALYSIS COEFFICIENTS

```

```

C21=COS(ARG)

```

```

S21=SIN(ARG)

```

```

C22=C21*A1-S21*B1

```

```

S22=C21*B1+S21*A1

```

```

C23=C21*A2-S21*B2

```



```

S22=C21*R2+S21*A2
C24=C21*A3-S21*R2
S24=C21*R3+S21*A3
C25=C21*A4-S21*R4
S25=C21*R4+S21*A4
C31=COS(2.0*ARG)
S31=SIN(2.0*ARG)
C32=C31*A2-S31*R2
S32=C31*R2+S31*A2
C33=C31*A4-S31*R4
S33=C31*R4+S31*A4
C34=C31*A1-S31*R1
S34=C31*R1+S31*A1
C35=C31*A2-S31*R2
S35=C31*R2+S31*A2
C41=COS(3.0*ARG)
S41=SIN(3.0*ARG)
C42=C41*A3-S41*R3
S42=C41*R3+S41*A3
C43=C41*A1-S41*R1
S43=C41*R1+S41*A1
C44=C41*A4-S41*R4
S44=C41*R4+S41*A4
C45=C41*A2-S41*R2
S45=C41*R2+S41*A2
C51=COS(4.0*ARG)
S51=SIN(4.0*ARG)
C52=C51*A4-S51*R4
S52=C51*R4+S51*A4
C53=C51*A2-S51*R2
S53=C51*R2+S51*A2
C54=C51*A2-S51*R2
S54=C51*R2+S51*A2
C55=C51*A1-S51*R1
S55=C51*R1+S51*A1
DO 1100 K=MP,MORTS,MR
J1=J+K-MP
J2=J1+M
J3=J2+M
J4=J3+M
J5=J4+M
R1=X(J1)
I1=Y(J1)
R2=X(J2)
I2=Y(J2)
R3=X(J3)
I3=Y(J3)
R4=X(J4)
I4=Y(J4)
R5=X(J5)
I5=Y(J5)
X(J1)=R1+R2+R3+R4+R5
Y(J1)=I1+I2+I3+I4+I5

```



```

X(J2)=R1*C21+I1*S21+R2*C22+I2*S22+R3*C23+I3*S23+R4*C24+I4*S24+
R5*C25+I5*S25
Y(J2)=I1*C21-R1*S21+I2*C22-R2*S22+I3*C23-R3*S23+I4*C24-R4*S24+
I5*C25-R5*S25
X(J3)=R1*C31+I1*S31+R2*C32+I2*S32+R3*C33+I3*S33+R4*C34+I4*S34+
R5*C35+I5*S35
Y(J3)=I1*C31-R1*S31+I2*C32-R2*S32+I3*C33-R3*S33+I4*C34-R4*S34+
I5*C35-R5*S35
X(J4)=R1*C41+I1*S41+R2*C42+I2*S42+R3*C43+I3*S43+R4*C44+I4*S44+
R5*C45+I5*S45
Y(J4)=I1*C41-R1*S41+I2*C42-R2*S42+I3*C43-R3*S43+I4*C44-R4*S44+
I5*C45-R5*S45
X(J5)=R1*C51+I1*S51+R2*C52+I2*S52+R3*C53+I3*S53+R4*C54+I4*S54+
R5*C55+I5*S55
Y(J5)=I1*C51-R1*S51+I2*C52-R2*S52+I3*C53-R3*S53+I4*C54-R4*S54+
I5*C55-R5*S55

```

```
1100 CONTINUE
```

```
1200 CONTINUE
```

```
GO TO 1000
```

```
1300 CONTINUE
```

```
IF (M.LE.1) GO TO 2400
```

```
C
```

```
C GENERAL FACTORS
```

```
C
```

```
DO 1400 J=2,PMAX
```

```
P=J
```

```
IF (M.EQ.(M/P)*P) GO TO 1500
```

```
1400 CONTINUE
```

```
CALL FCT FRR
```

```
1500 CONTINUE
```

```
JT=(P-1)**2+1
```

```
C
```

```
C
```

```
C
```

```
SET UP ARBITRARY FACTORS
```

```
DO 1600 J=1,JT
```

```
ARG=TWOPI*FLOAT(J-1)/FLOAT(P)
```

```
A(J)=COS(ARG)
```

```
B(J)=SIN(ARG)
```

```
1600 CONTINUE
```

```
MR=M
```

```
M=M/P
```

```
DO 2200 J=1,M
```

```
ARG=TWOPI*FLOAT(J-1)/FLOAT(MR)
```

```
C
```

```
C
```

```
C
```

```
ABSORB TWIDDLE FACTOR INTO ANALYSIS COEFFICIENTS
```

```
DO 1800 U=1,P
```

```
C(U,1)=COS(FLOAT(U-1)*ARG)
```

```
S(U,1)=SIN(FLOAT(U-1)*ARG)
```

```
DO 1700 V=2,P
```

```
JT=(U-1)*(V-1)+1
```

```
C(U,V)=C(U,1)*A(JT)-S(U,1)*B(JT)
```

```
S(U,V)=C(U,1)*B(JT)+S(U,1)*A(JT)
```



```
1700 CONTINUE
1800 CONTINUE
      DO 2200 K=MR,NORTS,MP
C
C      GENERAL ANALYSIS
C
      DO 1900 U=1,P
      JT=J+K-MP+(U-1)*M
      R(U)=X(JT)
      I(U)=Y(JT)
1900 CONTINUE
      DO 2100 U=1,P
      XT=0.0
      YT=0.0
      DO 2000 V=1,P
      XT=XT+R(V)*C(U,V)+I(V)*S(U,V)
      YT=YT+I(V)*C(U,V)-R(V)*S(U,V)
2000 CONTINUE
      JT=J+K-MP+(U-1)*M
      X(JT)=XT
      Y(JT)=YT
2100 CONTINUE
2200 CONTINUE
2300 CONTINUE
      GO TO 1300
2400 CONTINUE
      RETURN
      END
```



```

SURROUTINE SORT 1D
UNSCRAMBLING PROGRAM FOR ONE DIMENSIONAL FOURIER COEFFICIENTS

COMMON/CONST/NOPTS
COMMON/DAT/X(480),Y(480)
REAL S(480)

INTEGER JT
INTEGER DO,LIM(13),STEP(13),P,PMAX
INTEGER A,B,C,D,E,F,G,H,I,J,K,L,M,AL,BL,CL,DL,EL,FL,GL,HL,IL,JL,
.KL,LL,ML,AS,BS,CS,DS,ES,FS,GS,HS,IS,JS,KS,LS,MS

DIGIT REVERSE FOR USE WITH FOUR 1D . S MUST BE THE SAME SIZE AS
X AND Y.

EQUIVALENCES TO ALLOW INDEXING TO SET PARAMETERS AND ALLOW
SCALARS FOR USE IN THE DO LOOPS.

EQUIVALENCE (AS,STEP(1)),(BS,STEP(2)),(CS,STEP(3)),(DS,STEP(4)),
.(ES,STEP(5)),(FS,STEP(6)),(GS,STEP(7)),(HS,STEP(8)),(IS,STEP(9)),
.(JS,STEP(10)),(KS,STEP(11)),(LS,STEP(12)),(MS,STEP(13))
EQUIVALENCE (AL,LIM(1)),(BL,LIM(2)),(CL,LIM(3)),(DL,LIM(4)),
.(EL,LIM(5)),(FL,LIM(6)),(GL,LIM(7)),(HL,LIM(8)),(IL,LIM(9)),
.(JL,LIM(10)),(KL,LIM(11)),(LL,LIM(12)),(ML,LIM(13))

PMAX IS SET TO AGREE WITH FOUR 1D

PMAX=13

SET LIMITS AND STEP SIZES FROM INNER LOOPS GOING OUT

DO=13
M=NOPTS
100 CONTINUE

CHECK FOR FACTORS OF 4

IF (M.NE.(M/4)*4) GO TO 200
M=M/4

REALLY WANT 0-4*M-1 BUT WE GO FROM 1 TO 4*M. 4 STEPS OF M WITH
MAXIMUM DISPLACEMENT OF M INITIALLY

LIM(DO)=4*M
STEP(DO)=M
DO=DO-1
GO TO 100
200 CONTINUE

CHECK FOR REMAINING FACTORS

IF (M.LE.1) GO TO 500

FACTORS OF 2,3,5,7,11,13

```



```

DO 300 JT=2,PMAX
P=JT
IF (M.EQ.(M/P)*P) GO TO 400
300 CONTINUE
C
C   ERROR EXIT IF FACTORS ABOVE PMAX ARE NEEDED.
C
CALL FCT ERR
400 CONTINUE
M=M/P
C
C   REALLY WANT 0-P*M-1 BUT WE USE 1 TO P*M. P STEPS OF M WITH
C   MAXIMUM INITIAL DISPLACEMENT OF M
C
LIM(DO)=P*M
STEP(DO)=M
DO=DO-1
GO TO 200
500 CONTINUE
C
C   FINISH OUT THE DO LOOPS TO MAKE OUTER LOOPS EXECUTE ONLY ONCE
C
DO 600 JT=1,DO
LIM(JT)=1
STEP(JT)=1
600 CONTINUE
C
C   SET JT SO THAT JT RUNS FROM 1 TO NOPTS IN STEPS OF 1 WHILE M WILL
C   RUN WITH REVERSED DIGITS
C
JT=0
DO 700 A=1,AL,AS
DO 700 B=A,RL,RS
DO 700 C=B,CL,CS
DO 700 D=C,DL,DS
DO 700 E=D,EL,ES
DO 700 F=E,FL,FS
DO 700 G=F,GL,GS
DO 700 H=G,HL,HS
DO 700 I=H,IL,IS
DO 700 J=I,JL,JS
DO 700 K=J,KL,KS
DO 700 L=K,LL,LS
DO 700 M=L,ML,MS
JT=JT+1
S(JT)=X(M)
700 CONTINUE
C
C   COPY BACK OUT OF THE SCRATCH ARRAY
C
DO 800 JT=1,NOPTS
X(JT)=S(JT)
800 CONTINUE

```


C

```
      JT=0
      DO 900 A=1,AL,AS
      DO 900 B=A,BL,BS
      DO 900 C=B,CL,CS
      DO 900 D=C,DL,DS
      DO 900 E=D,EL,ES
      DO 900 F=E,FL,FS
      DO 900 G=F,GL,GS
      DO 900 H=G,HL,HS
      DO 900 I=H,IL,IS
      DO 900 J=I,JL,JS
      DO 900 K=J,KL,KS
      DO 900 L=K,LL,LS
      DO 900 M=L,ML,MS
      JT=JT+1
      S(JT)=Y(M)
900 CONTINUE
```

C

C

C

```
      COPY BACK OUT OF THE SCRATCH ARRAY
```

```
      DO 950 JT=1,NOPTS
      Y(JT)=S(JT)
950 CONTINUE
      RETURN
      END
```


SUBROUTINE FCT ERP
FACTORING ERROR

FACTORING ERROR IN FOUR 1D OR SORT 1D.

CURRENTLY TAKEN IF A FACTOR ABOVE 13 IS REQUIRED. (THE ARRAYS
ARE NOT BIG ENOUGH TO HANDLE THINGS ABOVE 13.)

WRITE (6,100)

100 FORMAT (1X,15HFACTORING ERROR)

RETURN

END

FORTRAN IV
PROGRAM TO CALCULATE
SYNTHETIC SEISMOGRAMS


```

C.....
C
C  THIS PROGRAM CALCULATES SYNTHESIZED GROUND MOTION
C.....
C
120 FORMAT(2F6.1,2I6)
121 FORMAT(1H1,5HUNIT=,F6.1,1X,4HNPT=,I6,1X,3HIP=,I6)
122 FORMAT(1X,25HEND OF THE RUN, THANK YOU)
123 FORMAT(1H1,25HFREQUENCY OF THE PULSE IS,F6.1,1X,3HCPS)
C
C  IP...NUMBER OF SECONDS PER INCH TO PLOT
C  PER...PULSE FREQUENCY
C
COMMON/VERT/PWDTP(3000)/HOR/PUHDP(3000)/TIM/PER(3000)/FR/FREQ(3000
.) /REAL/HRP(3000),ZRP(3000)/IMAG/HIP(3000),ZIP(3000)
COMMON/SCALE/HMAX,VMAX/DAT/X(3000),Y(3000)/CONST/NOPTS
COMMON/CST/ANGIP,UNIT,PER,NOE,NPT,IP,GINC/AREA/PUF(500)
C
C
READ(5,120) UNIT,PER,NPT,IP
WRITE(6,121) UNIT,NPT,IP
WRITE(6,123) PER
NOPTS=NPT
C
C
KK=4*500
CALL PLOTS(PUF(1),KK)
CALL PLOT(0.0,24.0,-3)
C
L=1
CALL TRANS (L)
C
AI=(FLOAT(NPT)/UNIT)+10.
CALL PLOT(AI,0.0,-3)
CALL PLOT(0.0,0.0,999)
WRITE(6,122)
STOP
END

```



```
SUBROUTINE LAGS(M,C)
REAL C(10)
K=M/2+1
L=M/2-1
DO 1 I=1,L
C(I+K)=C(K-I)
1 CONTINUE
WRITE(6,2)
2 FORMAT(1X,10AFTER LAGS/)
RETURN
END
```



```
SUBROUTINE CORR(MOM,FI)
REAL MOM,FI
IF(MOM) 1,1,4
1 IF(FI) 2,2,3
2 ANG=0.0
  GO TO 7
3 ANG=1.0
  GO TO 7
4 IF(FI) 5,5,6
5 ANG=-1.0
  GO TO 7
6 ANG=0.0
7 MOM=MOM+ANG*3.14159265
RETURN
END
```



```
SUBROUTINE MAX(N,X,XMAX)
  DIMENSION X(10)
  XMAX=0.0
  DO 10 I=1,N
    IF(ABS(X(I))-XMAX) 10,10,11
11  XMAX=ABS(X(I))
10  CONTINUE
    WRITE(6,20)
20  FORMAT(1X,9HAFTER MAX/)
  RETURN
  END
```



```
SUBROUTINE FACTOO(X,N)  
REAL X(10)  
DO 10 I=1,N  
X(I)=X(I)/FLOAT(N)  
10 CONTINUE  
RETURN  
END
```



```
SUBROUTINE PERIOD(P,N,TF)
REAL P(10)
DO 10 I=1,N
P(I)=FLOAT(I-1)/(TF*FLOAT(N))
10 CONTINUE
RETURN
END
```



```
SUBROUTINE COMCON(V,N)  
  REAL V(10)  
  DO 10 I=1,N  
    V(I)=-V(I)  
10 CONTINUE  
  RETURN  
END
```



```
SUBROUTINE PULSE1
COMMON/VERT/PWDTP(3000)/HOR/PUDTP(3000)/TIM/PER(3000)/FR/FREQ(3000
.) /REAL/HPP(3000),ZPP(3000)/IMAG/HIP(3000),ZIP(3000)
COMMON/SCALE/HMAX,VMAX/DAT/X(3000),Y(3000)/CONST/NOPTS
COMMON/CST/ANG1P,UNIT,PER,NOF,NPT,IP,GINC/AREA/BUE(500)
DO 1 I=1,NOF
  IF(PER-FREQ(I)) 2,3,3
2  A=1.
  GO TO 4
2  A=0.
4  HPP(I)=HPP(I)*A
  HIP(I)=HIP(I)*A
  ZPP(I)=ZPP(I)*A
  ZIP(I)=ZIP(I)*A
1  CONTINUE
  WRITE(6,5)
5  FORMAT(1X,12HAFTER PULSE1/)
  RETURN
END
```



```

SUBROUTINE TPLOT(IAT)
COMMON/VERT/PWDTP(3000)/HOR/PUOTP(3000)/TIM/PER(3000)/FR/FREQ(3000
.1/REAL/HRP(3000),ZRP(3000)/IMAG/HIP(3000),ZIP(3000)
COMMON/SCALE/HMAX,VMAX/DAT/X(3000),Y(3000)/CONST/NOPTS
COMMON/CST/ANG1P,UNIT,PEP,NDF,NPT,IP,GINC/AREA/RUE(500)
CH=-1.5
XSC=1./((IP*UNIT))
HSC=2./HMAX
VSC=2./VMAX
NP=NPT/2
IUNIT=UNIT
DO 1 I=1,NP
CALL PLOT(FLOAT(I-1)*XSC,PWDTP(I)*VSC,2)
1 CONTINUE
CALL SYMBOL(0.1,2.2,0.15,22HVERTICAL GROUND MOTION,0.0,22)
CALL PLOT(0.0,-4.0,-3)
DO 2 I=1,NP
CALL PLOT(FLOAT(I-1)*XSC,PUOTP(I)*HSC,2)
2 CONTINUE
CALL SYMBOL(0.1,2.2,0.15,24HHORIZONTAL GROUND MOTION,0.0,24)
CALL PLOT(0.0,CH,-3)
CALL PLOT(0.0,CH,-3)
CALL SYMBOL(2.0,0.0,0.15,13HCRYSTAL MODEL,0.0,13)
CALL SYMBOL(2.0,-0.7,0.15,23HANGLE OF INCIDENCE          DEGREES,
.0,0,23)
WRITE(6,4)
CALL NUMBER(4.6,-0.7,0.15,ANG1P,0.0,-1)
CALL SYMBOL(2.0,-1.2,0.15,31HPULSE FREQUENCY IS          C.P.S.,
.0,0,31)
WRITE(6,4)
CALL NUMBER(4.4,-1.2,0.15,PER,0.0,1)
CALL PLOT(0.0,-6.0,-3)
WRITE(6,4)
WRITE(6,4)
4 FORMAT(1X,12HTPLOT IS OKAY)
RETURN
END

```


SUBROUTINE TRANS(L)

```

C .....
C
C  CALCULATION OF TRANSFER FUNCTION
C  APPARENT SURFACE VELOCITY MUST BE GREATER THAN P VELOCITY IN THE TOP
C  LAYER AND S VELOCITY IN ANY LAYER
C
100 FORMAT(2I6)
101 FORMAT(F9.4,2F14.4)
102 FORMAT(1X,10HTHICK./KM/,2X,14HP VEL./KM/SEC/,1X,14HS VEL./KM/SEC/,
.2X,12HDEN./GP/CMC//)
103 FORMAT(2F10.5,I6)
104 FORMAT(2X,8HAP.VELOC.,4X,12HANG.INC.POT.,4X,12HANG.INC.SURF.)
105 FORMAT(F10.2,2X,F12.3,1X,F12.3,3X,F12.2)
106 FORMAT(1X,5HLAYER,2X,11HTHICK RATIO,2X,7HP RATIO,2X,7HS RATIO,3X,
.10HDEN. RATIO/)
107 FORMAT(1X,12,5X,F9.4,2F10.4/)
108 FORMAT(1X,F7.1,F7.4,4F7.2,2X,F8.4,3X,F8.4,7X,2F8.4)
109 FORMAT(1X,12HEND OF TRANS)
110 FORMAT(1H1,17HTRANSFER FUNCTION//)
111 FORMAT(1X,6HPERIOD,4X,4HREFQ,4X,2HTW,5X,3HHPW,4X,2HTU,5X,3HPHU,4X,
.42HHORIZONTAL/REAL-IMAG/,VERTICAL/REAL-IMAG//)
112 FORMAT(2X,4HANG1,7X,5HDANG1,2X,5HNOANG/)
113 FORMAT(2X,4HGMIN,5X,4HGINC,7X,3HNOF/)
114 FORMAT(1X,4H //)
115 FORMAT(1H1,12HCRUSTAL MODEL,I4//)
C
C
COMMON/VERT/PWDTP(3000)/HOR/PHDTP(3000)/TIM/PER(3000)/FR/ERFQ(3000
.)//REAL/HRP(3000),ZRP(3000)/IMAG/HIP(3000),ZIP(3000)
COMMON/SCALE/HMAX,VMAX/DAT/X(3000),Y(3000)/CONST/NOPTS
COMMON/CST/ANG1P,UNIT,DEF,MOF,NPT,IP,GINC
DIMENSION D(50),A(50),P(50),RHO(50),DGAM(50),DGAM1(50),DRA(50),
.DRP(50),DH(50)
C
C  CALCULATION OF TRANSFER FUNCTION
READ(5,100) NCM
DO 25 IAI=1,NCM
C
C  READ THE IDENTIFICATION OF THE CRUSTAL MODEL
C  NOL...NUMBER OF LAYERS
READ(5,100) NOL
C  READ THE LAYERS PARAMETERS.D=THICKNESS,A=P VELOCITY,P=S VELOCITY
C  RHO=DENSITY
C
C
WRITE(6,115) IAI
WRITE(6,102)
DO 3 I=1,NOL
READ(5,101) D(I),A(I),P(I),RHO(I)
WRITE(6,101) D(I),A(I),P(I),RHO(I)
3 CONTINUE
WRITE(6,114)
WRITE(6,114)

```



```

N=NOL
N1=NOL-1
N2=NOL-2

C
C READ ANG1=INITIAL ANGLE OF INCIDENCE AT THE SURFACE
C DANG1=INCREMENT OF THE ANGLES OF INCIDENCE
C NOANG=NUMBER OF ANGLES OF INCIDENCE TO BE CALCULATED
C

READ(5,103) ANG1,DANG1,NOANG
WRITE(6,112)
WRITE(6,103) ANG1,DANG1,NOANG
WRITE(6,114)
WRITE(6,114)

C
C GMIN=MINIMUM FREQUENCY DESIRED
C GINC=INCREMENT OF FREQUENCY
C NOF=NUMBER OF VALUES OF FREQUENCY DESIRED
C

READ(5,103) GMIN,GINC,NOF
WRITE(6,113)
WRITE(6,103) GMIN,GINC,NOF
WRITE(6,114)
WRITE(6,114)
ANG1P=ANG1-DANG1
DO 4 IA=1,NOANG
  ANG1P=ANG1P+DANG1
  SINI=SIN(ANG1P/57.29578)
  SININI=A(1)*SINI/A(NOL)
  C=A(NOL)/SINI
  AIM=ASIN(SININI)*57.29578
  WRITE(6,104)
  WRITE(6,105) C,ANG1P,AIM
  WRITE(6,114)
  WRITE(6,114)
DO 5 M=1,NOL
  COVA=C/A(M)
  COVR=C/R(M)
  DGAM(M)=2./((COVR**2)
  DGAM1(M)=DGAM(M)-1.
  DRA(M)=SQRT(ABS(COVA**2-1.))
  DRP(M)=SQRT(ABS(COVR**2-1.))
  DH(M)=PHO(M)*C*C
5 CONTINUE
TH=0.0
DO 6 L=1,N1
  TH=TH+D(L)
6 CONTINUE
WRITE(6,106)
DO 7 I=1,NOL
  PK=D(I)/TH
  OK=A(I)/A(NOL)
  VK=R(I)/R(NOL)
  RK=RHO(I)/RHO(NOL)
  WRITE(6,107) I,PK,OK,VK,RK
7 CONTINUE

```



```

WRITE(6,110)
WRITE(6,111)
DO 8 IER=1,NOF
GAF=FLOAT( IER-1)*GINC
ERFQ( IER)=GAF
IF(ERFQ( IER).EQ.0.0) GO TO 1
PER( IER)=1./ERFQ( IER)
1 WVNO=6.2831853*ERFQ( IER)/C
A11=1.
A12=0.0
A21=0.
A22=1.
A31=0.
A32=0.
A41=0.
A42=0.
C COMPUTE ELEMENTS OF A MATRIX FOR LAYERS
DO 9 M=1,N1
GAM=DGAM(M)
GAMM1=DGAM1(M)
RA=DRA(M)
RR=DRR(M)
H=DH(M)
P=WVNO*D(M)*RA
Q=WVNO*D(M)*RR
SIP=SIN(P)
W=SIP/PA
PP=RA*SIP
COP=COS(P)
SIO=SIN(Q)
RR=SIO/PR
Z=RR*SIO
COQ=COS(Q)
RHO=RHO(M)
RM=R(M)
DM=D(M)
R11=GAM*COP-GAMM1*COQ
R12=GAMM1*W+GAM*Z
R13=-(COP-COQ)/H
R14=(W+Z)/H
R21=+(GAM*PP+GAMM1*RR)
R22=-GAMM1*COP+GAM*COQ
R23=-(PP+RR)/H
R24=R13
R31=H*GAM*GAMM1*(COP-COQ)
R32=H*(GAMM1*GAMM1*W+GAM*GAM*Z)
R33=R22
R34=R12
R41=-H*(GAM*GAM*PP+GAMM1*GAMM1*RR)
R42=R31
R43=R21
R44=R11
FA11=R11*A11+R12*A21+R13*A21+R14*A41
FA12=R11*A12+R12*A22+R13*A22+R14*A42
FA21=R21*A11+R22*A21+R23*A21+R24*A41

```



```

FA22=R21*A12+R22*A22+R23*A32+R24*A42
FA31=R31*A11+R32*A21+R33*A31+R34*A41
FA32=R31*A12+R32*A22+R33*A32+R34*A42
FA41=R41*A11+R42*A21+R43*A31+R44*A41
FA42=R41*A12+R42*A22+R43*A32+R44*A42
A11=FA11
A12=FA12
A21=FA21
A22=FA22
A31=FA31
A32=FA32
A41=FA41
A42=FA42

```

9 CONTINUE

```

A21=-A21
A41=-A41
GAM=DGAM(N)
GAMM1=DGAM1(N)
RA=DPA(N)
RB=DRB(N)
H=DH(N)

```

C COMPUTE ELEMENTS OF F INVERSE FOR THE LAST LAYER

```

R11=-GAM*COVA**2
R12=1./(RHO(N)*A(N)*A(N))
R22=GAMM1*COVA**2/RA
R24=R12/RA
R44=1./(H*GAM)
R32=-R44/RB
R31=-R32*GAMM1*H
R42=1.0
FA11=R11*A11+R12*A31
FA12=R11*A12+R12*A32
FA21=R22*A21+R24*A41
FA22=R22*A22+R24*A42
FA31=R31*A11+R32*A31
FA32=R31*A12+R32*A32
FA41=R42*A21+R44*A41
FA42=R42*A22+R44*A42
DR=FA21*FA32-FA11*FA42-FA12*FA41+FA22*FA31
DI=FA11*FA32+FA21*FA42-FA12*FA31-FA22*FA41
DEN SQ=DR*DR+DI*DI
UPNR=FA32*DI-FA42*DR
UPNI=FA32*DR+FA42*DI
WPNI=FA41*DR+FA31*DI
WPNR=-FA31*DR+FA41*DI
PWDTP(IF3)=((2./DEN SQ)*SQRT(WPNR*WPNR+WPNI*WPNI))*COVA
PPHWP=ATAN(+WPNI/WPNR)
PUWTP(IF3)=((2./DEN SQ)*SQRT(UPNR*UPNR+UPNI*UPNI))*COVA
PPHUP=ATAN(+UPNI/UPNR)

```



```
C      CALL CORR(PPHWP,WDNI)
      CALL CORR(PPHUP,UPNI)
C
C      HIP(IFR)=PUDTP(IFR)*SIN(PPHUP)
      HRP(IFR)=PUDTP(IFR)*COS(PPHUP)
      ZRP(IFR)=PWDTP(IFR)*COS(PPHWP)
      ZIP(IFR)=PWDTP(IFR)*SIN(PPHWP)
C
      WRITE(6,108) PER(IFR),FREQ(IFR),PWDTP(IFR),PPHWP,PUDTP(IFR),
      .PPHUP,HRP(IFR),HIP(IFR),ZRP(IFR),ZIP(IFR)
      * CONTINUE
C
      IF(L.EQ.1) CALL MOTION(IAI)
      IF(L.EQ.2) CALL TRUNC(IAI)
C
      4 CONTINUE
      25 CONTINUE
      WRITE(6,109)
      RETURN
      END
```


SUBROUTINE MOTION(IAI)

```

C .....
C
COMMON/VERT/PWDTP(3000)/HOR/PUOTDTP(3000)/TIM/PER(3000)/FR/FREQ(3000
.) /REAL/HRP(3000),ZRP(3000)/IMAG/HIP(3000),ZIP(3000)
COMMON/SCALE/HMAX,VMAX/DAT/X(3000),Y(3000)/CONST/NOPTS
COMMON/CST/ANG1P,UNIT,PER,NOF,NPT,IP,GINC/AREA/BUF(500)
C
117 FORMAT(1X,4(I5,F12.4,1X,F12.4))
118 FORMAT(1H1,6X,12HTIME-V MOTION//)
119 FORMAT(1H1,6X,12HTIME-H MOTION//)
120 FORMAT(1H1,5HVMAX-,F6.4,1X,5HVMAX-,F6.4)
C
C
C
C
CALL PULSE1
C
C
N1=NOPTS/2
CALL ZERO(NOPTS,X)
CALL ZERO(NOPTS,Y)
CALL MOVE(NOF,ZRP,X)
CALL MOVE(NOF,ZIP,Y)
CALL LAGS(NOPTS,X)
CALL LAGS(NOPTS,Y)
CALL COMCON(Y,N1)
CALL FOUR 1D
CALL SORT 1D
CALL FACTOO(X,NOPTS)
CALL FACTOO(Y,NOPTS)
CALL PERIOD(PER,NOPTS,GINC)
CALL MOVE(NOPTS,X,PWDTP)
C
CALL ZERO(NOPTS,X)
CALL ZERO(NOPTS,Y)
CALL MOVE(NOF,HRP,X)
CALL MOVE(NOF,HIP,Y)
CALL LAGS(NOPTS,X)
CALL LAGS(NOPTS,Y)
CALL COMCON(Y,N1)
CALL FOUR 1D
CALL SORT 1D
CALL FACTOO(Y,NOPTS)
CALL FACTOO(X,NOPTS)
CALL MOVE(NOPTS,X,PUOTDTP)
C
WRITE(6,119)
WRITE(6,117)(I,PER(I),PUOTDTP(I),I=1,NPT)
WRITE(6,118)
WRITE(6,117)(I,PER(I),PWDTP(I),I=1,NPT)

```



```
C  
CALL MAX(NPT,PUDTP,HMAX)  
CALL MAX(NPT,PWDTP,VMAX)  
WRITE(6,120) HMAX,VMAX
```

```
C  
C  
CALL TPLOT(IAI)
```

```
C  
RETURN  
END
```


FORTRAN IV
TRUNCATED TRANSFER FUNCTION
PROGRAM

C THIS PROGRAM CALCULATES TRUNCATED TRANSFER FUNCTION

C.....

C 99 FORMAT(1X,25HEND OF THE RUN, THANK YOU)

100 FORMAT(2I6,3F7.2)

101 FORMAT(1H1,64HNPTS-,I6,3HIG-,I6,1X,3HCFR,F6.1,2HT-,F6.2,5HUNIT-,
F6.2)

C IG...NUMBER OF SPECTRA POINTS TO PLOT
C NPTS...INTEGRATION LIMIT
C T...TRUNCATION TIME

C
COMMON/VERT/PWDTP(3000)/HOR/PUOTP(3000)/AREA/PUF(500)
COMMON/DAT/X(3000),Y(3000)/TIM/PER(3000)/ER/ERFQ(3000)/CONST/NOP-
COMMON/REAL/HRP(3000),ZRP(3000)/IMAG/HIP(3000),ZIP(3000)
COMMON/SCALE/HMAX,VMAX/FINC/GINC
COMMON/BOL/ANG1P,UNIT,IG,NOF,CFR,T

C
C
READ(5,100) NPTS,IG,CFR,T,UNIT
WRITE(6,101) NPTS,IG,CFR,T,UNIT

C
C
L=2
CALL TRANS (L)

C
C
C
CALL PLOT(10.0,2.0,-3)
CALL PLOT(0.0,0.0,0.0,999)
WRITE(6,99)
STOP
END


```

SUBROUTINE TIME(IAI,K,L)
COMMON/VERT/PWDTP(3000)/HOR/PUDTP(3000)/AREA/PI F(500)
COMMON/REAL/HRP(3000),ZRP(3000)/IMAG/HIP(3000),ZIP(3000)
COMMON/DAT/X(3000),Y(3000)/TIM/PER(3000)/ER/ERFQ(3000)/CONST/NOPTS
COMMON/SCALE/HVAX,VMAX/FINC/GINC
COMMON/ROL/ANGIP,UNIT,IG,NOF,CER,T

```

```

C
IUNIT=UNIT
IK=IUNIT/4
A1=FLOAT(IAI)
XSCAL=1.0/UNIT
IF(K.EQ.1) XSCAL=5./UNIT
IF(K.EQ.2) V=1.
IF(K.EQ.1) V=2.
ZSCAL=V/VMAX
HSCAL=V/HVAX
IF(K.EQ.1) N=IFIX((CER/GINC)+1)
IF(K.EQ.2) N=NOPTS

```

```

C
CALL PLOT(0.0,PWDTP(1)*ZSCAL,3)
DO 1 I=1,N
CALL PLOT(FLOAT(I-1)*XSCAL,PWDTP(I)*ZSCAL,2)
1 CONTINUE
CALL SYMBOL(0.0,2.1,0.12,34VERTICAL,0.0,8)
CALL PLOT(0.0,-3.0,-3)
CALL PLOT(0.0,PUDTP(1)*ZSCAL,3)
DO 2 I=1,N
CALL PLOT(FLOAT(I-1)*XSCAL,PUDTP(I)*HSCAL,2)
2 CONTINUE
CALL SYMBOL(0.0,2.1,0.12,10HHORIZONTAL,0.0,10)
IF(K.EQ.1) GO TO 4
CALL SYMBOL(FLOAT(NOPTS-1)*XSCAL+0.5,-0.35,0.08,4HSEC.,0.0,4)
CALL SYMBOL(2.0,-1.5,0.12,25HTIME SYNTHESIS OF TRANSFER FUNCTION,
.0,0,35)
GO TO 6
4 DO 5 I=1,N,IK
CALL SYMBOL(FLOAT(I-1)*XSCAL,0.0,+0.30,13.0,0,-1)
A=ERFQ(I)
CALL NUMBER(FLOAT(I-1)*XSCAL,-0.35,0.08,4.0,0,1)
5 CONTINUE
CALL SYMBOL(FLOAT(N)*XSCAL+0.5,-0.35,0.12,5HREFQ.,0.0,5)
IF(L.EQ.1) CALL SYMBOL(2.0,-1.5,0.12,28HTPUNCATED TRANSFER FUNCTIO
NS,0.0,28)
IF(L.EQ.2) CALL SYMBOL(2.0,-1.5,0.12,32HNON-TRUNCATED TRANSFER FUN
CTIONS,0.0,32)
6 CONTINUE
CALL SYMBOL(2.0,-2.0,0.12,33HANGLE OF INCIDENCE DEGREES,
.0,0,33)
CALL NUMBER(4.1,-2.0,0.12,ANGIP,0.0,-1)
CALL PLOT(0.0,-05.5,-3)
WRITE(6,7)
WRITE(6,7)
7 FORMAT(1X,10HTIME IS OK)
RETURN
END

```



```

SUBROUTINE CUT
COMMON/VERT/PWDTP(3000)/HOR/PHDTP(3000)/AREA/RIIF(500)
COMMON/DAT/X(3000),Y(3000)/TIM/PER(3000)/ER/EFREQ(3000)/CONST/NOPTC
COMMON/REAL/HRP(3000),ZRP(3000)/IMAG/HIP(3000),ZIP(3000)
COMMON/SCALE/HMAX,VMAX/FINC/GINC
COMMON/ROL/ANGIP,UNIT,IG,NOF,CER,T
DO 1 I=1,NOF
  IF(CER-EFREQ(I)) 2,3,3
3  A=1.
  GO TO 4
2  A=0.
4  HRP(I)=HRP(I)*A
  HIP(I)=HIP(I)*A
  ZRP(I)=ZRP(I)*A
  ZIP(I)=ZIP(I)*A
1  CONTINUE
  WRITE(6,5)
5  FORMAT(1X,9HAFTER CUT/)
  RETURN
END

```



```
SUBROUTINE TCUT
COMMON/REAL/HPP(3000),ZRP(3000)/IMAG/HIP(3000),ZIP(3000)
COMMON/DAT/X(3000),Y(3000)/TIM/PER(3000)/EP/EFREQ(3000)/CONST/NOPTS
COMMON/VERT/PWDTP(3000)/HOR/PUDTP(3000)/AREA/PIF(500)
COMMON/BOL/ANG1P,UNIT,IG,NOF,CER,T
DO 1 I=1,NOPTS
  IF(T-PER(I)) 2,3,3
3  A=1.
  GO TO 4
2  A=0.
4  PWDTP(I)=PWDTP(I)*A
  PUDTP(I)=PUDTP(I)*A
1  CONTINUE
  RETURN
END
```



```
SUBROUTINE MOD(H,Z,P,N)
REAL H(10),Z(10),P(10)
DO 10 I=1,N
P(I)=SQRT(Z(I)**2+H(I)**2)
10 CONTINUE
RETURN
END
```



```
SUBROUTINE FREOUN(F,N,TT)
REAL F(10)
DO 10 I=1,N
F(I)=FLOAT(I-1)/(TT*FLOAT(N))
10 CONTINUE
RETURN
END
```


SUBROUTINE TRUNC(IAI)

```

C.....
COMMON/VERT/PWDTP(3000)/HOR/PUDTP(3000)/AREA/RUF(500)
COMMON/DAT/X(3000),Y(3000)/TIM/PER(3000)/ER/FREQ(3000)/CONST/NOPTS
COMMON/REAL/HPP(3000),ZRP(3000)/IMAG/HIP(3000),ZIP(3000)
COMMON/SCALE/HMAX,VMAX/FINC/GINC
COMMON/POL/ANGIP,UNIT,IG,NOF,CER,T

C
115 FORMAT(1X,7(2X,F12.4))
116 FORMAT(20X,20HREAL AND IMAG. PARTS//)
117 FORMAT(1X,3(F10.2,F12.4,1X,F12.4))
118 FORMAT(5X,3(1X,4HTIME,6X,7HV-COMP.,7X,7HH-COMP.))
119 FORMAT(10X,5HEREFO.,9X,14HVERTICAL COMP.,12X,16HHORIZONTAL COMP.,
.12X,9HV-MODULUS,2X,9HH-MODULUS/)
120 FORMAT(1H1,27HTRUNCATED TRANSFER FUNCTION//)
121 FORMAT(1H1,10HTIME SYNT.//)
122 FORMAT(1H1,5HHMAX-,F6.2,1X,5HVMAX-,F6.2)

C
DELT=1./UNIT
KK=4*500
CALL PLOTS(RUF(1),KK)
CALL PLOT(0.0,25.2,-3)

C
CALL MAX(NOF,PUDTP,HMAX)
CALL MAX(NOF,PWDTP,VMAX)
WRITE(6,122) HMAX,VMAX

C
K=1
L=2
CALL TIME(IAI,K,L)

C
CALL CUT

C
CALL ZERO(NOPTS,X)
CALL ZERO(NOPTS,Y)
CALL MOVE(NOF,ZRP,X)
CALL MOVE(NOF,ZIP,Y)
CALL LAGS(NOPTS,X)
CALL LAGS(NOPTS,Y)
N1=NOPTS/2
CALL COMCON(Y,N1)
CALL FOUR 1D
CALL SORT 1D
CALL FACTOO(X,NOPTS)
CALL FACTOO(Y,NOPTS)
CALL PERIOD(PER,NOPTS,GINC)
CALL MOVE(NOPTS,X,PWDTP)

C
CALL ZERO(NOPTS,X)
CALL ZERO(NOPTS,Y)
CALL MOVE(NOF,HRP,X)
CALL MOVE(NOF,HIP,Y)
CALL LAGS(NOPTS,X)
CALL LAGS(NOPTS,Y)
CALL COMCON(Y,N1)

```



```

CALL FOUR 1D
CALL SORT 1D
CALL FACT00(X,NOPTS)
CALL FACT00(Y,NOPTS)
CALL MOVE(NOPTS,X,PUDTP)

```

```

C
C
WRITE(6,121)
WRITE(6,118)
WRITE(6,117)(PER(I),PWDTP(I),PUDTP(I),I=1,N1)

```

```

C
CALL MAX(NOPTS,PUDTP,HMAX)
CALL MAX(NOPTS,PWDTP,VMAX)
WRITE(6,122) HMAX,VMAX

```

```

C
K=2
L=1
CALL TIME(IAI,K,L)

```

```

C
CALL TCUT

```

```

C
CALL ZERO(NOPTS,X)
CALL ZERO(NOPTS,Y)
CALL MOVE(NOPTS,PUDTP,X)

```

```

C
CALL FOUR 1D
CALL SORT 1D

```

```

C
CALL MOVE(NOPTS,X,HRP)
CALL MOVE(NOPTS,Y,HIP)
CALL ZERO(NOPTS,X)
CALL ZERO(NOPTS,Y)
CALL MOVE(NOPTS,PWDTP,X)

```

```

C
CALL FOUR 1D
CALL SORT 1D

```

```

C
CALL MOVE(NOPTS,X,ZRP)
CALL MOVE(NOPTS,Y,ZIP)
CALL MOD(ZRP,ZIP,PWDTP,NOPTS)
CALL MOD(HRP,HIP,PUDTP,NOPTS)
CALL FREQU(FREQ,NOPTS,DELT)

```

```

C
WRITE(6,120)
WRITE(6,116)
WRITE(6,119)
WRITE(6,115)(FREQ(I),ZRP(I),ZIP(I),HRP(I),HIP(I),PWDTP(I),
.PUDTP(I),I=1,NOF)

```

```

C
CALL MAX(NOF,PUDTP,HMAX)
CALL MAX(NOF,PWDTP,VMAX)
WRITE(6,122) HMAX,VMAX

```


C

```
K=1  
L=1  
CALL TIME(IAI,K,L)  
AI=(FLOAT(NORTS)/UNIT)+2.0  
CALL PLOT(AI,6.0,-3)
```

C

```
RETURN  
END
```


B29906